EZH2 induces methylation of ERG enhancing its transcriptional and transforming activity

Curti, Laura

UNIVERSITÉ DE GENÈVE
Section des Sciences Pharmaceutiques

FACULTÉ DES SCIENCES
Professeur Leonardo Scapozza

INSTITUTE OF ONCOLOGY RESEARCH (IOR)

Prostate Cancer group
Giuseppina Carbone, MD

EZH2 Induces Methylation Of ERG Enhancing Its Transcriptional And Transforming Activity

THÈSE

présentée à la Faculté Des Sciences de l'Université de Genève
pour obtenir le grade de Docteur ès sciences, mention sciences pharmaceutiques

par
Laura CURTI
de
Malnate (Italie)

Thèse N° 4913

VARESE

2016

Table of Contents

List of Abbreviations

ADT	Androgen Deprivation Therapy
AML	Acute myeloid leukemia
AR	Androgen Receptor
ARE	Androgen Responsive Element
CAM	Chick Chorioallantoic Membrane
ChIP	Chromatin Immunoprecipitation
ChIP-Seq	ChIP sequencing
CRPC	Castrate-resistant prostate cancer
DNMT	DNA methyltransferase
EBS	ETS binding site
EED	Ectoderm development protein
ER	Estrogen Receptor
ERG	ETS related gene
EZH2	Enhancer of Zeste Homolog 2
GAPDH	Glyceraldehyde-3-phosphate dehydrogenase
H3K27me3	Trimethylation of lysine 27 of the histone H3
HAT	Histone acetyltransferase
HDAC	Histone deacetylase
HGPIN	High grade intra-epithelial neoplasia
HMT	Histone methyltransferase
HSC	Hematopoietic stem cells
JMJD	Jumonji C domain-containing demethylases
LOH	Loss of Heterozygosity
mERG	methyl-ERG
p-AKT	phospho AKT
pERG	ERG overexpressing plasmid
PAP	Prostatic Acid Phosphatase
PCa	Prostate Cancer
PcG	Polycomb group
PDGFβR	Platelet-derived growth factor receptor
PI3K	Phosphatidylinositide 3-kinase
PIN	Intra-epithelial neoplasia
PRC	Polycomb Repressive Complex
PSA	Prostate Specific Antigen
PTEN	Phosphatase and tensin homolog gene
SAH	S-adenosylhomocysteine
SAM	S-adenosylmethionine
SUZ12	Suppressor of Zeste 12 homolog
TMPRSS2	Transmembrane serine protease 2
TSS	Transcription Start Site

Summary

Background: The TMPRSS2-ERG gene fusion is one of the most frequent gene rearrangements found in about 50% of human prostate tumors. Ten years from the discovery of the TMPRSS2-ERG gene rearrangement in prostate cancer its clinical impact is still uncertain. Despite the high frequency of ERG fusion, uncertainty persists regarding the molecular determinants of ERG-induced oncogenesis and its role in tumor progression. Understanding these aspects would clarify a fundamental tumorigenic pathway and open new perspectives for targeted therapeutic strategies for prostate cancer treatment.

Principal findings: We report a novel molecular interaction between the ETS transcription factor ERG and the H3K27 histone methyltransferase EZH2. We found that ERG possesses a H3K27-like highly conserved motif (RKS) centered at lysine 362 (K362), and that EZH2 was able to catalyze its mono-methylation. ERG methylation required ERG-EZH2 interaction and was observed in ERG positive cell lines and human tumors. Moreover, specific domains in ERG and EZH2 required for their interaction were identified.

K362 methylation and interaction with EZH2 enhanced both trans-activation and trans-repression mediated by ERG and contributed to global transcriptional and phenotypic reprograming in ERG fusion positive prostate cancer. Importantly, methylation defective ERG mutants had a significantly weaker transcriptional and transforming capability, while EZH2 mutants, lacking methyltransferase activity, failed to enhance ERG functions. ERG and EZH2 co-localized in several regions of the genome of ERG fusion positive prostate cancer cells, and most of these co-occupied genes constituted a set of highly deregulated genes in primary and metastatic ERG fusion positive tumors. Furthermore, a prognostic risk index gene signature derived from the ERG-EZH2 co-occupied gene set was highly predictive of overall survival in prostate cancer patients. Notably, PTEN loss, which is frequently observed in prostate tumors with ERG fusion and is associated with adverse prognosis, promoted ERG methylation via activation of AKT and EZH2 (S21) phosphory-

lation. We found that PTEN deprivation in ERG fusion positive cells boosted EZH2 phosphorylation and ERG methylation, increasing the transcriptional activity of ERG. Our results provide a mechanism for ERG tumor progression that could be promoted by other events, setting the basis for cross-talks with other oncogenic pathways in leading to cancer progression in ERG fusion positive tumors.

Conclusion/Significance: This study gives new insights in the mechanisms of prostate tumorigenesis, supporting a model in which ERG transcriptional and oncogenic activity would be increased. These findings provide a broadly relevant mechanism for tumor progression, and define a therapeutically actionable pathway that could have a broad impact on the management of ERG fusion positive prostate cancers.

Résumé

Contexte : La fusion génique TMPRSS2-ERG est l'un des réarrangements les plus fréquents dans le cancer de la prostate, en effet on retrouve cette translocation dans près de la moitié des tumeurs. Les retombées cliniques de cette découverte sont encore incertaines plus de dix ans après son identification. Malgré la fréquence élevée de la fusion du gène ERG, le mécanisme oncogénique ainsi que son rôle dans la progression tumorale restent encore à définir. L'étude de ces différents aspects permettrait d'une part d'approfondir les connaissances sur une voie de signalisation clé dans le processus tumoral, et d'autre part d'ouvrir le champ à de nouvelles perspectives thérapeutiques dans le traitement ciblé du cancer de la prostate.

Principales découvertes : Nous avons découvert une nouvelle interaction moléculaire entre la protéine ERG appartenant à la famille des facteurs de transcription ETS, et la méthyltransférase EZH2, ciblant l'histone H3K27. Nous avons trouvé que ERG possédait un motif RKS hautement conservé, H3K27-like, sur la lysine 362 (K362), et que EZH2 était capable de catalyser sa mono-méthylation. L'interaction ERG-EZH2, requise pour la méthylation de la protéine ERG, a été observée dans les lignées cellulaires ERG positives et dans les tumeurs humaines. De plus, des domaines spécifiques sur ERG et EZH2, nécessaires à leur interaction ont pu être identifiés.

La méthylation du résidu K362 et son interaction avec EZH2 a augmenté non seulement la trans activation mais également la trans répression médiée par ERG et contribué à la reprogrammation transriptionnelle et phénotypique dans les cancers de la prostate TMPRSS2-ERG positifs. De manière importante, les mutants ERG déficients en méthylation ont montré une diminution significative de la capacité transcriptionnelle et de transformation et parallèlement, les mutants EZH2, sans activité methyltransférase, n'ont pu augmenter les fonctions de ERG. ERG et EZH2 ont été co-localisés dans plusieurs régions du génome des cellules cancéreuses TMPRSS2-ERG positives. Les gènes appartenant à ces régions font partis d'un ensemble de gènes hautement dérégulés dans les tumeurs primaires et métastatiques

TMPRSS2-ERG positives. De plus, une signature génétique dérivée de l'ensemble des gènes co-occupant ERG-EZH2 a été hautement prédictive de la survie globale chez les patients atteints de cancer de la prostate. En outre, la perte de PTEN, qui est fréquemment observée dans les tumeurs de la prostate présentant la fusion TMPRSS2-ERG et qui est associée à un pronostic défavorable, permis la méthylation de ERG via l'activation de AKT et la phosphorylation de EZH2 (résidu S21).

Nous avons également trouvé que l'absence de PTEN dans les cellules TMPRSS2-ERG positives augmentait la phosphorylation de EZH2, ainsi que la méthylation de ERG, augmentant ainsi l'activité transcriptionnelle de ERG. Nos résultats permettent de mettre en évidence un mécanisme dans la progression tumorale des cellules ERG positives qui pourrait être favorisé par d'autres évènements, posant ainsi les bases pour des interactions entre voies de signalisations oncogéniques, et donnant lieu à la progression du cancer dans les tumeurs TMPRRS2-ERG positives.

Conclusion : Cette étude permet d'obtenir un nouvel aperçu des mécanismes de tumorigenèse du cancer de la prostate, soutenant un modèle dans lequel l'activité transcriptionnelle et oncogénique de ERG serait augmentée. Ces découvertes mettent en avant un mécanisme largement pertinent quant à la progression tumorale, et définissent une voie pouvant être thérapeutiquement ciblée et ainsi avoir un impact majeur sur la gestion des cancers de la prostate TMPRSS2-ERG.

Introduction

1. Prostate cancer

Prostate cancer (PCa) is the most commonly diagnosed non-skin cancer in men, accounting for more than 235.000 new cases and nearly 30.000 deaths annually in the United States (Siegel, Naishadham et al. 2013). Although the age-adjusted rate of cancer deaths has decreased steadily in the past 10 years, PCa remains the second leading cause of cancer deaths worldwide, and is now one of the most serious oncological diseases in men, with an incidence higher than that of all other solid tumors (Siegel, Naishadham et al. 2013).

The discovery of prostate-specific antigen (PSA) as a biomarker for PCa has made it possible to detect the disease in its early stages, and over the past three decades has revolutionized the diagnosis of PCa. PSA is a kallikrein-related serine protease, which, though produced in normal prostate secretions, is released into the blood when the normal prostate architecture is disrupted (Lilja, Ulmert et al. 2008). It is estimated that there is often a lag-time of 15 years or more from initially detectable PSA elevation to clinically manifested PCa. The widespread use of PSA testing, however, has led to a vast increase in the diagnosis of patients with clinically localized low Gleason grade carcinomas that may not require treatment, as their tumors are relatively indolent. The Gleason score classifies tumors from 1 to 5, based on their most prevalent glandular architecture: lower scores indicate a well-differentiated glandular pattern, while higher scores represent entirely undifferentiated tumors (Gleason and Mellinger 1974). As there is a potential to over-treat indolent diseases, in recent years there has been considerable debate about the benefits versus the risks of PSA screening. Consequently, one of the major clinical challenges associated with PCa diagnosis and treatment is posed by the current inability to readily distinguish indolent from aggressive tumors in PCa patients who present low Gleason grade tumors after biopsy (Sartor, Hricak et al. 2008). Therefore, understanding the molecular basis of cancer initiation should lead to the identi-

fication of novel tumor biomarkers and new mechanistic insights into disease progression, improving prognostic abilities.

The only well-established risk factors for PCa are older age, black ethnicity, and a family history of the disease (Center, Jemal et al. 2012). Lifestyle components also contribute to PCa development, as evidenced by the identification of marked incidence differences between industrialized Western countries and East Asian countries. The higher incidence in Western countries is commonly attributed to dietary factors, such as increased meat and dairy intake along with reduced fruit and vegetable consumption, although this is a matter of some controversy (Golabek, Powroznik et al. 2015; Yang, Kenfield et al. 2015). In addition, although there is evidence for a strong genetic component of PCa, and several genetic loci have been implicated in hereditary PCa, the functional role of these genes in PCa pathogenesis is speculative.

The normal human prostate is a tubular-alveolar gland that surrounds the urethra at the base of the bladder, and produces important components of the seminal fluid. At the histological level, the human prostate is composed of a well-developed stromal compartment containing nerves, fibroblasts, infiltrating lymphocytes and macrophages, endothelial cells, capillaries, and smooth muscle cells surrounding glandular acini, which contain a pseudo-stratified epithelium with three differentiated epithelial cell types: luminal, basal and neuroendocrine (Figure 1). The luminal epithelial cells form a continuous secretory-layer of polarized columnar cells that are responsible for the production of PSA, prostatic acid phosphatase (PAP), and kallikrein-2, which are secreted as part of the seminal fluid. Luminal cells express characteristic markers such as cytokeratins 8 and 18, as well as high levels of androgen receptor (AR), which is essential for normal prostate development. Basal cells, located beneath the luminal epithelium, are limited by a basement membrane that divides the stroma from the epithelial compartment. Basal cells express p63 and the high-molecular-weight cytokeratins 5 and 14, while expressing AR at low or

undetectable levels. They do not produce prostatic secretory proteins. Consistent with a possible stem cell function, basal cells also express factors that protect from DNA damage, such as the anti-apoptotic gene Bcl2 (Abate-Shen and Shen 2000). Basal cells represent the proliferative compartment of the prostate since they are undifferentiated, proliferating, and androgen-independent, whereas luminal cells, which represent the major population composing the epithelium, are differentiated, non-proliferating and androgen-dependent.

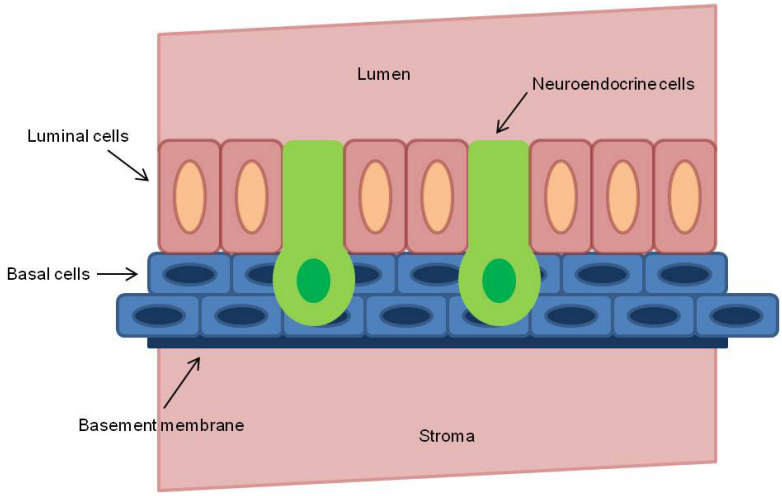

Figure 1. **Human prostate.** Schematic description of the pseudo-stratified epithelium of a normal human prostate.

The third cell type is represented by neuroendocrine cells, which are rare AR-negative cells whose function is not completely known and that express endocrine markers, such as chromogranin A and synaptophysin (Shen and Abate-Shen 2010).

Whereas the terms basal and luminal cells are adequate when referring to cells that are specific for each layer, further studies noted that some cells in the basal layer express luminal markers, while others in the luminal layer express basal markers. These findings suggest that heterogeneous subpopulations of differentiating cells are present in the prostate epithelium. These subpopulations contain cells with intermediate phenotype between that of the early progenitor basal cells and the ter-

minally differentiated secretory-luminal cells, and can migrate between both layers. They are not easily classified but, for example, the expression of AR – low for less differentiated cells and high for terminally differentiated cells – could help to better define this group of intermediate cells.

Substantial evidence supports the existence of a stem cell population in the prostate. In conditions of androgen-deprivation, approximately 90% of luminal cells and a small percentage of basal cells undergo apoptosis and die. However, after re-administration of androgens, the prostate epithelium regenerates in approximately 2 weeks, indicating that it contains a long-term population of castration-resistant stem cells (Lawson and Witte 2007).

Like most other epithelial cancers, PCa arises from precursor lesions, called prostatic intra-epithelial neoplasia (PIN), and progresses to locally invasive disease and ultimately metastasis. Each stage is associated with characteristic morphologic and histopathologic alterations, such as disruption of the basal cell layer, which occurs early in the disease, and a progression to androgen-independence, which is associated with advanced disease and metastasis. Prostate adenocarcinoma originates from the epithelia of the gland, and since primary prostate tumors often contain multiple independent histological foci of cancer that are often genetically distinct, it is generally regarded as multifocal cancer. By contrast, molecular and cytogenetic analyses show that multiple metastases in the same patient are clonally related, suggesting that metastatic cancer may arise from the selective advantage of individual clones during cancer progression. Generally, prostate tumors are characterized by a loss of basal cells and reduced matrix diversity, and express a luminal phenotype driven by AR. However, the co-expression of a subset of luminal and basal markers has often been found in many tumors, supporting the hypothesis that prostate tumors arise from the disruption of differentiation pathways, which normally restricts luminal and basal markers expression to their respective cell types.

In addition, the cell of origin, the cell that is the oncogenic target that gives rise to the tumor, has not been clearly identified in PCa (Frank and Miranti 2013).

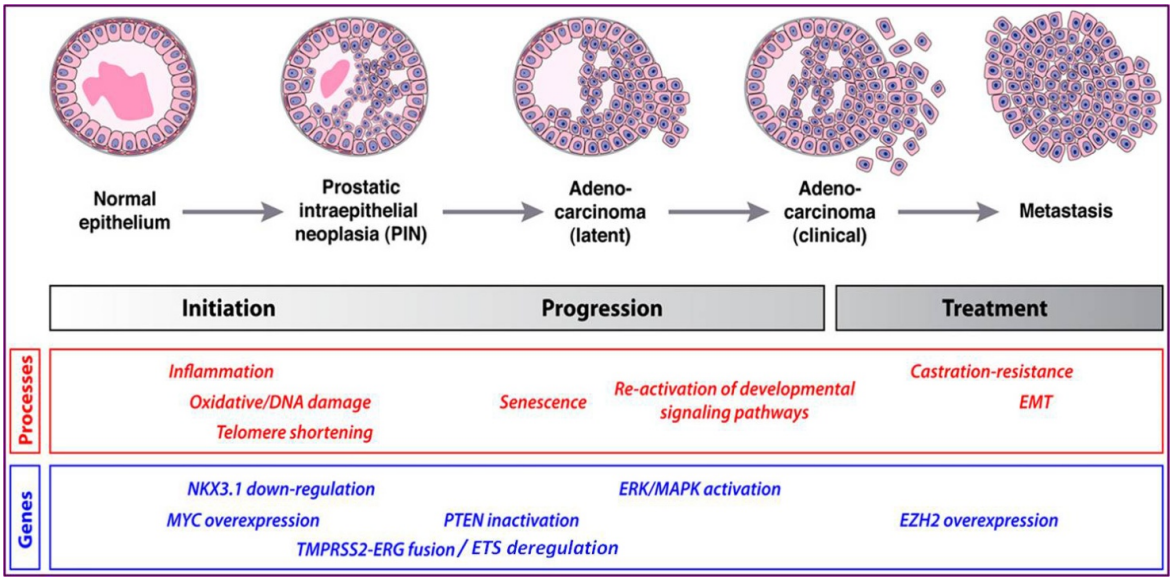

Figure 2. **PCa progression.** Stages of progression and molecular processes involved in human PCa. Adapted from *Shen and Abate-Shen, 2010*.

The histological and clinical heterogeneity of PCa is also reflected at the molecular level. Although PCa is characterized by several stages of progression, little evidence exists for a clearly defined series of genetic events leading to PCa development, and it is also unknown whether these events are associated with a precise, temporal sequence or a fortuitous relationship (Figure 2) (Thomas, Jacobs et al. 2008). Establishing the temporal sequence of genomic events in PCa is critical for defining prostate cancer progression and aggressiveness at the molecular level. A reliable molecular "map" of progression could prove invaluable in a number of ways, such as for patients on active surveillance or for improved risk stratification for patients with intermediate-risk prostate tumors. A myriad of studies regarding gene expression and copy number profiles provide a relatively comprehensive picture of the alterations in PCa at the genomic and gene expression levels (Tomlins, Rhodes et al. 2005; Thomas, Jacobs et al. 2008; Shen and Abate-Shen 2010; Berger,

Lawrence et al. 2011; Boyd, Mao et al. 2012). Although the spectrum of specific genomic lesions in prostate tumors is diverse, with considerable molecular heterogeneity between tumors, alterations in specific signalling pathways are recurrent (Barbieri and Tomlins 2014). Indeed, there are several candidate genes and pathways, identified by molecular studies, which are thought to be important at each stage of progression (Figure 2 and Table 1).

The prostate cancer genome displays relatively few focal chromosomal gains or losses (most commonly focal loss at PTEN) and overall low mutation rates compared with other cancers. However, PCa is characterized by a large number of chromosomal rearrangements and extensive copy number alterations involving multiple chromosomes. This phenomenon, termed "chromoplexy", often leads to loss of one or both copies of critical tumor suppressor genes, such as Nkx 3.1, PTEN, TP53, and CDKN1B, as well as oncogenic fusions such as TMPRSS2-ERG, which is observed in ~50% of prostate tumors. Genomic and transcriptomic analyses have provided evidence that prostate tumors can be subclassified based on gene expression and SCNA (Somatic Copy Number Alteration) signature, with some success in predicting aggressive features of the disease or impact on prognosis (Lapointe, Li et al. 2004; Lapointe, Li et al. 2007; Taylor, Schultz et al. 2010). Interestingly, specific alterations such as mutations and deletions in PTEN and TP53 are enriched in ETS-positive tumors, while other drivers, such as SPOP mutations, CHD1 deletions and SPINK1 overexpression, occur exclusively in ETS-negative prostate tumors (Barbieri and Tomlins 2014). Advances in molecular subclassification of prostate tumors raise the possibility of a transition from a poorly understood, heterogeneous disease with a variable clinical course to a collection of homogenous subtypes, identifiable by molecular criteria, associated with specific genetic abnormalities, and perhaps amenable to specific management strategies. The major genomic alterations that characterize PCa, e.g. AR lesions, PTEN loss, Nkx 3.1 repression, SPOP mutations, and ETS deregulation, are described below.

Table 1. **Candidate genes and pathways deregulated during PCa progression**.

Gene or Pathway	Function	Evidence	References
Hedgehog pathway	Development and regeneration	Marked activation of the hedgehog pathway has been reported to have a crucial role in the development as well as in the progression of PCa to more aggressive and even therapy-resistant disease states. Targeting Hh signaling could therefore be a potential option for the treatment of PCa.	(Karhadkar, Bova et al. 2004; Gonnissen, Isebaert et al. 2013)
α-methylacyl-CoA racemase (AMACR)	Fatty acid metabolism	This enzyme is involved in peroxisomal β-oxidation of branched-chain fatty acids. It is one of the most overexpressed genes in HGPIN compared to normal prostate and it is potentially an important prostate tumor marker.	(Ananthanarayanan, Deaton et al. 2005; Jiang, Zhu et al. 2013)
Fatty acid synthase (FASN)	Fatty acid metabolism	Highly overexpressed in aggressive localized and metastatic prostate tumors. Expression in PCa is linked to phosphorylation and nuclear accumulation of AKT.	(Van de Sande, Roskams et al. 2005; Migita, Ruiz et al. 2009; Flavin, Peluso et al. 2010)
Myc	Growth control	One of the master regulators of cell proliferation. Myc is often amplified in localized and metastatic PCa. Myc expression in the mouse prostate results in prostate tumor development.	(Jenkins, Qian et al. 1997; Koh, Bieberich et al. 2010; Kim, Roh et al. 2012)
PIM-1	Growth control	A serine-threonine kinase that interacts with Myc. Expression of PIM-1 characterizes a Myc-like signature in human PCa, and PIM-1 is highly expressed in murine PCa driven by Myc expression. High levels of PIM-1 predict recurrence in localized prostate tumors.	(Ellwood-Yen, Graeber et al. 2003; Zippo, De Robertis et al. 2007; Holder and Abdulkadir 2014)
Glutathione-S-transferase pi-class (GSTP1)	Protection from carcinogenesis	GSTP1 protects against reactive chemical species, including ROS. Transcriptional silencing of GSTP1 through promoter hypermethylation is one of the most frequent events in PCa (>90%). The precursor lesion PIN also shows GSTP1 hypermethylation.	(Henrique and Jeronimo 2004; Yuan, Qian et al. 2008)
Phosphatase and tensin homolog (PTEN)	PI3K signalling	PTEN antagonizes the PI3K/Akt signalling pathway and is frequently deleted in PCa. Loss of PTEN expression in mouse models results in PCa.	(Wang, Gao et al. 2003; Phin, Moore et al. 2013)
Cyclin-dependent kinase inhibitor 1B (p27)	PI3K signalling	Expression of this cyclin-dependent kinase inhibitor is often lost in PCa. Its down regulation is mediated by PI3K and the ubiquitin ligase SKP2.	(Macri and Loda 1998; Chu, Hengst et al. 2008)
Neutral endopeptidase (NEP)	PI3K signalling	NEP stabilizes PTEN and is frequently lost in the development of PCa.	(Osman, Yee et al. 2004; Osman, Dai et al. 2006)

Hepsin (HPN)	Protease	This serine protease is one of the most consistently overexpressed genes reported in PCa profiling studies. Hepsin expression in the mouse prostate causes disruption of the basement membrane and weakening of epithelial-stroma adhesions.	(Klezovitch, Chevillet et al. 2004; Wu and Parry 2007; Holt, Kwon et al. 2010)
Androgen receptor (AR)	Steroid receptor	Alterations of the AR signalling play an important role in early pathogenesis rather than in mediating the transition to castration resistance disease.	(Shen and Abate-Shen 2010; Karantanos, Corn et al. 2013)
NKX3.1	Transcriptional regulator	The NKX3.1 locus frequently demonstrates LOH in PIN and PCa. NKX3.1 null mice develop PIN. NKX3.1 acts as a haploinsufficent tumor suppressor, and loss of one allele affects cellular proliferation and gene expression.	(Magee, Abdulkadir et al. 2003; Shen and Abate-Shen 2010)
Enhancer of Zeste homolog 2 (EZH2)	Transcriptional regulator	A polycomb group protein that acts as a transcriptional repressor, EZH2 is required for proliferation in different cell types. EZH2 protein is increased in metastatic PCa and high expression in localized PCa predicts recurrence.	(Varambally, Dhanasekaran et al. 2002; Sauvageau and Sauvageau 2010)
ETS	Transcriptional regulator	Oncogenes ERG (21q22.2), ETV1 (7p21.2), ETV4 (17q21), and ETV5 (3q27) very highly expressed in a subset of prostate tumors.	(Tomlins, Rhodes et al. 2005)

Androgen Receptor

The androgen receptor (AR) occupies a central role in the biology of both normal prostate development and PCa progression (Shen and Abate-Shen, 2010). AR is a member of the nuclear hormone receptor superfamily that directs the transcriptional regulation of genes governing a wide variety of cellular processes, including cell cycle, cell proliferation, survival, and differentiation (Schiewer, Augello et al. 2012). Upon activation by androgens, AR dissociates from heat shock proteins, dimerizes, and translocates from the cytoplasm into the nucleus, where it recognizes and binds to the 15-bp palindromic androgen response elements (ARE) on target genes (Heemers and Tindall 2007). AR is the most important transcription factor for the lineage-specific differentiation of the prostate, inducing the expression of prostate-specific genes such as PSA and TMPRSS2, and maintaining the differentiated prostate epithelial phenotype (Wright et al., 2003). In normal prostate epithe-

lium, androgen signalling, through AR, is essential for inducing growth and proliferating signals of prostate development. Indeed, in the absence of functional AR, the prostate fails to develop (Cunha and Lung 1978); upon androgen deprivation, the androgen dependence of prostate tissue is manifested by rapid cellular apoptosis and involution to the regressed state, underlining the importance of the AR signal pathway in all aspects of prostatic growth and differentiation (Shen and Abate-Shen 2010).

PCa initiation and progression is also uniquely dependent on AR. Androgen signalling is a critical signalling pathway in both primary and advanced PCa, and approximately 80-90% of prostate tumors are dependent on androgen at initial diagnosis. A androgen-deprivation therapy (ADT) remains the standard treatment for advanced PCa. ADT is known to provide remission of the disease, best evidenced by a decline of PSA in about 90% of patients. After a mean time of 2-3 years, however, the disease progresses despite continuous hormonal manipulation. This type of cancer is known as castrate-resistant prostate cancer (CRPC) (Harris, Mostaghel et al. 2009). Metastatic castration-resistant prostate cancer (mCRPC) is associated with a poor prognosis and a mean survival time of only 16–18 months (Marques, Dits et al. 2010). Lesions in the AR gene itself play an important role in early pathogenesis of the disease rather than in resistance to therapy. Considerable evidence now supports the idea that development of CRPC is related to continuous AR transcriptional activity in prostate cancer cells. Several cellular and molecular alterations are related to the post-castration activation of the AR, including an incomplete blockade of AR-ligand signalling, AR amplification, AR mutations, aberrant AR co-regulator activities, and AR splice-variant expression (Karantanos, Corn et al. 2013). Although recent data show AR amplification in about 40%, and point mutations in an additional 10% of treated, metastatic tumors, these lesions are absent in clinically localized prostate tumors (Barbieri and Tomlins 2014). Furthermore, in normal cells the transcriptional activity of AR is finely controlled by

the coordinated recruitment of specific co-regulatory proteins (among others, collaborative factors, co-repressors, and co-activators), which might become aberrantly expressed in PCa, resulting in a deregulated AR transcriptional network (Shen and Abate-Shen 2010). Interestingly, deregulation of these genes is present in both primary and metastatic tumors, indicating that although AR itself is not altered in clinically localized disease, other elements of the signalling pathway may be affected.

A distinct and intriguing role for androgen signalling in driving prostate carcinogenesis has been proposed based on the whole genome of prostate tumors. The importance of genomic rearrangements in PCa is well established, and it has been demonstrated that rearrangements may occur when the loci are brought into close physical proximity to each other (Mani, Tomlins et al. 2009). Interestingly, rearrangement breakpoints are more common near androgen receptor binding sites (Berger, Lawrence et al. 2011), raising the possibility that androgen receptor-mediated transcription brings together distant genomic loci and that it predisposes to genomic rearrangements through transcriptional stress. Accordingly, androgen stimulation can bring together the TMPRSS2 and ERG loci and promote gene fusion (Bastus, Boyd et al. 2010; Haffner, Aryee et al. 2010). Whole-genome sequencing in a German cohort supported a high incidence of androgen-driven structural rearrangements, correlating with younger age at diagnosis (Weischenfeldt, Simon et al. 2013). These data suggest that androgen-mediated transcriptional activity could act as an initial driver of many genomic rearrangements in PCa, and reinforce the idea that androgen signalling is a critical signalling pathway in both primary and advanced PCa (Barbieri and Tomlins 2014).

Extensive interaction between AR signalling and other oncogenic signalling pathways may allow for crosstalk and functional redundancy. This type of interplay between AR, interactors that affect its activity, and other pathways may help explain the inevitable failure of therapy targeting the androgen axis; further investigation defining these interactions may identify new key therapeutic targets.

PTEN

One pathway with a well-known role in PCa is the phosphatidylinositide 3-kinase (PI3K) signalling pathway. Current evaluations suggest that this signalling pathway is up-regulated in 30-50% of prostate tumors (De Velasco and Uemura 2012; Phin, Moore et al. 2013). PI3K signalling is initiated by the activation of a number of tyrosine kinase receptors, including platelet-derived growth factor receptor (PDGFR), insulin-like growth factor receptor (IGFR), and epidermal growth factor receptor (EGFR). Once activated, these receptors phosphorylate PI3K at the cell membrane. Phosphorylated PI3K, in turn, phosphorylates phosphatidylinositol-4,5-diphosphate (PIP2), leading to the accumulation of phosphatidylinositol-3,4,5-triphosphate (PIP3). PIP3 recruits AKT and phosphoinositide-dependent protein kinase 1 (PDK1), which phosphorylates AKT. Phosphorylated AKT (pAKT) activity extends over a wide range of substrates, such as the multiple molecules involved in cell survival and proliferation, including MDM2, c-Myc, and GSK3β, but most importantly activates the mammalian target of rapamycin (mTOR), which plays a significant role in tumorigenesis (Feldman and Feldman 2001) (Figure 3). The phosphatase and tensin homolog gene (PTEN) is the primary negative regulator of the PI3K/AKT survival pathway and is the most frequently deleted tumor suppressor gene in PCa. Monoallelic loss of PTEN is present in up to 60% of localized prostate tumors, while complete loss of PTEN in PCa is linked to metastasis and androgen-independent progression (Phin, Moore et al. 2013). PTEN signalling regulates cell division and, when sufficient growth has taken place, can also direct cells to enter a natural cell death pathway by inducing G1-phase cell cycle arrest through the retinoblastoma protein (Paramio, Navarro et al. 1999; Radu, Neubauer et al. 2003). As PTEN is a regulator of PI3K signalling, a loss thereof leads to over-activation of AKT which, in turn, is associated with uncontrolled cell proliferation, decreased apoptosis, and enhanced tumor angiogenesis (Carnero, Blanco-Aparicio et al. 2008).

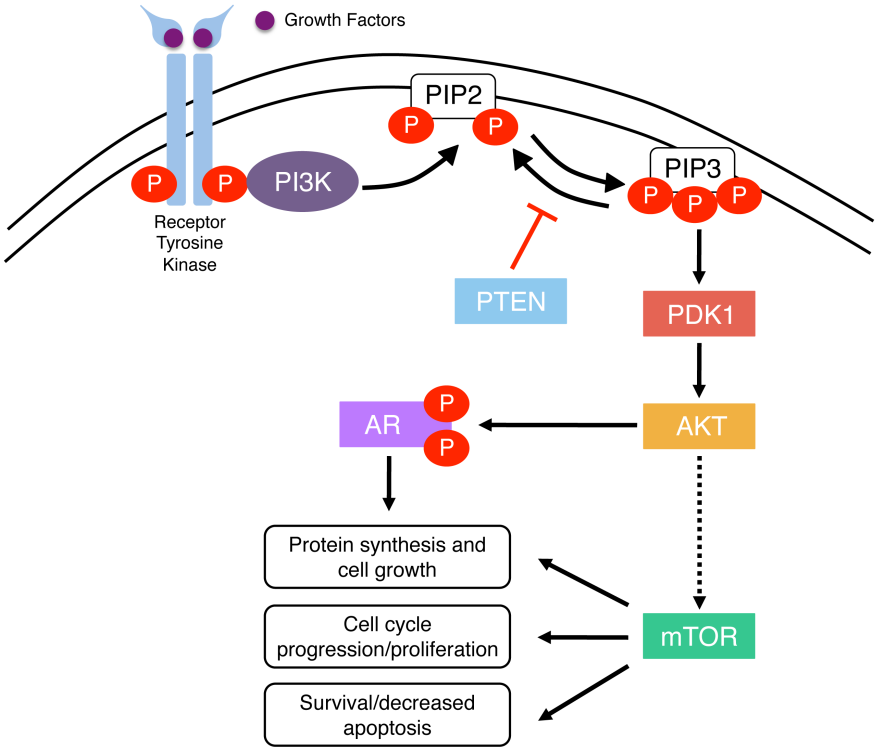

Figure 3. **The PI3K/PTEN/Akt pathway.** Binding of growth factors to the tyrosine kinase receptor activates the receptor complex, which in turn recruits and activates PI3K. Activated PI3K converts PIP2 to PIP3, which subsequently mediates the phosphorylation of AKT through PDK1.Phosphorylated AKT is active on a wide range of substrates, but one of its most important targets is mTOR, which is involved in cell growth, proliferation, and survival. Activated AKT also interacts with androgenreceptor (AR) in an androgen-independent manner, leading to over-activation of the AR signalling pathway in castration resistant prostate cancer. PTEN is a tumor suppressor that negatively regulates the pathway by removing the 3-phosphate from PIP3, converting it back to PIP2. Loss of PTEN leads to over-activation of AKT which, in turn, is associated with uncontrolled cell proliferation, decreased apoptosis, and enhanced tumor angiogenesis. Adapted from *Phin, Moore and Cotter, 2013*.

The PTEN tumor suppressor gene maps to human chromosome 10q23.3; this region is known to exhibit high rates of LOH in a variety of human malignancies, including kidney-, lung-, breast-, and prostate cancer (Kwabi-Addo, Giri et al. 2001). In PCa, the PTEN gene can be altered by small changes in DNA sequence or point mutations that lead to the inactivation of PTEN protein function (Dong 2006). In addition, the PTEN gene may also be inactivated by epigenetic events, such as promoter methylation (Whang, Wu et al. 1998; Konishi, Nakamura et al. 2002). Moreover, in recent years, it has become evident that the PTEN gene is also affected by relatively large deletions and genomic rearrangements in PCa (Phin, Moore et al. 2013). Other mechanisms including transcriptional repression, microRNA (miRNA)

regulation (Poliseno, Salmena et al. 2010), disruption of competitive endogenous RNA (CeRNA) networks (Tay, Kats et al. 2011), and post translational modifications have also been implicated in the loss of PTEN function and in the initiation of tumorigenesis (Wang and Jiang 2008; Singh and Chan 2011). Given the enormous amount of mechanisms involved in the loss of PTEN, it is clear that PTEN status is a powerful biomarker that promises effective diagnosis and improved patient stratification and management.

Analyses of PTEN deletion in genetically engineered mouse models have revealed its cooperativity with the inactivation of other key genes that are deregulated in prostate tumorigenesis, and have also provided insights into new therapeutic options for the treatment of PCa. Inactivation of PTEN has been shown to cooperate with loss of function of the Nkx 3.1 gene, up-regulation of c-Myc proto-oncogene or TMPRSS2-ERG fusion (Kim, Cardiff et al. 2002; Carver, Tran et al. 2009; Kim, Eltoum et al. 2009; King, Xu et al. 2009). Moreover, the observation that complete inactivation of PTEN in mouse prostate tumors leads to cellular senescence (Chen, Trotman et al. 2005) has led to the idea that novel therapeutic approaches might promote senescence for selective targeting of prostate tumor cells through knockdown of PTEN function (Alimonti, Nardella et al. 2010). Notably, in prostate cancers, PTEN reduction or loss predisposes to the emergence of castration-resistant prostate cancer (Mulholland, Dedhar et al. 2006; Shen and Abate-Shen 2010). In particular, perturbation of PTEN expression in human prostate cancer cell lines or targeted deletion of PTEN in mouse prostate cancers is sufficient for the development of castration resistance (Bertram, Peacock et al. 2006; Gao, Ouyang et al. 2006; Wu, Conaway et al. 2006). It has been observed that activation of the PI3K pathway is associated with repressed androgen signalling in mouse and human prostate cancers, and, importantly, that the generated castrate-resistant phenotype is reversible because inhibition of the PI3K pathway restores AR protein levels and signalling in PTEN-deficient prostate cells (Carver, Chapinski et al. 2011). These findings

demonstrate that inhibition of the PI3K pathway in PTEN-negative PCa can up-regulate AR and activate AR target gene expression (Carver, Chapinski et al. 2011) (Figure 3). Despite the evidence that PTEN loss can promote castration resistance, there is little insight into the mechanism. Some reports have suggested that PTEN loss activates AR, through PI3K-mediated stabilization of AR protein levels or Akt-mediated phosphorylation and transcriptional activation of AR. Conversely, other studies have demonstrated that PI3K activation promotes degradation of AR and inhibits AR transcriptional activity (Lin, Hu et al. 2003; Mulholland, Tran et al. 2011). Anyway, this bidirectional cross-talk between two critical survival pathways in PCa provides the molecular rationale for simultaneously targeting both AR and PI3K signalling pathways.

Nkx 3.1

Down-regulation of the Nkx 3.1 homeobox gene represents a frequent, critical event in PCa initiation, and is likely to involve multiple mechanisms (Abate-Shen, Shen et al. 2008). Nkx 3.1 is a member of the NK subfamily of homeobox genes, which are implicated in processes of cell fate specification and organogenesis in many species, including Drosophila, in which they were first identified (Kim and Nirenberg 1989). The Nkx family is characterized by divergent residues within the homeodomain, including a tyrosine at position 54, residues that are thought to contribute to differential DNA binding specificity relative to that of the canonical Antennapedia-class homeodomains. Indeed, binding site selection experiments have identified "TAAGTA" as a consensus site for human Nkx 3.1 (Steadman, Giuffrida et al. 2000), which differs from the consensus sequences identified for other homeo-proteins that typically contain a "TAAT" core (Catron, Iler et al. 1993). Several studies of Nkx family homeoproteins, including those of the Nkx3 class, indicate that they act as transcriptional repressors in cell culture assays and *in vivo* (Steadman,

Giuffrida et al. 2000; Murtaugh, Zeng et al. 2001). Other studies, however, indicate that Nkx 3.1 possesses transcriptional activator activity in certain tissue contexts (Carson, Fillmore et al. 2000; Gelmann, Steadman et al. 2002).

Nkx 3.1 is located in a chromosomal region that displays LOH in up to 85% of high-grade PIN lesions and adenocarcinomas (Shen and Abate-Shen 2010). In addition, irrespective of whether LOH has occurred, the Nkx 3.1 gene undergoes epigenetic down-regulation, perhaps through promoter methylation (Asatiani, Huang et al. 2005), suggesting that most likely there is a selection for reduction of Nkx 3.1 expression throughout PCa progression. Nkx 3.1 is the earliest known marker of prostate formation during development, and continues to be expressed at all stages of prostate differentiation, and in adulthood. A loss of its function leads to defects in prostatic protein secretions and ductal morphogenesis, indicating that it is necessary for prostate development (Bhatia-Gaur, Donjacour et al. 1999). Nkx 3.1 loss of function has also been shown to contribute to prostate carcinogenesis; since Nkx 3.1 mutant mice are predisposed to prostate carcinoma and also because its loss of function cooperates with that of other tumor suppressor genes in cancer progression (Shen and Abate-Shen 2003). These findings demonstrate that Nkx 3.1 plays important roles both in prostate development and PCa pathogenesis; while it is essential for normal morphogenesis and function of the prostate, its inactivation leads to prostatic epithelial hyperplasia and dysplasia that model a pre-neoplastic condition. It has also been shown that Nkx 3.1 expression in the androgen-deprived prostate marks a rare population of prostate epithelial stem cells that is a cell of origin for PCa in mouse models (Wang, Kruithof-de Julio et al. 2009). Analyses of Nkx 3.1 function in human tumor cells and genetically engineered mice have provided insights into its potential roles in cancer initiation. In particular, Nkx 3.1 inactivation in mice results in a defective response to oxidative damage, while its expression in human prostate cancer cell lines protects against DNA damage, and is regulated by inflammation (Ouyang, DeWeese et al. 2005; Markowski, Bowen et al.

2008; Bowen and Gelmann 2010). A causal role for Nkx 3.1 in these processes has been suggested by analyses of genes that are dysregulated following perturbation of Nkx 3.1 expression in mouse models or human cell lines (Muhlbradt, Asatiani et al. 2009; Song, Zhang et al. 2009). These and other findings have led to a model in which Nkx 3.1 represents a haploinsufficient tumor suppressor gene that acts as a "gate-keeper" gene for PCa initiation (Kim, Bhatia-Gaur et al. 2002; Gelmann 2003; Magee, Abdulkadir et al. 2003).

SPOP and CHD1

The SPOP gene encodes the substrate-recognition component of a Cullin3-based E3-ubiquitin ligase. Mutations in the SPOP gene occur in 6%-15% of multiple independent cohorts, representing the most common point mutations in primary PCa. Missense mutations are found exclusively in the structurally substrate-binding region of SPOP, indicating that prostate cancer-derived mutations will alter substrate binding (Barbieri, Baca et al. 2012). Among SPOP substrates, the AR co-activator SRC-3 has stimulated a great deal of interest. Wild-type SPOP normally binds and promotes SRC-3 degradation; however, prostate cancer-derived SPOP mutants lose this ability, leading to increased androgen signalling in certain model systems (Geng, He et al. 2013). SPOP mutations are mutually exclusive with deletions and mutations in the TP53 tumor suppressor, TMPRSS2-ERG fusion and other ETS rearrangements. Moreover, SPOP mutant tumors generally lack lesions in the PI3K pathway (Barbieri, Baca et al. 2012; Grasso, Wu et al. 2012; Lindberg, Mills et al. 2013). SPOP mutant tumors also show a distinct pattern of genomic aberrations, they specifically harbour deletions of the CHD1 gene at 5q21 and in the 6q21 regions, which are significantly associated with SPOP mutations (Barbieri, Baca et al. 2012). CHD1 encodes a chromodomain helicase DNA-binding protein that acts to remodel chromatin states, and is involved in transcriptional control across the genome. CHD1 is recurrently

deleted in PCa. Rearrangements and point mutations have also been identified, while lesions in CHD1, particularly focal homozygous deletions, are restricted to ETS-negative tumors (Barbieri, Baca et al. 2012; Grasso, Wu et al. 2012). Interestingly, prostate tumors harbouring CHD1 deletion have a significant increase in genomic rearrangements (Liu, Lindberg et al. 2012; Baca, Prandi et al. 2013). Taken together, these findings support SPOP mutations and CHD1 deletions as driver lesions that underlie a distinct ETS-negative molecular subclass of PCa.

ETS

Fusions involving androgen-regulated genes and members of the ETS transcription factor family are the most commonly-known molecular alterations in PCa, identified in a majority of cases (Tomlins, Rhodes et al. 2005; Rubin, Maher et al. 2011). The molecular characterization of prostate tumors often begins with ETS-positive and ETS-negative subclasses. Whole-genome-, epigenetic-, and gene expression profiling studies support tumors harbouring ETS fusions (ETS-positive) as distinct biological entities compared with those without (ETS-negative). Advanced stages of PCa are associated with the increased expression of multiple ETS proteins, including ETS1, ETS2, ERG, ESE2, ETV1 and ESE1 (Gavrilov, Kenzior et al. 2001; Alipov, Nakayama et al. 2005; Kunderfranco, Mello-Grand et al. 2010; Longoni, Sarti et al. 2013), and the decreased expression of others, such as PEA3, PDEF and ESE3 (Gu, Zerbini et al. 2007; Rostad, Mannelqvist et al. 2007; Cangemi, Mensah et al. 2008). Considering that some ETS transcription factors are involved in malignant transformation and tumor progression, including invasion, metastasis, and neo-angiogenesis through the activation of cancer-related genes, they could be potential molecular targets for selective cancer therapy. This family of transcription factors and its role in PCa development and progression are better described below.

2. ETS Transcription factors

ETS-domain proteins are a group of DNA-binding transcriptional factors involved in many different cellular processes. ETS1 is the founding member of the family and whose name – and that of the entire resulting family – was initially derived from the viral oncogene *v-ets*, found in the avian transforming retrovirus E26 (E Twenty Six), which induces both erythroblastic and myeloblastic leukemias in chickens (Leprince, Gegonne et al. 1983).

To date, 27 ETS family members have been identified in humans. All the ETS family proteins share a highly conserved DNA-binding domain of about 85 amino acid residues that recognizes a central, invariant 5′-GGA(A/T)-3′ motif within the context of a 9- to 10-bp DNA sequence, defined as the *ETS binding site* (EBS) (Papas, Watson et al. 1986; Wang, Petryniak et al. 1992) (Figure 4). Structural studies showed that the ETS domain is a conserved variant of the *winged helix-turn-helix motif*, a subtype of a DNA-binding motif that consists of two α-helices separated by a tight turn, and contains an extended loop between two β-strands (wing) that also contacts DNA. Indeed, the ETS domain is composed of three α-helices and four stranded, anti-parallel β-sheets. The two invariant arginines located in the third α-helix, the amino acid residues in the "wing" between β-strands 3 and 4, and also a loop between α-helices 2 and 3, provide key ETS protein interactions with the major groove in DNA (Donaldson, Petersen et al. 1996; Sharrocks 2001; Agarkar, Babayeva et al. 2010; Regan, Horanyi et al. 2013).

The ETS domain is also a target for protein-protein interactions and a single amino acid alteration, at the carboxy-terminal end of the DNA-recognition helix 3 in the domain, can markedly alter its DNA-binding specificity and its interaction with other transcription factors (Cooper, Newman et al. 2014) (Figure 5).

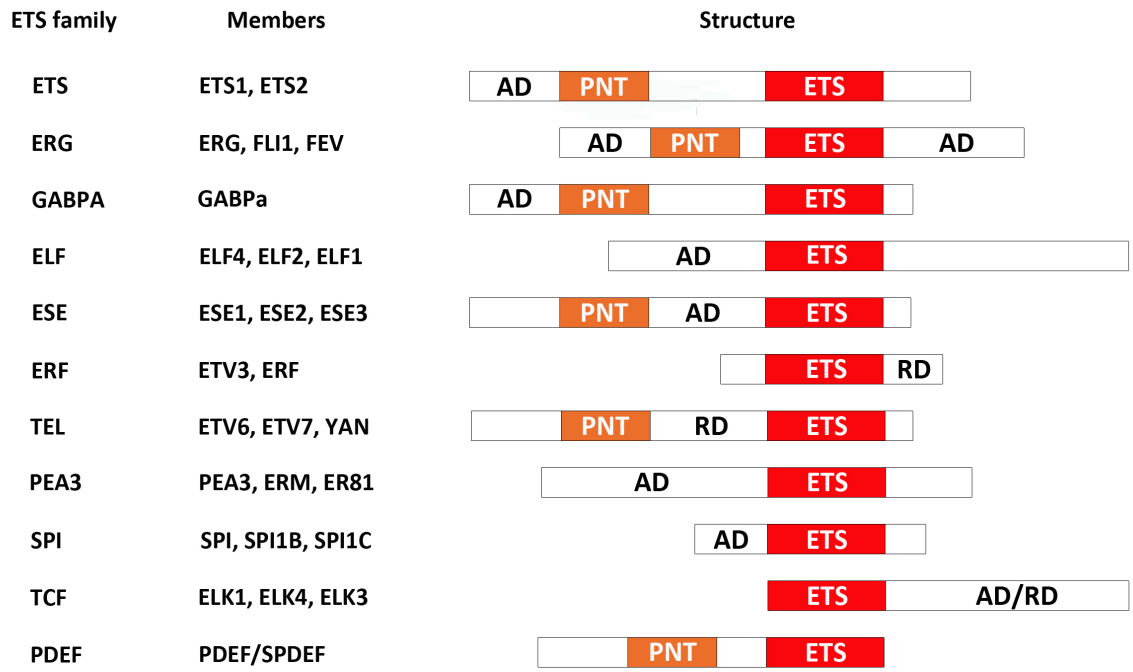

Figure 4. **Structural and functional domains of ETS transcription factor family members.** Boxes identify the DNA binding domain (ETS), transcriptional activation domain (AD), basic helix-loop-helix pointed domain (PNT), and transcriptional repressor domain (RD).

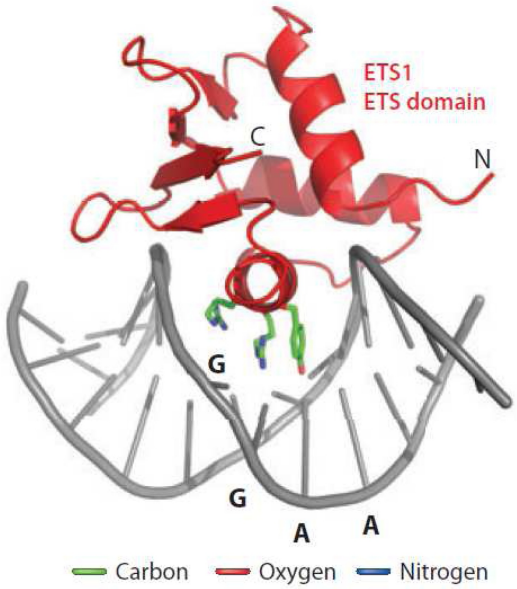

Figure 5. **ETS domain structure.** Ribbon diagram of the ETS1 ETS domain bound to a DNA duplex. In stick format are shown the side chain of R391, R394 and Y395 which provide base-specific contacts to core GGAA. Taken from *Hollenhorst, McIntosh and Graves, 2011*.

Approximately one-third of ETS family members possesses a second structured evolutionarily-conserved domain called the Pointed domain (PNT) that

forms a helix-loop-helix structure for protein-protein interactions (Kim, Phillips et al. 2001) or can oligomerize and alter DNA-binding affinity (Green, Coyne et al. 2010). This conserved domain plays unique roles in different ETS proteins.

Moreover, two other domains have been characterized: the B-box domain, found in three members of the TCF subfamily, and which forms an induced structural element that interacts with serum response factor (SRF) on DNA (Hassler and Richmond 2001) and the OST domain, which appears unique to GABPA and serves in cofactors recruitment (Kang, Nelson et al. 2008).

On the basis of their structural composition and similarities in the DNA-binding domain, ETS proteins can be divided into 11 subfamilies (ETS, ERG, GABPA, ELF, ESE, ERF, TEL, PEA3, SPI, TCF and PDEF) (Figure 4).

The overall diversification of the known biochemical properties of the ETS members suggests that different family members will play distinct biological roles. However, despite evidence that different ETS proteins can execute diverse roles, an extensive overlap in the expression of various family members is found in many human tissues. Genome-wide studies of ETS occupancy using either ChIP-chip or ChIP-seq reveal that a single ETS protein can bind to hundreds to thousands of ETS binding sites in a particular cell type. However, these studies also show that multiple ETS factors can occupy any given single ETS binding site within a particular cell type indicating redundant binding (Farnham 2009; Yu, Mani et al. 2010; Hollenhorst, McIntosh et al. 2011). In this case, the DNA sequence flanking the GGAA/T central core appears to play an important role in determining the preferential binding of individual ETS family members. For example, changing the sequence of 5'-GCGGAAGCG-3' in the MSV (Moloney Sarcoma Virus) enhancer to GCGGATGCG significantly reduces ELF1 binding but does not affect ETS1 binding, whereas altering this sequence to GCGGAAGAA completely abolishes ETS1 binding but has little effect on ELF1 binding (Wang, Petryniak et al. 1992). In addition to the different binding consensus sequences, which characterize different ETS proteins, there are

other aspects that enhance the specificity of targets among different members of the ETS family.

Outside of the highly conserved ETS domain, structural or functional domains and post-translational modifications illustrate the potentially unique properties of subfamilies or individual ETS proteins. Post-translational modifications, such as phosphorylation, glycosylation, sumoylation, acetylation, and ubiquitinylation are additional levels of ETS proteins regulation; they dynamically and reversibly influence protein–protein interactions, protein–DNA interactions, sub-cellular localization, stability, and activity, thereby significantly increasing the functional complexity of ETS factors regulation (Tootle and Rebay 2005). For example, phosphorylation of ETS1 is essential for ETS1 to recruit its co-activator and form a ternary complex with AP-1, leading to promotion of extracellular matrix breakdown through transcriptional activation of different genes (Yang, Hauser et al. 1996; Wasylyk, Bradford et al. 1997); phosphorylation of ESE1 increases the stability of ESE1, which enhances its transformation potency (Manavathi, Rayala et al. 2007); phosphorylation and sumoylation of TEL are important for TEL-mediated functions and TEL localization (Wood, Irvin et al. 2003; Maki, Arai et al. 2004). Lastly, acetylation of multiple relevant acetylation sites in the C-terminus of the fusion protein EWS-FLI1 increases its binding ability, protein stability, and transcriptional potency, showing that also acetylation can regulate ETS proteins functions (Schlottmann, Erkizan et al. 2012).

Furthermore, different ETS proteins also have distinct spatial and temporal expression patterns. Some ETS, such as ETS1, TEL, or TCF members, are ubiquitously expressed (Nakayama, Ito et al. 2001; Okuducu, Zils et al. 2006; Ghosh, Basu et al. 2012; Kar and Gutierrez-Hartmann 2013), while some, such as ETS2, ERG, ESE1, and others, are expressed in a tissue-specific manner (Vlaeminck-Guillem, Carrere et al. 2000; Xu, Dwyer et al. 2008). In addition, different ETS have different transcriptional activity. Although most ETS proteins have been shown to be

transcriptional activators, a considerable number has been shown to be repressors, while several family members have been shown to display both repressive and activating capabilities. Lastly, cooperation with co-activator or co-repressor proteins is also crucial for regulating transcription in a specific manner that inhibits promiscuous binding (Sharrocks 2001).

ETS transcription factors play crucial roles in the regulation of a variety of cellular functions including cell growth (Sakurai, Yamada et al. 2003), cell development (Maroulakou and Bowe 2000; Ciau-Uitz, Wang et al. 2013), cell differentiation (Kurpios, MacNeil et al. 2009; Kanaya, Hase et al. 2012), cell proliferation, apoptosis (Oikawa, Yamada et al. 1999; Tamir, Howard et al. 1999; Teruyama, Abe et al. 2001; Birdsey, Dryden et al. 2008; Wu, Zhang et al. 2013), and oncogenic transformation (Wasylyk, Hagman et al. 1998; Oikawa and Yamada 2003; Holterman, Franovic et al. 2010; Chen, Chi et al. 2013) (Figure 6).

They control the expression of many cell type-specific growth factors, growth factor receptors, and integrin families involved in cellular proliferation. Moreover, signalling by the growth factors and their receptors finally modulates the functional activities of several ETS proteins via MAP kinase, Jak/Stat signalling, and others. For example, expression of the HGF (hepatocyte growth factor) receptor, encoded by the c-*met* gene, is up-regulated by ETS1 and c-*met* activation, by HGF, induces c-*ets-1* transcription via a Ras-MAP kinase signalling pathway, indicating that ETS1 acts both upstream and downstream of c-*met* (Gambarotta, Boccaccio et al. 1996; Paumelle, Tulasne et al. 2002).

It has been shown that ETS proteins are involved in the apoptotic process. Some ETS prevent apoptosis, while some directly induce the expression of apoptosis-related genes and so promote apoptosis under certain conditions. Expression levels, cellular contexts, and other factors influence the capability of an ETS transcription factor to prevent or induce apoptotic cell death. For example, ETS1 and ETS2 have been reported to be pro-apoptotic as well as anti-apoptotic in some cases (Wei,

Srinivasan et al. 2009). Furthermore, some ETS members take part in lineage development and cell differentiation. Several ETS proteins are preferentially expressed in certain lineages of hematopoietic cells, and also play important roles in their development, commitment and differentiation. TEL is essential for embryonic angiogenesis in the yolk sac, where the common precursors of vascular and hematopoietic lineages are present, and, by controlling the bone marrow microenvironment, also essential in adult hematopoiesis (Wang, Kuo et al. 1997). PU.1 levels are critical in the decision to induce myeloid or lymphoid differentiation; high levels promote macrophage differentiation, while low levels induce B-cell fate (DeKoter and Singh 2000). FLI1 appears to be essential for the development and differentiation of megakaryocytes (Hart, Melet et al. 2000; Starck, Weiss-Gayet et al. 2010) and, together with ETS1, PU.1, and GATA1, is involved in erythropoiesis (Clausen, Athanasiou et al. 1997; Athanasiou, Mavrothalassitis et al. 2000; Liew, Rand et al. 2006). Several ETS members, such as ERG, TEL, ETS1, and others, play important roles in vascular development and angiogenesis (Randi, Sperone et al. 2009; Heo, Choi et al. 2010). Members of the PEA3 subfamily and other ETS proteins appear to be involved in the development of the central and peripheral nervous system (Lin, Saito et al. 1998; Arber, Ladle et al. 2000). Also, it has been reported that overexpression of PEA3 accelerates myogenic differentiation (Taylor, Dupont-Versteegden et al. 1997) and that other ETS members, such as ETS1, ETS2 and PU.1, are involved in osteogenic differentiation (Raouf and Seth 2000).

Since proteins of the ETS family control such a large number of cellular processes it is not surprising that their aberrant expression contributes to malignant transformation and tumor progression.

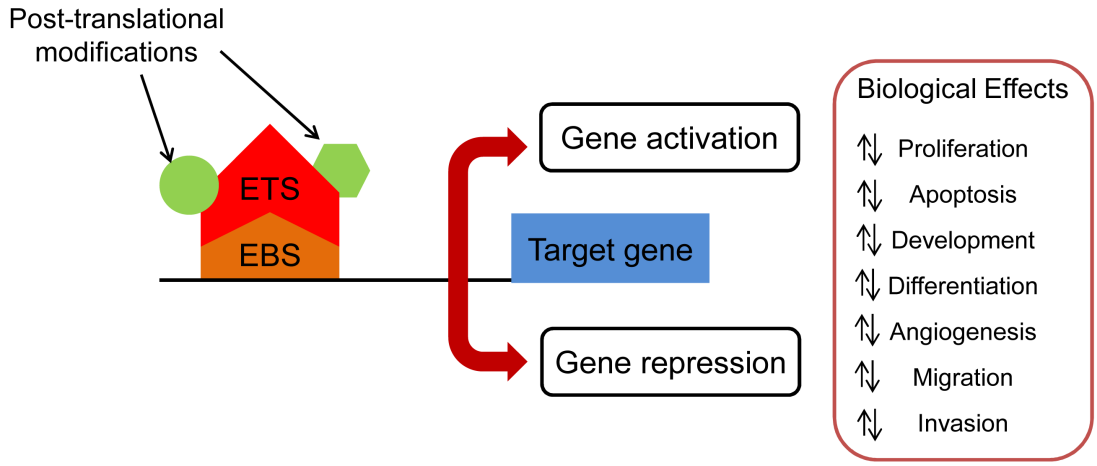

Figure 6. **ETS functions.** ETS factors regulate the expression of a myriad of genes. Acting as activator or repressor of target genes, they can affect many cellular processes.

ETS factors and prostate cancer

Aberrant expression of ETS proteins has been documented in various types of human malignancy, including PCa, where they have been found to be frequently deregulated. Recent analysis of microarray datasets from primary PCa and normal prostate clinical samples, performed in our laboratory, showed that several ETS genes, particularly ERG, ESE3, and ESE1, were differentially expressed in tumor samples compared with normal prostate (Kunderfranco, Mello-Grand et al. 2010). Using specific criteria, our lab identified three major tumor subgroups characterized by the predominant deregulation of an ETS factor: 1) tumors with high ERG expression (ERG^{high}); 2) tumors with high ESE1 expression ($ESE1^{high}$); and 3) tumors with low ESE3 expression ($ESE3^{low}$). A fourth group (NoETS) included tumors that had normal-like levels of all ETS. Previous studies in our laboratory indicated that the expression of epithelial-specific ETS factor ESE3 is frequently reduced at the RNA and protein level in clinical samples of prostate cancer compared with normal prostate. Half of the PCa samples had an almost complete loss of ESE3 expression (≥ 80 % reduction), while about 80% of them had at least a 2-fold reduction of ESE3 compared with normal prostate (Cangemi, Mensah et al. 2008). In PC3 and Du145 prostate cancer cells, ESE3 is silenced by methylation of an evolutionarily conserved

CpG site in its promoter; however, after 5-aza-2'-deoxycytidine treatment its expression is restored. Methylation of this site is inversely correlated with ESE3 expression in a prostate epithelial cell transformation model, occurring only in Ras-transformed and tumorigenic cells and not in normal, immortalized cells. This evidence suggests that ESE3 silencing is functionally linked to oncogenic transformation. Moreover, ESE3 plays an important role in apoptosis, directly binding to the caspase-3 promoter and increasing its expression. Lastly, re-expression of ESE3 in prostate cancer cells inhibits clonogenic survival and induces apoptotic cell death, consistent with the tumor suppressor role of this protein (Cangemi, Mensah et al. 2008). Decreased expression of ESE3 may result in loss of important regulatory mechanisms in prostate epithelial cells, and contribute to the pathogenesis of prostate cancer (Cangemi, Mensah et al. 2008). Furthermore, we demonstrated in a recent paper that ESE3 controls prostate epithelial cell differentiation and stem-like potential by regulating the expression of key epithelial-to-mesenchymal transition and cancer stem cell genes. Collectively, these findings define a key role for ESE3 in the development of a subset of prostate tumors (Albino, Longoni et al. 2012).

Other ETS transcription factors are frequently overexpressed in human PCa (Table 2). ETS1 has been reported to be overexpressed in latent and clinically manifest carcinomas, and a strong expression of ETS1 has been associated with poor tumor differentiation (Alipov, Nakayama et al. 2005). Moreover, evidence of the importance of ETS1 in the development and progression of the disease has been provided (Shaikhibrahim and Wernert 2012). ETS2 is overexpressed in high Gleason-score primary and metastatic prostate cancer. Interfering with ETS2 expression or activity has a negative impact on cell proliferation and survival (Sementchenko, Schweinfest et al. 1998; Carbone, McGuffie et al. 2004). Not only are ETS transcription factors involved in promoting prostate oncogenesis, but some ETS members, as mentioned previously in relation to ESE3, can function as a negative regulator of carcinogenesis. PDEF is another ETS protein with a critical role in

regulating genes involved in cell motility, invasion, and adhesion of epithelial cells, including prostate cancer cells. Indeed, inhibition of PDEF expression triggers a transcriptional program of genes involved in migration, invasion, adhesion, and epithelial de-differentiation (Gu, Zerbini et al. 2007).

Table 2. **Summary of ETS factors involved in prostate tumorigenesis.**

ETS member	Mechanism of tumorigenesis in PCa
ERG	Overexpression of TMPRSS2-ERG fusion and androgen dependent robust activation of ERG target genes (Tomlins, Rhodes et al. 2005).
ESE1	Overexpression in both primary and metastatic cancers; association with inflammatory pathways (Longoni, Sarti et al. 2013).
ETS1	Overexpression and association with poor tumor differentiation (Alipov, Nakayama et al. 2005). Important role in transformation and progression (Shaikhibrahim and Wernert 2012).
ETS2	Overexpression in metastatic prostate cancers. Involved in cell proliferation and survival (Sementchenko, Schweinfest et al. 1998; Carbone, McGuffie et al. 2004).
ESE3	Its loss increases cell survival and supports epithelial-to-mesenchymal transition (Cangemi, Mensah et al. 2008; Albino, Longoni et al. 2012).
PDEF	Its loss is linked to epithelial de-differentiation and increases cells capability to migrate and invade (Gu, Zerbini et al. 2007).

Generally, ETS proteins are aberrantly expressed owing to increased transcriptional activity or chromosomal rearrangements such as gene amplification or translocations. Amplification of ETS genes is not a dominant mechanism in driving cancer. To date, in leukemia and lymphoma, only few cases involving ETS1, ETS2, and ETV6 have been identified (Baldus, Liyanarachchi et al. 2004; Chae, Kim et al. 2010; Garcia, Arancibia et al. 2013). By contrast, malignant cellular transformation occurs often via chromosomal translocations, resulting in ETS gene fusions and abnormal regulation of gene expression.

ETS gene fusions frequently happen in human leukemia. The ETS member TEL is involved in more than 40 different translocations in human hematological cancers, where its PNT domain, ETS domain, or both, are fused in-frame with partners such as AML1 (Romana, Mauchauffe et al. 1995) and EVI1 (Peeters,

Wlodarska et al. 1997), as well as with tyrosine kinases such as PDGFβR (Golub, Barker et al. 1994), TRKc (Eguchi, Eguchi-Ishimae et al. 1999), ABL (Papadopoulos, Ridge et al. 1995; Golub, Goga et al. 1996), and JAK2 (Lacronique, Boureux et al. 1997). This fusion generally leads to oligomerization of the PNT domain of TEL, which is necessary for the constitutive activation of the tyrosine kinase, and resultant transformation and pathogenesis. In Ewing's sarcoma, a childhood cancer of the soft tissue, the ETS gene FLI1 translocates from its original position of 11q22 to chromosome 22, producing transcripts derived from the fusion of the amino-terminal region of the EWS gene with the carboxyl-terminal DNA binding domain of the FLI1 itself (Riggi and Stamenkovic 2007). Upon fusion, EWS-FLI1 becomes a more potent transactivator than FLI1 itself, and many targets of EWS-FLI1, both direct and indirect, have been found to be involved in EWS tumor maintenance. It has also been shown that the amino-terminal domain of EWS gene can become fused to the C-terminal domains of several members of the ETS family of transcription factors, including ERG, ETV1, ETV4, and FEV (Janknecht 2005).

Recurrent chromosomal aberrations were thought to be prevalent and primarily characteristic of leukemias, lymphomas, and sarcomas. Now, however, owing to the finding of recurrent translocations involving ETS genes, ETS transcription factors have emerged as significant elements in prostate tumorigenesis. Important studies have identified chromosomal rearrangements that activate members of the ETS family, such as ERG, ETV1, ETV5, and ETV4 in the majority of prostate carcinomas (Tomlins, Rhodes et al. 2005; Iljin, Wolf et al. 2006; Mehra, Tomlins et al. 2007; Mosquera, Perner et al. 2007; Tomlins, Laxman et al. 2007; Hu, Dobi et al. 2008; Rouzier, Haudebourg et al. 2008). In 2005, through a simple, statistical approach termed "cancer outlier profile analysis" (COPA), Tomlins et al identified and described a small number of fusion transcripts, specific to PCa, that were the consequence of a chromosomal rearrangement involving the androgen responsive 5' elements of the TMPRSS2 gene (which codes the androgen-regulated

trans-membrane protease, serine 2) and some ETS genes (Tomlins, Rhodes et al. 2005). Gene fusions of the 5'-untranslated region (UTR) of TMPRSS2 (21q22.3) with the ETS members ERG (21q22.2), ETV1 (7p21.2), ETV5 (3q28), and ETV4 (17q21), provide a mechanism for robust, androgen-mediated induction of specific ETS factors, which in turn activates multiple ETS responsive genes with roles in PCa development. While the TMPRSS2-ERG fusions are the most predominant in prostate cancer, fusion genes involving ETV1, ETV4, and ETV5 constitute approximately 1-10% of cases (Shaikhibrahim, Lindstrot et al. 2011; Shaikhibrahim and Wernert 2012). Gene fusions are found in the majority of prostate tumors, but the role that these fusions play in the development and progression of PCa is far less understood.

ERG

The ETS transcription factor ERG (E-twenty-six related gene) is coded by the ERG gene, whose transcription produces at least five proteins, ERG-1/p41, ERG-2/p52, ERG-3 /p55, ERG-4/p49, and ERG-5/p38 as a result of a combination of alternative mRNA splicing, alternative polyadenylation or differential initiation codon (Owczarek, Portbury et al. 2004). The longest variant, termed ERG-3 or p55, has been chosen as the "canonical" variant and is 486 amino acids in length. By comparison, the ERG-2/p52 isoform lacks a short segment of 24 amino acids in the central portion of the protein upstream of the ETS domain, while the ERG-1/p41 variant lacks both the 24-amino acid segment and a portion of around 100 amino acids at the beginning of the amino-terminal region. While all the ERG isoforms can bind the ETS binding site in a specific manner, acting as transcriptional regulators, it is still not known whether these transcripts have different functions *in vivo*.

As previously mentioned, the ETS family of transcription factors, to which ERG belongs, is essential for numerous cell processes, including normal hemato-

poiesis and immune development. ERG, together with FLI1 and ETS1, is initially expressed in the blood island of the yolk sac where the common precursors of vascular and hematopoietic lineages (hemangioblasts) are present (Maroulakou and Bowe 2000). In particular, it is a critical regulator of adult hematopoietic stem cells (HSC) and is essential for maintaining self-renewal at times of high HSC cycling during stress hematopoiesis (Ng, Loughran et al. 2011). Moreover, ERG regulates multiple endothelial functions, playing a central role in endothelial biology. It is the most abundantly expressed ETS factor in resting endothelial cells and its expression, although not uniquely endothelial, is restricted mostly to the hematopoietic-endothelial lineage. This ETS factor drives the expression of genes strictly related to the endothelial lineage and angiogenesis, such as endoglin, the von Willebrand factor, ICAM-2, and VE-Cadherin (Randi, Sperone et al. 2009), and is also essential for endothelial homeostasis and differentiation (McLaughlin, Ludbrook et al. 2001). During embryonic development, ERG gene expression predominates in mesodermal tissues, and is particularly associated with endothelium and cartilage, where it seems to have a specific function in the regulation of endothelial and chondrocyte genes (Vlaeminck-Guillem, Carrere et al. 2000). ERG is also a key regulator of vascular development and angiogenesis (Birdsey, Dryden et al. 2008). In fact, several ERG target genes have been implicated in angiogenesis, including the ERG-dependent expression of VE-Cadherin which is essential for endothelial junctional stability and endothelial survival (Birdsey, Dryden et al. 2008), both critical processes in angiogenesis. It has been currently published that ERG expression is required for embryogenesis and vascular integrity, providing clear evidences for ERG as an essential regulator of endothelial cell development (Han, Pacifici et al. 2015). A recent study has also shown that ERG can regulate endothelial cell motility and migration by driving HDAC6 expression, and regulating tubulin acetylation and actin localization (Birdsey, Dryden et al. 2012), thereby supporting the role of ERG as a master regulator of endothelial biology.

Although many of the pathways through which ERG exerts its roles are still to be defined, in recent years it has become clear that the aberrant expression of ERG can produce profound phenotypes, indicating that a change in ERG activity can have a tremendous impact. Overexpression of the ERG gene product, located on chromosome 21, has been implicated in the myeloproliferative disorders frequently seen in Down Syndrome patients (Ng, Hyland et al. 2010); it has also been shown that ERG has a dedifferentiating effect (Tsuzuki, Taguchi et al. 2011), and confers greater invasiveness to cell lines (Klezovitch, Risk et al. 2008; Zong, Xin et al. 2009). Furthermore, the aberrant expression of ERG increases cell migration and resistance to anoikis of prostate cancer cell lines (Kunderfranco, Mello-Grand et al. 2010). Analysis of PCa transcriptomes has revealed that ERG mRNA is overexpressed in approximately two-thirds of patients with prostate tumor, and that the molecular mechanism which leads to aberrant ERG expression can be attributed to a chromosomal rearrangement that results in fusion of the 5'- end of a prostate-specific, androgen-responsive, transmembrane serine protease gene (TMPRSS2) to ERG (Tomlins, Rhodes et al. 2005; Rosen, Sesterhenn et al. 2012).

While, as previously stated, TMPRSS2-ERG fusion has been identified in approximately 50% of prostate tumors, it has been observed in more than 90% of prostate tumors with ETS-family gene rearrangements. The high prevalence of this rearrangement suggests that this region is a hot spot for chromosomal rearrangements in PCa. Seventeen different types of TMPRSS2-ERG fusion transcripts involving various regions of the TMPRSS2 and ERG genes have been identified in human prostate tumors (Figure 7) (Clark, Merson et al. 2007). Eight of these transcripts are unlikely to encode functional ERG proteins owing to the introduction of premature stop codons. The remaining 9 predicted functional TMPRSS2-ERG fusion transcripts form truncated ERG proteins: 2 encode normal ERG proteins, 6 encode for amino-

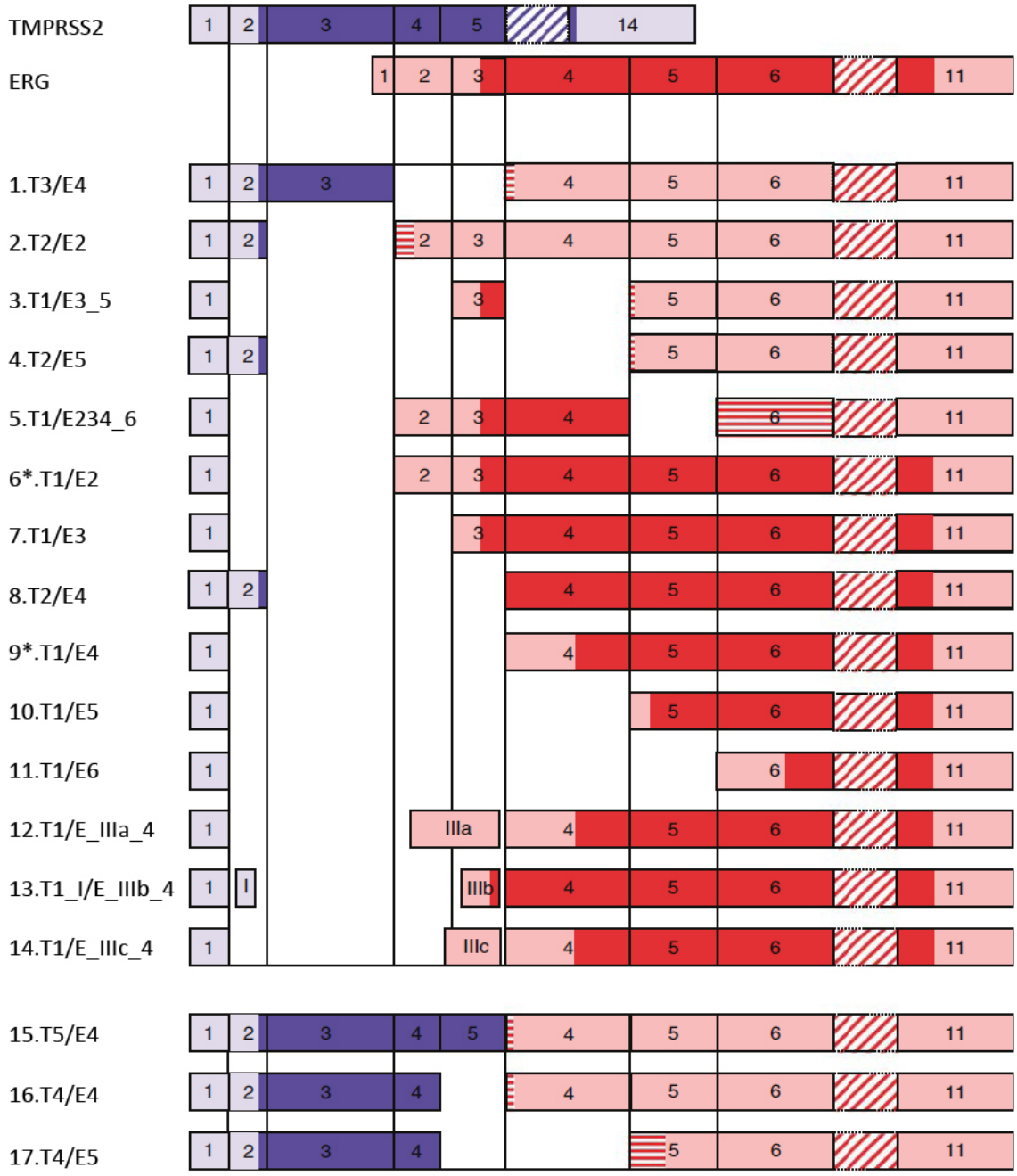

Figure 7. **Structure of TMPRSS2-ERG hybrid transcripts.** Sequences derived from TMPRSS2 are shown in blue, while those derived from ERG are shown in red. Light colours represent untranslated regions. Transcripts 6 and 9 (highlighted by *) are the same as those detected by *Tomlins et al.* (2005). Modified by *Clark et al., 2007.*

terminal truncated ERG proteins, and 1 encodes for a bona fide TMPRSS2-ERG fusion protein (Clark, Merson et al. 2007). Since the C-terminal region of ERG contains the ETS binding domain and the transactivation domain, it is likely that in the TMPRSS2-ERG fusion the biological functions of DNA binding and protein-protein

interactions via the ETS domain remain intact. For this reason, it is possible that differrent ERG fusion isoforms have similar biological functions to their wild-type counterparts. The 5′ region of the TMPRSS2 gene included in the fusion transcripts are generally non-coding and are usually not translated into protein product. However, there are several transcript variants that result in both TMPRSS2 and ERG exons being translated into protein. The fusion transcripts TMPRSS2 exon 1 fused to ERG exon 4 (previously reported by Tomlins et al., 2005) or ERG exon 5 (designated T1/E4 and T1/E5, respectively, in figure 7) are the most frequently expressed type of TMPRSS2-ERG fusion. Alternative splicing of transcripts encoded by a single ERG gene fusion has also been reported to occur in acute myelogenous leukemia (AML), where, in individual AML patients, expression of three alternatively spliced FUS-ERG transcripts is observed, but only one transcript type encodes a functional protein (Ichikawa, Shimizu et al. 1994; Kong, Ida et al. 1997). These studies demonstrate that the expression of multiple fusion mRNAs is common, and for this reason the alternative splicing of the TMPRSS2-ERG gene is proposed as the most likely basis for the multiple different types of fusion mRNAs observed (Figure 7). Since this discovery, there has been considerable interest in understanding the mechanism by which the TMPRSS2-ERG fusion may promote progression to PCa. In 2008, Tomlins et al tried to determine functional roles for TMPRSS2-ERG fusion in prostate cancer, taking advantage of a model of transgenic mice expressing the truncated ERG product under the control of a probasin promoter, which drives androgen-regulated transgene expression exclusively in the prostate. They noticed that although ERG induces a neoplastic phenotype in the mouse prostate (mPIN), thus providing support for an oncogenic role in human prostate cancer, it is not sufficient for the development of prostate cancer in mice. Their *in vitro* studies also showed that, while the TMPRSS2-ERG fusion product markedly increases invasion, it is unable to transform benign prostatic epithelial cell lines. Both of these results, however, are consistent with the occurrence of TMPRSS2–ERG fusion in the context

of pre-existing genetic lesions during the course of human prostate cancer development (Tomlins, Laxman et al. 2008).

In understanding the interplay between TMPRSS2-ERG activation, PIN, and prostate cancer oncogenesis, the role of PTEN seems crucial. PTEN is among the most commonly mutated tumor suppressor genes in human cancer, and, like many other tumor suppressors, targets proteins in signalling pathways that regulate cell growth and survival, and contributes to cancer when lost or inactivated. In PCa, it seems that a substantial proportion of both PIN and prostate cancer lesions contain abnormalities of PTEN (Yoshimoto, Cutz et al. 2006), suggesting that PTEN and its downstream target Akt may play an important role in early human PCa.

In 2009, two important studies drew attention to a close collaboration between ETS transcription factors and PTEN tumor suppressor (Carver, Tran et al. 2009; King, Xu et al. 2009) (Figure 8). Both studies were started based on evidence that TMPRSS2-ERG alone is insufficient to initiate prostate neoplasia, and that cooperating oncogenic lesions are required. King et al examined a cohort of ERG rearrangement positive and negative human prostate tumors for associated PTEN copy number loss or MYC amplification as measured by high-resolution array-based comparative genome hybridization (aCGH), and found that tumors with PTEN loss were highly enriched for ERG rearrangement, while MYC amplification was not associated with ERG rearrangement. Furthermore, when they crossed TMPRSS2-ERG mice with PTEN haploinsufficient mice, all of the mice (8/8) showed PIN development by six months of age. Comparable results were obtained by Carver et al. They analysed 40 prostate cancer specimens for ERG genetic rearrangements and PTEN protein expression in consecutive sections from a tumor tissue microarray, and, notably, 14 of the 15 ERG FISH-positive samples had reduced or absent PTEN expression, highlighting that PTEN loss and ERG genetic rearrangement are concomitant events. They then wanted to determine whether aberrant prostatic expression of ERG would cooperate with PTEN loss to promote PCa development

and progression in mice. For this purpose, they generated PTEN haploinsufficient mice expressing ERG under the control of the probasin promoter. At approximately two months of age, these mice developed high-grade prostatic intraepithelial neoplasia (HGPIN) and multifocal invasive adenocarcinoma, together with a reduction in cancer latency, by six months of age. Conversely, control PTEN heterozygous mice developed HGPIN at approximately eight months of age and did not develop adenocarcinoma. Moreover, PTEN and AKT/pAKT levels in the two genotypes were similar, proving that prostate-specific overexpression of ERG does not directly affect PTEN levels. Collectively, these data demonstrate that ERG gene rearrangement cooperates with PTEN loss, leading to the progression of HGPIN to invasive adenocarcinoma and indicating that PTEN loss could function as a "second hit" in TMPRSS2-ERG fusion positive prostate cancer. This observation was also supported by tissue recombinant studies, where ERG overexpression in combination with either PTEN knockdown or expression of constitutively activated AKT resulted in the development of adenocarcinoma (Zong, Xin et al. 2009). Other studies have investigated the biological effects of ERG knocking down ERG expression in TMPRSS2-ERG fusion positive VCaP cell xenograft model systems (Sun, Dobi et al. 2008; Tomlins, Laxman et al. 2008; Wang and Jiang 2008). These showed that ERG depletion in VCaP prostate cancer cells inhibits cell growth, cell invasion and xenograft tumor growth.

In order to better understand how ERG promotes PCa progression, it is also necessary to take into consideration the molecular cross-talk between ERG and others important components, like the AR or transcriptional co-repressors associated with malignancies such as histone deacetylases (HDACs) and histone methyl-transferase (HMTs) commonly overexpressed in PCa (Varambally, Dhanasekaran et al. 2002; Weichert, Roske et al. 2008) (Figure 9).

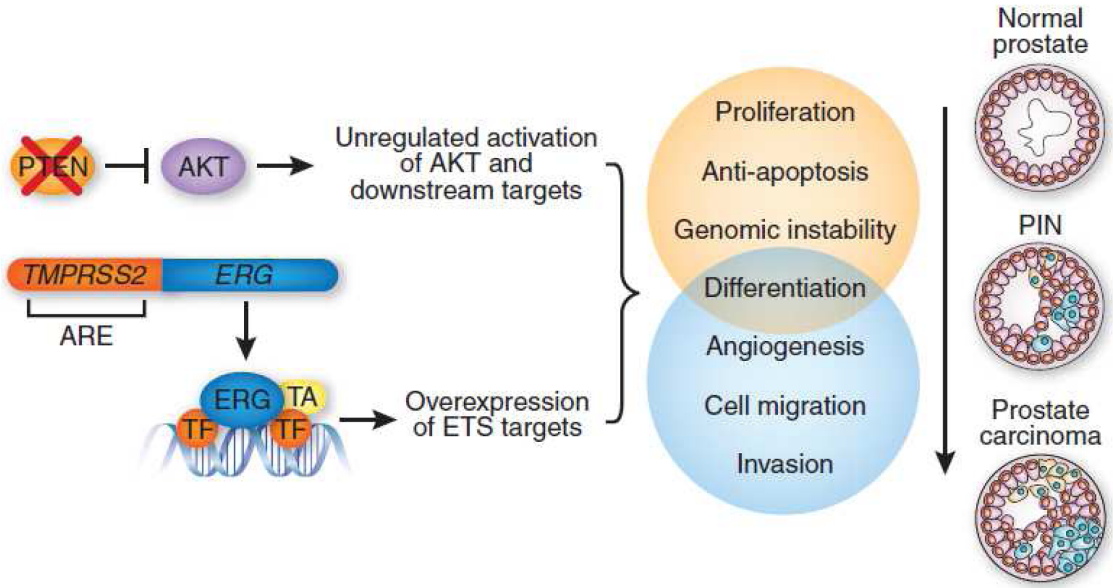

Figure 8. **PTEN loss and TMPRSS2-ERG collaboration.** Loss of PTEN with concomitant activation of AKT could act in partnership with the TMPRSS2-ERG translocation, promoting prostate cancer progression through downstream pathways that increase the selective advantage. ARE. androgen responsive element; TA, transcriptional activator; TF, transcription factor. Taken from *Squire, 2009.*

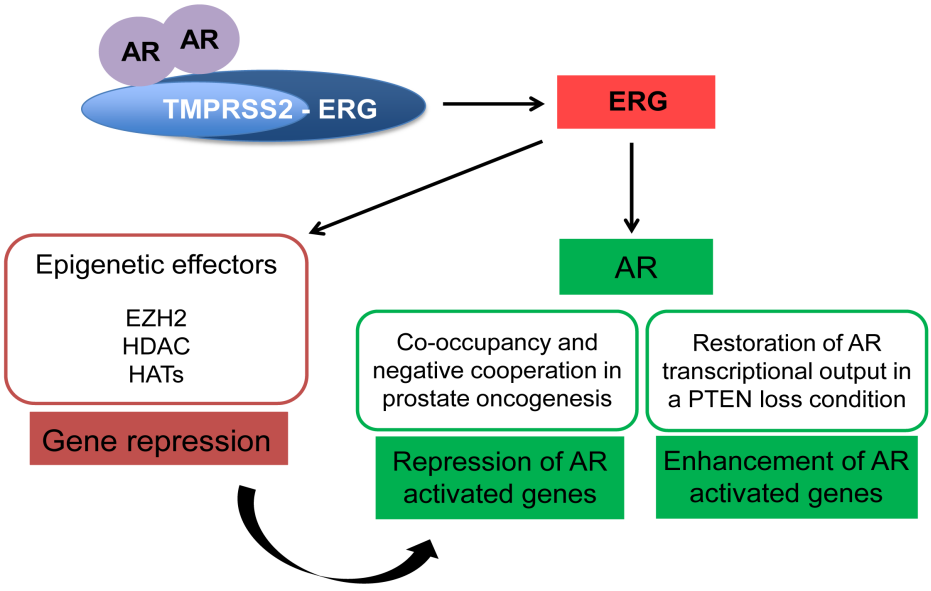

Figure 9. **ERG activation and molecular cross-talks.** TMPRSS2-ERG fusion leads to androgen-dependent robust induction of ERG protein. ERG regulates the expression of several target genes including some encoding for epigenetic effectors and associated to gene repression. ERG can also interplay with the androgen receptor (AR). On one hand, ERG co-occupies a majority of AR target genes and antagonises its normal activity, recruiting EZH2 or other epigenetic effectors to mediate the inhibition of androgen-dependent transcription. On the other hand, ERG expression can enhance AR transcriptional activity, in a context of PTEN deficiency.

Although the AR has a critical role in PCa progression, the detailed mechanism of attenuation and functional consequences associated with AR and ERG transcriptional cross-talk are currently still unclear. ChIP-Seq analysis of ERG, both in cell lines and tumor samples that overexpress this transcription factor, identified a striking level of co-occupancy (44%) with the androgen receptor (Yu, Mani et al. 2010; Chng, Chang et al. 2012). The involvement of the AR in normal prostate development, coupled with the prevalence of ETS-binding sequences at AR-bound regions, implies a cooperative interaction that could play a role in ETS-mediated prostate oncogenesis. Co-immunoprecipitation assays revealed an endogenous, DNA-independent interaction between AR and ERG proteins in cell lines as well as in prostate cancer tissues, involving the ETS domain of the ERG protein (Yu, Mani et al. 2010). Expression studies indicate that a potential mechanism of oncogenic ERG protein at these sites is to antagonise or enhance AR normal function (Yu, Mani et al. 2010; Chng, Chang et al. 2012; Chen, Chi et al. 2013) (Figure 9). ERG overexpression significantly decreases AR transcript in multiple prostate cell lines; concordantly, ERG depletion in VCaP cells leads to AR up-regulation, further supporting an inhibitory role of ERG on the AR gene (Yu, Mani et al. 2010). Besides directly regulating AR itself, ERG is recruited to a majority of AR target genes at gene-specific loci, repressing androgen regulation of a lineage-specific differentiation program. Results obtained by Yu et al and Chng et al suggest that the antagonist effect of ERG on AR transcriptional activity could in part be attributed to the reduction of AR recruitment to its cis-regulatory elements by ERG. Moreover, EZH2 and also HDACs are recruited to AR and ERG co-localized sites, and cooperate with ERG in mediating the inhibition of androgen-dependent transcription. Indeed, some studies show that the Polycomb member EZH2 is significantly up-regulated in ERG^{high} tumors compared with both normal prostate and NoETS tumors, and that ERG acts as a transcriptional activator of EZH2 by binding to its promoter, thereby demonstrating a direct link between EZH2 and ERG expression (Kunderfranco,

Mello-Grand et al. 2010; Yu, Mani et al. 2010). Furthermore, ERG binds to the promoter of a number of previously reported EZH2 target genes, suggesting an ERG-direct regulation of EZH2-mediated epigenetic silencing, and an EZH2 contribution in repressing AR target genes. Even though different studies show that ERG suppresses AR function, in a recent study Chen et al maintain that a robust ERG-mediated transcriptional activity, observed only in the setting of PTEN loss, can restore AR transcriptional output, and induce the up-regulation of genes involved in cell death, migration, inflammation, and angiogenesis (Chen, Chi et al. 2013). Generating a conditional mouse model with the TMPRSS2-ERG transgene crossed with Pb-Cre4 mice, that express ERG specifically in the prostate, they confirm that ERG alone, even in the context of robust, high-level protein expression, is insufficient to cause prostate cancer. Significantly, however, when combined with homozygous PTEN loss, the mice develop accelerated, highly penetrant invasive adenocarcinoma. Examining the genome-wide localization of AR by ChIP-Seq, they found a marked increase in the number of AR peaks in ERG mice compared with wild-type, without there being any changes in the amount of AR protein or circulating testosterone. Moreover, ERG expression had no significant effect on AR target genes in PTEN intact mice, but significantly restored AR transcriptional output in the setting of PTEN loss, where AR-regulated genes were generally decreased in expression. More important, they also found that transcriptome changes induced by ERG were greatly amplified in magnitude by PTEN loss. Since they obtained similar results for ETV1, they concluded that overexpression of ETS transcription factors mediate context-dependent oncogenic transformation by influencing AR transcriptome and priming the prostate epithelium to cooperate with aberrant upstream signalling in prostate oncogenesis.

3. Epigenetics and Prostate cancer

As in many other human cancers, PCa development and progression are driven by an interplay of genetic and epigenetic changes. Indeed, as previously described, PCa is characterized by recurrent chromosomal changes, such as gains, losses, and translocations. Furthermore, epigenetic alterations are also believed to represent important contributing factors in prostate carcinogenesis, and may also provide useful biomarkers for disease progression. In fact, a view is emerging that epigenetic disruption of progenitor cells may be an initial step in cancer development, leading to a polyclonal precursor population within which subsequent genetic and epigenetic events may occur (Cooper and Foster 2009).

The term "epigenetic" refers to mechanisms of inherited change of gene expression that do not involve changes in DNA sequence or copy number (Cooper and Foster 2009). There are two main types of epigenetic aberration. The first type concerns DNA methylation, during which DNA methyltransferases (DNMTs) catalyse the addition of a methyl group to the 5'-carbon of cytosine in CpG sequences. DNA methylation aberrations can occur as either hypo- or hypermethylation. Both forms can lead to chromosomal instability and transcriptional gene silencing, and both have been implicated in a variety of human malignancies, including PCa (Baylin, Makos et al. 1991). The second type of aberration involves chromatin structure. In eukaryotes, DNA is packaged into repeating units of nucleosomes by folding itself around histone complexes. The nucleosomes in turn are packed into higher-order structures to allow chromatin compaction, which provides an essential mechanism adopted by mammalian cells to control gene expression (Strahl and Allis 2000). The local structure of chromatin can heavily influence the degree to which a gene can be transcribed, since it determines how accessible the gene is to the transcriptional machinery. Over the years, it has become apparent that histones are one of the key determinants of local chromatin structure,

which is not only affected by histone presence, but also more importantly by covalent post-translational modifications to histone tails (Yang and Yu 2013). The N-terminal tails of histones, positioned peripheral to the nucleosome core, are subject to various covalent modifications, such as acetylation, methylation, phosphorylation, ubiquitination, and sumoylation by specific chromatin-modifying enzymes. The pattern of these modifications has been referred to as "the histone code", and acts as a second layer of epigenetic regulation of gene expression affecting chromatin structure and remodelling (Jenuwein and Allis 2001). Histone modifications can lead to either repression or activation, depending upon which residues are modified and the type of modifications present (Sharma, Kelly et al. 2010). Overall, histone modifications impact on chromatin conformation and consequently influence gene transcription, DNA repair, DNA replication, and cell cycle checkpoints (Sawan, Vaissiere et al. 2008). Acetylation and deacetylation of histone tails are catalysed by histone acetyltransferases (HATs) and deacetylases (HDACs), respectively. Histone acetyltransferases have been shown to increase the activity of several transcription factors, including nuclear hormone receptors such as AR, by inducing histone acetylation, which facilitates promoter access to the transcriptional machinery (Welsbie, Xu et al. 2009). Conversely, HDACs reduce levels of histone acetylation, and are associated with transcriptional repression. Another well-studied histone modification concerns histone methylation. Different from the lysine acetylation mentioned above, lysine methylation leads to transcriptional activation or repression, depending on which residue is modified, and density of methylation (Sharma, Kelly et al. 2010). For example, histone H3 methylation has been observed at multiple lysine sites, including H3K4, K9, K27, and K36, and the addition of up to three methyl groups at each lysine produces a total of four methylation states: unmethylated, monomethylated, dimethylated and trimethylated. Histone methylation is now considered a reversible process: histone methyltransferase (HMTs) are respon-

sible for adding the methyl group, whereas histone demethylases (HDMs) remove it. Methylation of the histone tails could also take place on the arginine residues.

The most important difference between genetic and epigenetic alterations is that epigenetic changes are potentially reversible. In fact, using specific inhibitors that target enzymes such as DNMTs, HMTs, and HDACs, it is possible to re-establish the original situation, whereas it is very difficult to restore the exact sequence when the DNA sequence is altered by mutations. Chromatin remodelling mechanisms have emerged as a major event, showing alterations among human cancers; the de-regulation of proteins involved in chromatin regulation can affect genome-wide control of gene expression and play key roles in DNA repair and genome maintenance. Since epigenetic alterations are common in human cancers, and also play a key role in tumor progression, a better understanding of epigenetic alterations can help the process of drug design and discovery for cancer treatment.

The most remarkable epigenetic change in PCa concerns DNA methylation. Overall, more than 50 genes have been reported to be hyper-methylated in PCa, and whereas hyper-methylation of specific genes is evidently associated with an early phase of prostate tumor development, global DNA hypo-methylation is related to progression (Schulz and Hoffmann 2009). In addition, prostate tumors exhibit global changes in chromatin structure and histone modifications owing to the altered expression of specific chromatin-modifying enzymes. For instance, it has been reported that in metastatic prostate cancers, the H3K27 methyltrasferase Enhancer of zeste homolog 2 (EZH2) and the corresponding demethylase JMJD3 are overexpressed (Xiang, Zhu et al. 2007). Likewise, overexpression of the histone deacetylase HDAC1 is regularly found in prostate tumors harbouring the major TMPRSS2-ERG fusion (Iljin, Wolf et al. 2006; Setlur, Mertz et al. 2008). Over the past two decades, it has been discovered that a wide spectrum of epigenetic aberrations in PCa is connected to EZH2 dysregulation. Indeed, post-translational histone modifications, including EZH2-induced histone methylation, are a category of

epigenetic events that play a crucial role in PCa pathogenesis. Perturbations in histone modifications can heavily impact chromatin structure and genome stability, resulting in inappropriate gene expression or silencing, which can lead to cellular transformation (Sparmann and van Lohuizen 2006). In addition, EZH2 can directly interact with several DNMTs, so that also DNA methylation is an event closely linked to EZH2 activity (Vire, Brenner et al. 2006).

EZH2 is a histone methyltransferase responsible for one of the key modifications associated with prostate carcinogenesis (Figure 10). It is the catalytic subunit of the Polycomb repressive complex 2 (PRC2), a well-known repressive complex that leads to target gene silencing by promoting the trimethylation of lysine residue 27 of histone H3 (H3K27me3) (Figure 11). Generally, polycomb group proteins (PcG) are involved in the maintenance of the gene expression pattern of different cells set during early development, by modifying chromatin structure. They play key roles in developmental patterning, X-chromosome inactivation, and stem cell maintenance (Plath, Fang et al. 2003; Lee, Jenner et al. 2006; Shen, Kim et al. 2009). In mammals, there are two main polycomb group complexes: PRC1 and PRC2.

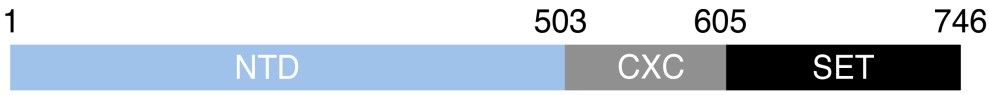

Figure 10. **EZH2 structure.** Boxes identify the main domain of EZH2: the cysteine-rich CXC domain; the catalytic SET domain; and the N-terminal domain (NTD) which provides binding sites for several interactors.

The human PRC2 complex includes five subunits: EZH2, EED (ectoderm development protein), SUZ12 (suppressor of zeste 12 homolog), RbAp46/48 (retinoblastoma-associated protein 46/48), and AEBP2 (Adipocyte enhancer-binding protein 2). EZH2, via the SET domain, is responsible for catalysing H3K27me3, and silencing tumor suppressor genes (Sauvageau and Sauvageau 2010).

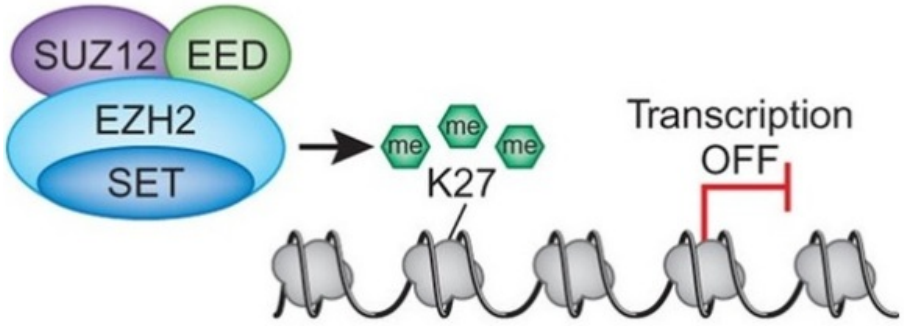

Figure 11. **EZH2 activity.** EZH2 normally trimethylates histone H3 at lysine 27 (H3K27) by its catalytic SET domain to inhibit gene expression. Taken from *Martinez-Garcia andLicht, 2010*.

EZH2 levels are abnormally elevated in cancer tissues compared with corresponding normal tissues, and hyperactivation of EZH2, either by over-expression or mutations, is found in a variety of malignancies that include prostate, breast, bladder, ovarian, gastric, melanoma, lung, and lymphoma (Shen, Cui et al. 2013). EZH2 was first found to be associated with PCa in 2002 by a cDNA microarray study, which demonstrated its up-regulation in metastatic prostate cancer (Varambally, Dhanasekaran et al. 2002). In this report, EZH2 was highlighted as the most significantly up-regulated gene when comparing metastatic cancer with localized cancer. In addition, through tissue microarray analysis of prostate samples, they also identified a positive relationship between EZH2 protein levels and disease aggressiveness. Several follow-up studies further confirmed that expression of EZH2 shows a correlated pattern with the stage of development of PCa (Berezovska, Glinskii et al. 2006; Saramaki, Tammela et al. 2006). In addition, EZH2 is over-expressed in localized cancers with a higher risk of recurrence after radical prostatectomy, suggesting that EZH2 overexpression could be a valuable prognostic indicator of patient out-come (Varambally, Dhanasekaran et al. 2002). Similarly, overexpression of EZH2 was also found in invasive and metastatic breast cancer, where increased levels of the protein is a strong indicator of poor clinical outcome (Kleer, Cao et al. 2003). For these reasons, EZH2 can serve as a useful biomarker for

diagnostic and prognostic purposes. Interestingly, in contrast to the overexpression pattern of EZH2 in solid tumor cancer, EZH2 aberrations manifest themselves in the form of point mutations in lymphoma and myeloid neoplasms, suggesting that EZH2 mutations exist in a cancer type-specific manner (Yang and Yu 2013). It has been reported that EZH2 harbours various heterozygous mutations at tyrosine 641 (Y641) in the C-terminal SET domain (Figure 10). In contrast to the wild-type, which has a substrate preference for unmethylated H3K27 and monomethylated H3K27me1, the Y641 mutants have enhanced catalytic efficiency for dimethylated H3K27me2. Thus, both the wild-type and the Y641 mutants can work together to increase the levels of H3K27me3 (Sneeringer, Scott et al. 2010; Yap, Chu et al. 2011).

Analysis of patient samples significantly correlate elevated EZH2 expression with increased proliferation, invasiveness, and metastasis of PCa. It has been reported that EZH2 is significantly enhanced in tumors with a high Gleason score and PSA recurrence (van Leenders, Dukers et al. 2007), and that endogenous down-regulation of EZH2 reduces proliferation and invasion in prostate cancer cells (Bryant, Cross et al. 2007). Moreover, it has emerged that EZH2 has a role in promoting metastasis formation by repressing the expression of different metallo-proteinase inhibitors in prostate cancer cells (Shin and Kim 2012). Currently, EZH2 is believed to function predominantly as a transcriptional repressor; to carry out this role, it usually cooperates with other epigenetic silencing enzymes. Several studies have shown that EZH2 physically and functionally interacts with DNMTs (Vire, Brenner et al. 2006) and HDACs (van der Vlag and Otte 1999; Tie, Furuyama et al. 2001), suggesting that there is a potential interplay between these different classes of epigenetic modulation enzymes in the control of gene expression, resulting in the conversion of the target genes into a more deeply silenced chromatin state (Figure 12).

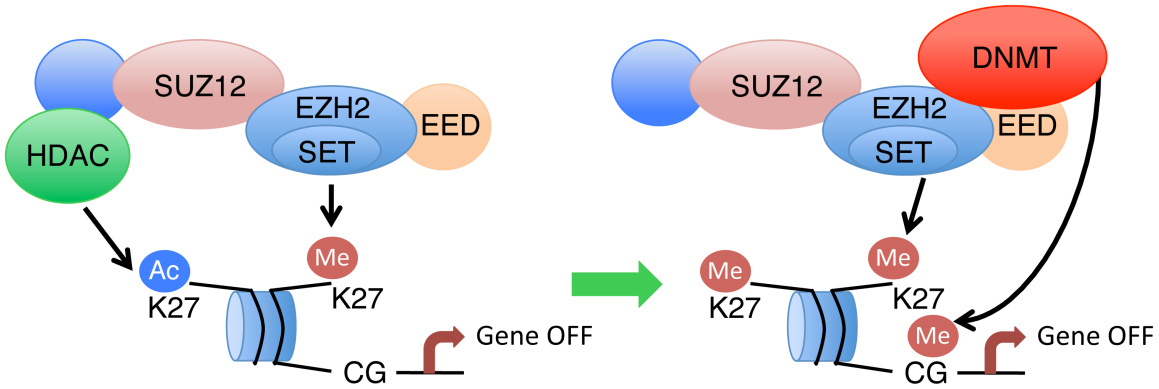

Figure 12. **Cooperation between different epigenetic silencing enzymes.** Schematic model showing the interplay between EZH2, histone deacetylase (HDAC) and DNA methyltransferase (DNMT). Target genes are silenced through the methylation of lysine 27 (K27) by the PRC2. If K27 is pre-acetylated, HDAC may first deacetylates it, increasing the silenced chromatin state. Moreover, DNMTs may also be recruited by PRC2. Methylation of CpG DNA of target genes makes the chromatin state more deeply silenced. Ac=acetylation; Me=methylation. Modified by *Tan et al., 2014*.

Functional links between EZH2, HDACs, and DNMTs have been found in colon-, prostate-, liver-, lung-, ovarian-, and breast tumors, and all three types of epigenetic silencing machinery may contribute to the control of abnormal gene expression in cancer cells (Simon and Lange 2008). EZH2 itself is also tightly regulated and controlled at the transcriptional, post-transcriptional, as well as post-translational levels (Yang and Yu 2013) (Figure 13). Indeed, phosphorylation of different EZH2 residues can heavily affect its activity. It has been reported that EZH2 can be phosphorylated at serine 21 by activated AKT and that this modification leads to suppression of EZH2 methyltransferase activity by impeding EZH2 binding to histone H3, which in turn results in a decrease of lysine 27 trimethylation and derepression of silenced genes (Cha, Zhou et al. 2005). Also phosphorylation of threonine 345 and 487 by the cyclin-dependent kinase 1 (CDK1) and 2 (CDK2) are determining factors for EZH2 activity. Phosphorylation of T345 is important for the recruitment of EZH2 to the promoter of its target genes, and blockage of its phosphorylation diminishes the oncogenic activity of EZH2 (Zeng, Chen et al. 2011); phosphorylation of T487 seems to promote dissociation of EZH2 from SUZ12 and EED, leading to suppression of H3K27 trimethylation and consequent derepression

of target gene expression (Wei, Chen et al. 2011). Lastly, phosphorylation at tyrosine 641 (Y641) by JAK2 promotes EZH2 degradation (Sahasrabuddhe, Chen et al. 2015).

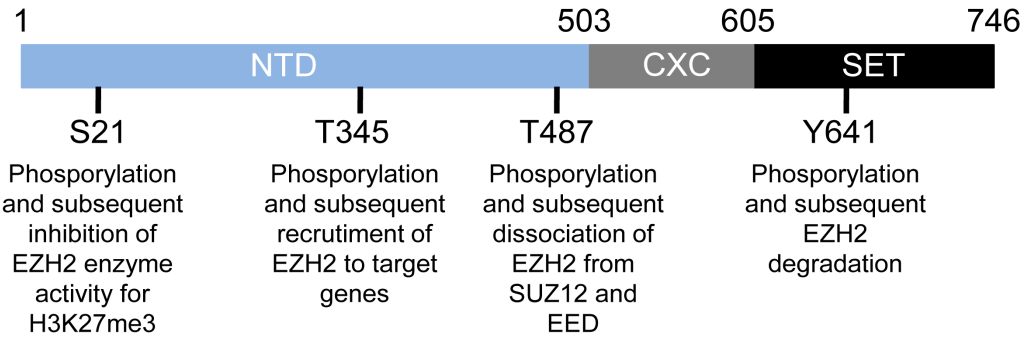

Figure 13. **Post-translational modifications of EZH2.** EZH2 could be phosphorylated at serine 21 (S21), at threonine 345 (T345) and 487 (T487) in the N-terminal domain, and at tyrosine 641 (Y641) in the SET domain.

In addition to its role as a transcriptional repressor, a novel role for EZH2 has recently emerged, that of acting as a transcriptional activator of target genes (Shi, Liang et al. 2007; Lee, Li et al. 2011; Xu, Wu et al. 2012). The first to posit EZH2 as a transcriptional activator in breast cancer cells were Shi et al. in 2007. They demonstrated that EZH2 physically interacts with estrogen receptor α (ER) and β-catenin (thereby connecting the estrogen and Wnt signalling circuitries), functionally enhances gene transactivation by estrogen and Wnt pathways and phenotypically promotes cell cycle progression. In 2011, Lee et al confirmed the role of EZH2 as a dual function transcription regulator in breast cancer, demonstrating its ability to act either as a transcriptional activator or repressor of NF-κB target genes (Figure 14). In ER-negative breast cancer, overexpressed EZH2 forms a complex with RelA and RelB molecules to confer constitutive activation of NF-κB target genes expression without requiring other PRC2 subunits. By contrast, in ER-positive breast cancer cells, where RelB expression is repressed, ER recruits EZH2 as a member of the PRC2 to NF-κB target gene promoters, and functions as a canonical epigenetic repressor.

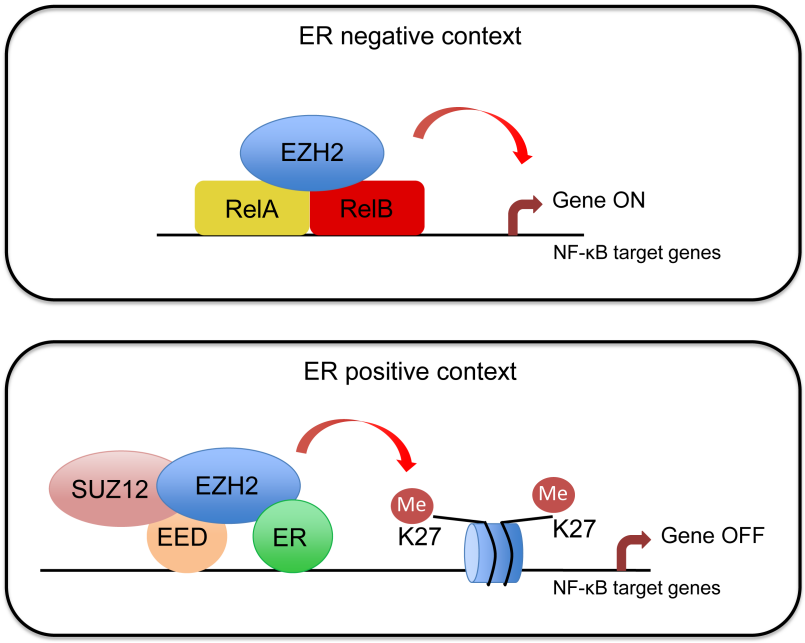

Figure 14. **Context-dependent roles of EZH2.** In ER-negative basal-like breast cancer cells, EZH2 interacts with and acts as a co-activator of RelA and RelB to promote the expression of NF-κB target genes (upper figure). In ER-positive breast cancer cells, ER recruits EZH2 as a member of the PRC2 to the promoter of the NF-κB target genes, leading to epigenetic silencing of those genes (lower figure). Modified by *Lee et al, 2011.*

The differential expression of ER and RelB in the two contexts can be crucial for switching the role of EZH2 in regulating NF-κB target genes expression. Considering this model, they state that EZH2 could function in both canonical and non-canonical manners to repress or activate NF-κB target gene expression in a context-dependent, specific mode (Lee, Li et al. 2011) (Figure 14). Recently, Xu et al reported that EZH2 plays an important role in castration-resistant PCa, and that its oncogenic function depends not on silencing but on transcriptional induction of its target genes (Xu, Wu et al. 2012). They identified a subset of EZH2 PRC2-independent sites that lack nearby H3K27me3, which they called EZH2 "solo" peaks, suggesting that in androgen-independent cells, EZH2 gains a unique set of chromatin binding sites that lack the characteristic EZH2 mark. In addition, they identified a significant enrichment of AR binding motif at EZH2 solo peaks, and a robust physical interaction between AR and EZH2. Since phosphorylation of EZH2 alters its enzymatic activity, they examined the phosphorylation status of EZH2. They demonstrated that

phosphorylation of EZH2 at serine 21, mediated directly or indirectly by the PI3K-AKT pathway, can switch its function from a Polycomb repressor to a transcriptional co-activator of AR and potentially other factors (Figure 15).

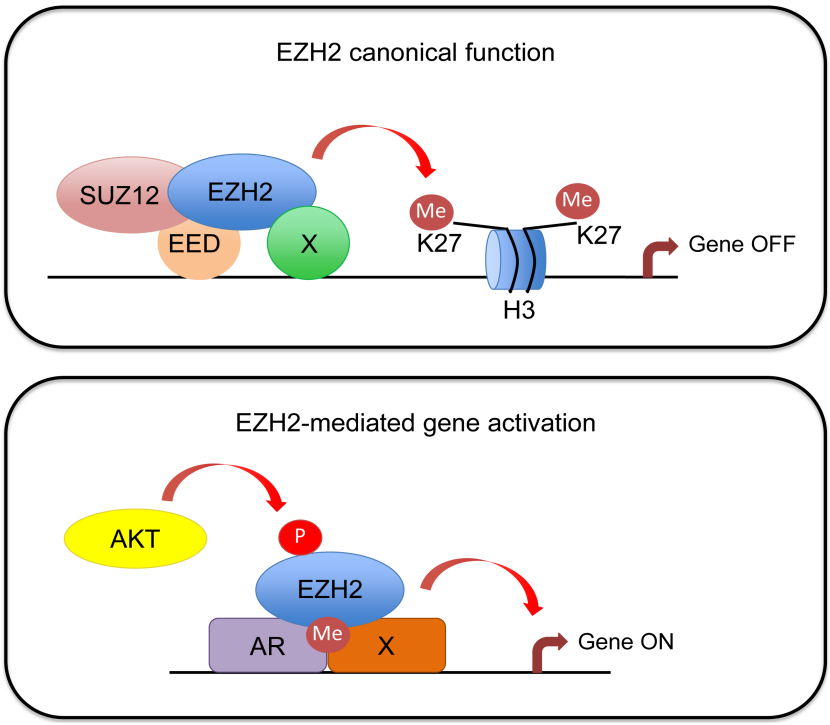

Figure 15. **Molecular mechanism of action of EZH2.** Polycomb dependent mechanism (*upper figure*): EZH2 functions as a part of PRC2, mediating transcriptional repression. When recruited by DNA-binding proteins (X) to the target gene promoters, it catalyses the trimethylation of Histone H3 at lysine 27, resulting in chromatin compaction and gene silencing. Polycomb independent mechanism (*lower figure*): AKT mediated phosphorylation of EZH2 at serine 21 decreases the H3K27me3 activity of EZH2. Phosphorylated EZH2 can function independently of other PRC2 proteins and may methylate androgen receptor (AR) or other proteins enhancing their transcriptional activity. Modified by *Deb, Thankur and Gupta, 2013*.

Moreover, recent studies have underlined a new mechanism of EZH2-mediated methylation of non-histone proteins, which can regulate different processes. It has been reported that EZH2 can monomethylate the lysine on a RKS histone-like sequence on RORα transcription factor, leading to its subsequent ubiquitination and degradation (Lee, Lee et al. 2012). The transcription factor GATA4 is another EZH2 non-histone target. He et al demonstrated that EZH2 binds to and methylates GATA4, attenuating its transcriptional activity by reducing its interaction

with, and acetylation by, p300 (He, Shen et al. 2012). However, it seems that EZH2-mediated methylation does not exclusively lead to degradation or repression. Indeed, it has been shown that EZH2 binds to, and methylates, also the STAT3 transcription factor; in this case, STAT3 methylation enhances its activity and is also a critical modification that leads to STAT3 activation (Kim, Kim et al. 2013) (Figure 16).

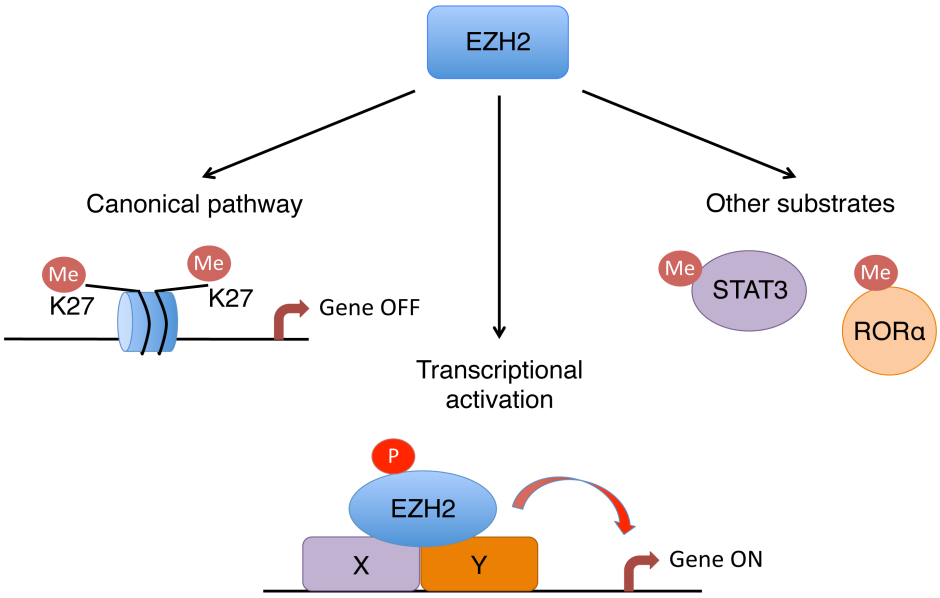

Figure 16. **Various functions of EZH2 in human cancer.** EZH2 function as transcriptional repressor together with other PRC2 components; EZH2 can act as transcriptional activator independent of PRC2; EZH2 can also methylate substrates other than histone H3 such as transcription factors. Modified by *Yamaguchi and Hung, 2014.*

Considering the number of processes in which EZH2 is involved, and also the importance that its activity plays in tumor progression and metastasis spread, inhibiting EZH2 activity might be a promising and appealing anti-cancer therapy. Indeed, over the past few years, several potent inhibitors of EZH2 have been discovered. Among these inhibitors, 3-deazaneplanocin A (DZNep), an S-adenosyl-homocysteine (SAH) hydrolase inhibitor, can induce apoptosis in breast and colon cancer cells, inducing EZH2 depletion and the associated H3K27me3 (Tan, Yang et

al. 2007). DZNep interferes with SAM and SAH metabolism, and can indirectly inhibit the methylation reaction (Figure 17). In fact, DZNep treatment was shown to result in reactivation of EZH2 repressed target genes, inhibited cell growth, and reduced tumor formation in various cancers (Piunti and Pasini 2011). Moreover, it has minimal toxicity *in vivo* when used as an antiviral compound in Ebola virus infected mice (Bray, Driscoll et al. 2000), and together with its importance in cancer epigenetic pathways, may be a promising drug candidate for anti-cancer treatment. Recently, McCabe et al discovered a potent, highly selective, S-adenosylmethionine-competitive, small molecule inhibitor called GSK126. This compound can effectively inhibit proliferation of EZH2 mutant diffuse large B-cell lymphoma cell lines, and significantly inhibits the growth of EZH2 mutant diffuse large B-cell lymphoma xenografts in mice (McCabe, Graves et al. 2012).

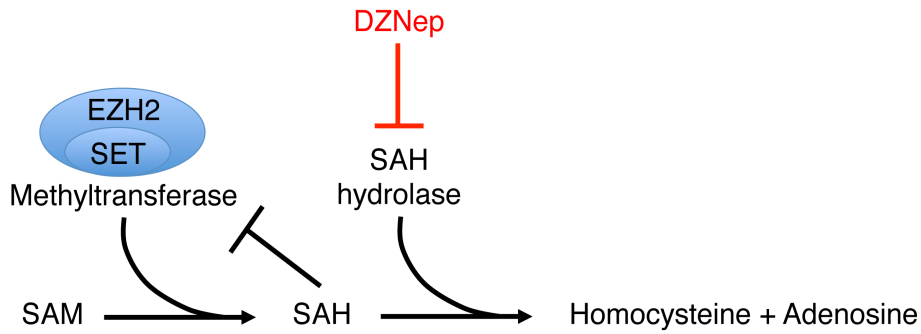

Figure 17. **Mechanism of action of DZNep.** S-adenosylmethionine (SAM) is the methyl donor for methylation reactions. SAM is metabolized to S-adenosylhomocysteine (SAH) by methyltransferases. SAH is then converted into homocysteine and adenosine by SAH hydrolase. DZNep inhibits SAH hydrolase, causing an increase in SAH levels, which in turn inhibits the methyltransferases like EZH2. Adapted from *Miranda et al, 2009*.

Since PCa has been regarded as a model of "epigenetic catastrophe" (Yegnasubramanian, Kowalski et al. 2004), it is an ideal system in which epigenetic drugs could be studied. Among the enzymes that can serve as molecular targets for anti-cancer therapy, EZH2 holds great promise for effectively inducing apoptotic cell death when its activity is abolished in prostate cancer cells. Although there has been progress in generating EZH2 inhibitors for the use of cancer treatment, a deeper

understanding of the multifaceted biological roles of EZH2 is still needed, in order to facilitate the development of pharmacological agents with maximal efficacy and minimal toxicity. Thus, it is believed that EZH2 is an encouraging candidate for molecular targeting in PCa treatment, and representing as it does an innovative approach to combating the disease through epigenetic mechanisms.

Aim of the work

ETS transcription factors constitute a family of signal-dependent transcriptional regulators with important roles in cell proliferation, differentiation and carcinogenesis. The TMPRSS2-ERG gene fusion is found in about half of prostate tumors and represents one of the most frequent genetic rearrangements in human cancers. As a result of that gene fusion, a mechanism for overexpression of the ETS transcription factor ERG is provided. Although that overexpression can produce profound phenotype, the biological role of the aberrant expression of ERG in initiation and progression of prostate cancer is still unclear. Even if it is emerging that ERG requires additional cooperating factors to fully exert its oncogenic role, the molecular details of these interactions are not yet well defined. For this reason, interactors, cross-talks and cooperation between multiple signalling pathways, which might be involved in the progression of ERG-positive tumors need to be identified. Another important protein often overexpressed in human prostate cancers, and associated with tumor progression, is the catalytic subunit of the Polycomb repressive complex 2, Enhancer of zest homolog 2 (EZH2). We and others revealed the presence of a cross-talk between ETS transcription factors and epigenetic effectors and found that altered expression of ERG lead to the induction of EZH2, which in turn mediated epigenetic silencing of several genes. The novel notion about PRC2-independent functions of EZH2, and its ability to interact with and methylate also non-histone proteins, encouraged further studies on these proteins in order to verify a possible direct link between ERG and EZH2. Not less important, EZH2 is a promising candidate for molecular targeting in PCa, combating the disease through epigenetic mechanisms. Accordingly, the overall goal of this project was to evaluate a possible molecular interaction between ERG and EZH2 in prostate cancer cells, and how EZH2 could influence ERG oncogenic activity. Identifying a mechanism of ERG-induced oncogenesis involving EZH2 could have a relevant impact on the clinical management of prostate cancer, and might provide the rationale for a possible epigenetic therapy in ERG-positive prostate cancer.

Material and Methods

Cell Cultures, Cell Transfection, Selection of Stable Cell lines and Drugs

RWPE1, VCaP, LNCaP, PC3, and NCI-H660 were obtained from American Type Culture Collection and maintained in Keratinocyte serum-free growth medium (Gibco) supplemented with human recombinant Epidermal Growth Factor (rEGF) and Bovine Pituitary Extract (BPE) (RWPE1), DMEM (VCaP) or RPMI-1640 (all others) supplemented with 10% fetal bovine serum (FBS), according to the provider's instructions. RWPE1 are ERG-negative normal prostate epithelial cells. VCaP cells are ERG translocation positive, AR-positive and androgen dependent. LNCaP cells are ERG-negative, AR-positive, androgen-dependent and carry the ETV1 gene translocation (Table 3).

Table 3:
Characteristics of the different cell lines used.

Name	Origin	Tumorigenic	Comments
RWPE1	Human prostate normal epithelial cells	No	AR positive Androgen sensitive ERG negative
VCaP	Human prostate carcinoma established from vertebral bone metastasis	Yes	AR positive Androgen sensitive TMPRSS2-ERG (T1/E4) translocation positive
LNCaP	Human prostate carcinoma established from left supraclavicular lymph node metastasis	Yes	AR positive Androgen sensitive ETV1 translocation positive ERG negative
PC3	Human prostate carcinoma established from bone marrow metastasis	Yes	AR negative Androgen independent ERG negative
NCI-H660	Extrapulmonary small cell carcinoma originating from the prostate gland, established from a lymph node metastasis	Yes	AR negative PTEN null TMPRSS2-ERG translocation positive Androgen independent

LNCaP with stable expression of ERG were generated as previously described (Kunderfranco, Mello-Grand et al. 2010). LNCaP with stable expression of ERG-K362A were generated by transfection of the pCEFL-ha-ERG3-K362A expressing vector using JetPRIME reagent (Polyplus-transfection SA) and selection in G418. Control cells were obtained by transfection with pcDNA3.1 and selection in G418. In both cases, G418 resistant cells were expanded, and expression of ERG-K362A was determined by qRT-PCR and Western blotting. VCaP with stable PTEN depletion were generated by viral infection of control (EV) and PTEN shRNAs (shPTEN) (Sigma), and subsequent selection with puromycin. PTEN down-regulation was evaluated by qRT-PCR and Western blotting. For transient gene knockdown, cells were transfected with siRNAs directed to ERG (Qiagen, Hilden, Germany), EZH2 (Ambion-life Technologies), SUZ12 (Ambion-life Technologies), PTEN (Ambion-life Technologies) or a control siRNA, directed to the firefly luciferase gene, siGL3 (Ambion-life Technologies). Sequences of all siRNAs used are shown in Table 4. Cells were plated in six-well plates and transfected with 100 nM of siRNA using Lipofectamine 2000 (Invitrogen) and were harvested after 48h. PC3 cells were transiently transfected with different ERG and EZH2 expression constructs using JetPRIME reagent (Polyplus-transfection SA). The following constructs were used: pCEFL-ha-ERG3 (kindly provided by S. Izraeli), pcDNA3-myc-EZH2 (kindly provided by Jer-Tsong Hsieh) and pCDNA3-myc-EZH2-ΔSET (kindly provided by TaI-Lung Cha). ERG mutated or truncated constructs (i.e., ha-ΔC-ERG3, ha-P-I-ERG3, ha-P-ERG3, ha-N-ERG3, his-ΔN-ERG3, ERG-K362A) and EZH2 truncated constructs (i.e., EZH2-ΔCXC and EZH2-1-340) were generated as described below.

When indicated, cells were treated with DZNep (Cayman Chemical) and MK-2206 (Selleckchem, Life Technologies) at indicated concentrations and times.

Table 4:
Small interfering RNAs used in knockdown experiments.

siGL3	5′ CUUACGCUGAGUACUUCGAtt 3′ 5′ UCGAAGUACUCAGCGUAAGtt 3′
Negative Control (NC) for DLA	Catalog n. 4611 (Ambion)
siERG	Catalog n. SI03089443 (Qiagen)
siEZH2	5′ CAAAGAAUCUAGCAUCAUAtt 3′ 5′ UAUGAUGCUAGAUUCUUUGtt 3′
siSUZ12	5′ GGAUGUAAGUUGUCCAAUAtt 3′ 5′UAUUGGACAACUUACAUCCtt 3′
siPTEN	5′ GCAUACGAUUUUAAGCGGAtt 3′ 5′ UCCGCUUAAAAUCGUAUGCag 3′
shPTEN	Clone ID:NM_000314.4-2996s21c1 (Sigma)

Generation of mutated constructs

To generate ERG mutated constructs (i.e., ha-ΔC-ERG3, ha-P-I-ERG3, ha-P-ERG3, ha-N-ERG3, his-ΔN-ERG3, ERG-K362A) and EZH2 mutated constructs (i.e., EZH2-ΔCXC, and EZH2-1-340) Quik Change Site-Directed Mutagenesis Kit from Stratagene was used using pCEFL-ha-ERG3 or pcDNA3-myc-EZH2 expressing vectors as templates, respectively. All obtained constructs were sequenced to verify the inserted mutation. Mutagenesis primers are reported in Table 5.

Protein analysis and antibodies

Cell lysates were prepared lysing cells in RIPA lysis buffer (50 mM Tris-HCl pH 7.4; 150 mM NaCl; 1 mM EDTA; 1% NP-40; 0.25% sodium deoxycholate; 4 mM sodium orthovanadate; 1 mM PMSF; 1 mM sodium fluoride) with complete mini-EDTA protease inhibitor cocktail (Roche) and phosphatase inhibitor cocktail (PhosStop, Roche) for 30 minutes on ice. Proteins were quantified using BCA protein assay (Pierce) according to the manufacturer's instructions. 40-60 μg of proteins were resolved on 10% SDS PAGE and analysed by Western blot using enhanced

chemiluminescence system (Amersham-Pharmacia). Membranes were probed with antibodies against ERG (sc-353 Santa Cruz Biotechnology Inc.), EZH2 (BD Biosciences), PTEN (#9552 Cell Signalling Technology Inc.), p-AKT (Ser473 #4051 Cell Signalling Technology Inc.), total AKT (#9272 Cell Signalling Technology Inc.), HA-probe (F7, Santa Cruz), Histidine (anti-polyHistidine, H1029, Sigma Aldrich), c-Myc (BD Biosciences), pan-methylated Lysine (ab23366 Abcam), GAPDH (Millipore MAB374) and α-TUBULIN (Calbiochem). The anti-methyl-ERG (anti-mERG) antibody (affinity purified rabbit polyclonal, AbMart) was custom-made and generated using a lysine (K362) mono-methylated ERG peptide. Specificity of the antibody was determined by peptide competition assay, as described below.

Peptide competition assay

Three identical lysates of VCaP cells were run on a gel. Prior to immunoblotting, 8 μg of the mERG antibody were incubated 1 hour at room temperature with 5 fold excess (40 μg) of peptide. A methylated (M-peptide) and unmethylated (C-peptide) competitor peptides, corresponding to the epitope recognized by the antibody, were used in parallel. The antibody that was bound to the M-peptide (blocking peptide) could no longer bind to the epitope present in the protein on the Western blot (neutralized antibody). After membrane blocking, samples were separately incubated over-night at 4°C with the antibody not pre-incubated, with the neutralized antibody and lastly with the non-neutralized antibody. The signals obtained with the antibody alone represent the maximum signal, while the signals which disappear with the blocked antibody are specific to the antibody.

RNA analysis

Total RNA was extracted using Trizol (Invitrogen) and Direct-zol RNA-MiniPrep kit (Zymo Research). All RNA samples were treated with DNase to remove any contaminant genomic DNA. Quantitative real-time RT-PCR (qRT-PCR) was performed using 20 ng of RNA as template for SYBR Green RT-PCR one-step qRT-PCR kit (Qiagen) on the ABI 7000 machine (Applied Biosystems). Samples were analysed in triplicate. The level of each gene was calculated by comparing the Ct value in the samples to a standard curve generated from serially diluted RNA from a reference sample and normalizing it to the amount of β-actin as previously described (Cangemi et al., 2008). Next, the relative quantities were normalized to the control samples (siGL3, NC, pcDNA or DMSO). Sequences of all PCR primer sets used in the study are shown in Table 5.

Chromatin Immunoprecipitation (ChIP) and ChIP-reChIP

Cells were collected and exposed to formaldehyde (37%) to cross-link protein-DNA complexes, and processed as previously described (Cangemi, Mensah et al. 2008). After sonication, chromatin extracts were immunoprecipitated with antibodies against ERG (sc-354 X, Santa Cruz Biotechnology Inc.), EZH2 (AC22, Active Motif), acetylated histone H3 (Active Motif), tri-methylated histone H3 at lysine 27 (H3K27me3) (Upstate Biotechnology), SUZ12 (Active Motif), and IgG (Millipore) as control.

For ChIP-reChIP experiments, cells were treated and processed as for a normal chromatin immunoprecipitation. Before the second round of immunoprecipitation, washed beads were eluted with 10 mM DTT at 37°C for 30 minutes. Subsequently, the second round of immunoprecipitation was carried out as described above. To determine the amount of immunoprecipitated DNA, quantitative real-time PCR was performed using KAPA SYBR Fast qPCR kit (KAPA

Biosystems) on the ABI 7000 machine (Applied Boiosystems) and primers spanning the region of interest (Table 5). The amount of immunoprecipitated DNA was calculated in reference to a standard curve and normalized to Input DNA (Cangemi, Mensah et al. 2008). When ChIP was performed in ERG overexpressing cells or upon siRNAs mediated knockdown, the amount of DNA was normalized to the control sample, represented as 1. All experiments were repeated at least three times and representative results are shown.

Table 5:
Primer sets used for qRT-PCR, ChIP and mutagenesis.

Gene ID	Assay	Forward (FWD) and reverse (REV) primer sequences
IL-6	qRT-PCR	FWD: CCACACAGACAGCCACTCAC
IL-6	qRT-PCR	REV: TTTCAGCCATCTTTGGAAGG
NKX 3.1	qRT-PCR	FWD: AGAAAGGCACTTGGGGTCTT
NKX 3.1	qRT-PCR	REV: TCCTCTCCAACTCGATCACC
ARID2	qRT-PCR	FWD: GAAGGAGCTGGATCTTCACG
ARID2	qRT-PCR	REV: AAGCAAAGGCAGCGTTAGAA
BMI1	qRT-PCR	FWD: TTCTTTGACCAGAACAGATTGG
BMI1	qRT-PCR	REV: GCATCACAGTCATTGCTGCT
CADPS	qRT-PCR	FWD: CCGAATGGATAAGCCTCAAA
CADPS	qRT-PCR	REV: ATAACTGCACATGGCAAACG
CTNNA1	qRT-PCR	FWD: CATGTTTTGGCTGCATCTGT
CTNNA1	qRT-PCR	REV: CAGCAGCCTTCATCAAATCA
DAAM1	qRT-PCR	FWD: TGCACTTCCAGCTGAGAAAA
DAAM1	qRT-PCR	REV: TCAGTGCTGTCTTTAAACTCTCT
MAT2A	qRT-PCR	FWD: AGGGATGCCCTAAAGGAGAA
MAT2A	qRT-PCR	REV: ATTTTGCGTCCAGTCAAACC
IL-6 promoter EBS	ChIP	FWD: ACAGCTGGGAAGACGAGAAA
IL-6 promoter EBS	ChIP	REV: GGAAGTTCGTGTTCATGATAAAA
NKX 3.1 promoter EBS	ChIP	FWD: TGCGGATAAAGGAACCACCA
NKX 3.1 promoter EBS	ChIP	REV: AGGCATGACAAGTAGGTGCAGC
NKX 3.1 promoter ARE	ChIP	FWD: TCGCGGTGAGAAAATCAGTGT
NKX 3.1 promoter ARE	ChIP	REV: TGAAAAGCATGCCCTGGTG
ARID2 promoter	ChIP	FWD: ACATCGCCTCCACCCCTA
ARID2 promoter	ChIP	REV: CGGGGAACAATAGACTCGAC

BMI1 promoter	ChIP	FWD: GGCTCGCATTCATTTTCTGC
BMI1 promoter	ChIP	REV: GCCTCGCCTCCTACGTAC
CADPS promoter	ChIP	FWD: CTCCCCAATCGGCAAGAT
CADPS promoter	ChIP	REV: GGCAAGGGGGAGAATCAAT
CTNNA1 promoter	ChIP	FWD: AGAATGACATGGGGAACAGC
CTNNA1 promoter	ChIP	REV: TAAGCACGTGGTGATTCAGG
DAAM1 promoter	ChIP	FWD: ACAAACTAGGTCGGCAGGAA
DAAM1 promoter	ChIP	REV: GGACAGAGAACACACACCCT
MAT2A promoter	ChIP	FWD: TTGGGAATGCACCTTGTTCT
MAT2A promoter	ChIP	REV: ACAAGAACGCCGGGTTTAAT
GAPDH promoter	ChIP	FWD: TCCTCCTGTTTCATCCAAGC
GAPDH promoter	ChIP	REV: TAGTAGCCGGGCCCTACTTT
ΔC-ERG3	Mut.	CGCCTACAAGTTCGACTAACACGGGA TCGCCCAGG (stop codon)
P-I-ERG3	Mut.	CAGGCAGTGGCCAGATCTTAACTTTGG CAGTTCCTCCTGG (stop codon)
P-ERG3	Mut.	CCTCAGAGAGACTCCTCTTCCATAATT GACTTCAGATGATGTTG (stop codon)
N-ERG3	Mut.	GCTACATGGAGGAGAAGCACTAACCA CCCCCAAACATGACC (stop codon)
ERG-K362A	Mut.	CCGGCGCTGGGGAGAGCGGGCGAGC AAACCCAACATG (Alanine instead of lysine)
EZH2-ΔCXC	Mut.	CCGGTTGTGGGCTGCACACTAGAGAA AGATACAGCTG (stop codon)
EZH2-1-340	Mut.	GCTGCTGCTCTCACCGCTTAGCGGATA AAGACCCCACC (stop codon)

Co-immunoprecipitation

Co-immunoprecipitation experiments were performed using Protein G PLUS/Protein A-Agarose mixture (Calbiochem-Millipore) which was incubated with 1-2 μg of anti-HA (F7, Santa Cruz Biotechnology Inc.), anti-ERG (sc-354X, Santa Cruz Biotechnology Inc.), anti-EZH2 (AC22, Active Motif) and anti-MYC (BD Pharmingen) antibodies for 30 minutes at 4°C under rotation. After centrifugation, BSA 0.2% was added to the beads-antibody complex for 30 minutes at 4°C under rotation. Lastly, 100-300 μg of lysates were incubated with the blocked complex for

2h at 4°C under rotation. Precipitates were washed four times with RIPA lysis buffer, resuspended in Loading sample buffer 2X and proteins were resolved on 10% SDS-PAGE and analysed by Western blot. Histidine pull-down was performed using Dynabeads His-Tag Isolation & Pulldown magnetic beads (Invitrogen). The HA and Myc plasmid tags are small peptides which derive from the hemagglutinin protein (HA tag), and c-myc protein (Myc tag). They are little peptides and apparently they did not interfere with the system after transfection.

Dual-Luciferase Reporter Assay

Cells were plated in 48-well plates and 24h later transfected with the pGL3-ETS responsive element (Panomics), pGL3-IL-6 promoter reporter (provided by Stephanie Cabarcas), pGL3-NKX3.1 promoter reporter (provided by J. M. Bentel) along with control empty vector pcDNA3.1 or ERG, ΔN-ERG3, ERG-K362A, EZH2, EZH2-ΔSET expression vectors. Renilla pRLSV40 (Promega) was used as control to monitor transfection efficiency. Luciferase activity was measured after 24h using the Dual-Luciferase Reporter Assay System (Promega) as previously described (Cangemi, Mensah et al. 2008). Data are expressed as Firefly luciferase activity normalized to the Renilla luciferase activity, and then represented as fold change to pcDNA or control, as Relative Luciferase Activity (RLA). Reporter assays were performed in triplicate and repeated in three independent experiments.

Immunofluorescence

Cells were grown on glass cover-slips, fixed with 4% formaldehyde, and permeabilized with Methanol-Acetone 1:1 solution. Next, slides were blocked with BSA 5% for 30 minutes and then incubated with anti-ERG (sc-353 Santa Cruz Biotechnology Inc.), anti-mERG (AbMart), anti-EZH2 (BD Biosciences) antibodies for 1h at room temperature. Next, slides were incubated with anti-rabbit Alexa 594 or

anti-mouse Alexa 488 (Invitrogen) for 1h in the dark. For mERG antibody peptide competition assay, slides were incubated with the M- or C-peptide during the blocking phase with BSA 5%. Pictures were taken with Zeiss Axiovert (40X and 100X objectives) using Axiocam Mrc3 and processing with AxioVision 4.5 (Carl Zeiss AG, Feldbach, Switzerland).

Anoikis and Migration Assay

Cell survival in anchorage-independent conditions (anoikis assay) was assessed by plating 10^4 LNCaP cells in poly-hema coated 96-well plates. Cell viability was measured using a colorimetric assay (MTT, Sigma) and reading absorbance at 570 nm in a microplate reader at indicated time points.

Cell migration was assessed using the scratch wound healing assay (Liang, Park et al. 2007). Cells were grown to confluence in 12-well plates and left over-night in OPTIMEM (Gibco). Then, scratches were performed on the cell monolayer, complete medium was added to the cultures and images were taken at time 0 and 72 h. All assays were performed in triplicates and results were represented as percentage mean ± SD from three independent experiments.

Soft Agar Assay

For soft agar assay, cells were harvested and resuspended in a mixture of 1.8% low-grade agarose and RPMI for each 60 mm dish. Cells (10^4 cells/dish) were seeded on the top of solidified bottom agar, and then incubated at 37°C, 5% CO_2. After 3-4 weeks, colonies were fixed and stained with 0.01% crystal violet in 20% ethanol and counted with an automated colonies counter (ImageJ). The assay was performed in triplicates and results were represented as mean ± SD from three independent experiments. Representative images are shown.

Immunocytochemistry

For immunocytochemistry (ICC), cells were harvested and washed with PBS using centrifugation to remove residual proteins, and then were resuspended in PBS to a final concentration of $5x10^6$ cells/mL. Next, cells were attached to slides using centrifugation method (Thermo Scientific Shandon cytospin Cytocentrifuge) at 800 rpm for 5 minutes. At a later stage, cells were fixed and permeabilized with Methanol-Acetone 1:1 solution. After blocking with 5% BSA, cells were incubated 1 hour at room temperature with anti-pS21 EZH2 antibody (Bethyl Laboratories), followed by a biotinylated secondary antibody (LSAB2-DAKO). Then, streptavidin-HRP (Horseradish peroxidase) conjugate and 3-3'Diaminobenzidine (DAB) chromogen were used to detect the binding. Cell nuclei were counterstained blue by hematoxylin solution, and sections were dehydrated and mounted in a suitable organic mounting medium.

Gene expression profile

RNA was collected from LNCaP with stable expression of wild type ERG (ERG-WT), ERG mutant (ERG-K362A) or empty vector (EV). We performed 8x60k Sure Print G3 Human GE Arrays. RNA was amplified, labelled, and hybridized according to the two-colours microarray-based gene expression analysis protocol (Agilent Technologies). Slides were scanned with the dual-laser scanner Agilent G2505B and analysed as described. Differentially expressed genes were obtained by selecting probes with absolute log2 fold change >0.37 and adjusted P value <0.05. Data are MIAME-compliant and have been deposited in GEO. Functional annotation of selected gene list was performed using MetaCore tool, an integrated software suite for functional analysis that uses knowledge captured from the peer-reviewed literature to perform pathway enrichment and other kinds of analysis.

Genome wide analysis of ERG and EZH2 occupancy

To determine the genome-wide co-localization of ERG-EZH2 complexes, we analysed ChIP-sequencing datasets (GSE28951) performed in VCaP cells (Chng, Chang et al. 2012). Reads from EZH2-combined (2h DHT and 2h ETOH, 71,308,293 reads), ERG-combined (2h DHT, 18h DHT, 38,344,993 reads) and Input (16,775,051 reads) were mapped to the hg19 human genome assembly and only uniquely mapped reads were kept. Using MACS software (Zhang, Liu et al. 2008), we elicited 14,780 peaks from the EZH2-combined data set and 48,274 peaks from the ERG-combined data set. Peaks were annotated with our software (peak-tool) using all regions of the gencode-v19 database (Harrow, Frankish et al. 2012). The tool reported the presence of peaks in gene-promoters, gene-bodies, enhancers, and their distances to the TSSs. Peak-tool uses the GENCODE comprehensive database of human genes, as well as the ENCODE list of human enhancers, to annotate a list of user provided peaks. Each peak is annotated and its genomic location is classified as one of the following four possibilities:

a) Promoter (peak lies -2kb to +0.5kb relative to TSS of a gene)

b) Enhancer

c) Intragenic (peak lies within Intron / Exon of a gene)

d) Intergenic

The gene name and the isoform name associated with the Promoter and Intragenic peaks are reported by the tool along with the distance of peak to the TSS. Peak-tool is open-source and is available from https://github.com/goxed/peak-tool/.

ERG-EZH2 co-regulated gene signature

Publicly available datasets were downloaded from GEO, processed and analysed. The Sboner dataset (GSE16560) includes 281 primary prostate tumors with indication of the ERG fusion status, vital status and overall follow-up (Sboner,

Demichelis et al. 2010). The Grasso dataset (GSE35988) includes 122 samples (59 primary, 35 metastatic prostate tumors and 28 normal) with indication of the ERG fusion status (Grasso, Wu et al. 2012). The Taylor dataset (GSE21034) includes 131 primary and 19 metastatic, without annotation of the ERG fusion status (Taylor, Schultz et al. 2010). The TCGA (The Cancer Genome Atlas) dataset (downloaded from http://gdac.broadinstitute.org/) includes 497 primary prostate tumors with indication of fusion status.

To build the ERG-EZH2 co-regulated gene signature we selected the ERG-EZH2 co-occupied genes most differentially expressed (T-test pvalue<0.05) in ERG fusion positive compared to negative tumors from the Sboner dataset. This list included 118 genes. Comparison among different classes of samples, clustering, and survival analysis were performed using BRB-ArrayTools (developed by Dr. Richard Simon and BRB-ArrayTools Development Team). Clustering was performed using the one minus correlation metric and average linkage after genes were centered and scaled.

Gene set enrichment analysis (GSEA) was performed by using the tool from the Broad Institute (http://www.broadinstitute.org/gsea/index.jsp). T-test was used as metric for ranking genes after 1000 permutations.

Cumulative risk index and Kaplan-Meier (KM) plot

Among the ERG-EZH2 gene signature, 41 genes (19 down-regulated and 22 up-regulated) had a prognostic impact when used individually. We combined the expression of the 41 genes to calculate a cumulative prognostic risk index. The prognostic risk index was calculated and dichotomized in high and low risk by taking the median as threshold. The calculated risk index has as continuous variable and a statistically significant hazard ratio (HR=4.7, CI95%=[2.922 – 4.566] and Wald p-value=1.8e-10). For drawing the KM curves, the median risk index was used to

divide the patients into high and low risk. KM figures were plotted using R and the survival package.

Statistics

Statistical significance of differential findings between experimental groups was assessed by Student's t test.

Genes UPREGULATED by WT ERG and not by ERG-K362A

Gene Name	
PAGE1	TCEB3-AS1
LINC01208	C22orf42
HERC2	RBKS
FST	FAM189A2
ESPNL	RCAN2
LY86	PLA2G2F
HERC2P4	SNORA23
ANXA1	MGP
PARVB	SNORA51
LINC00870	KLK8
CD163L1	SCARNA18
LOC158435	RNU105A
C20orf196	SNORD110
FLJ37786	TMEM158
C9orf92	ID2
PRSS23	EFNA5
TCONS_l2_00015858	SNORA36A
XLOC_009943	TMEM65
IGFBP3	SNORA36A
SNORA28	LONRF2
LOC101928443	SEMA6B
THSD7A	AY927536
FUBP3	MTERFD2
ADRA2A	LRRC73
PXMP4	AI198876
SNORD46	SNORA21
SNORD15B	EDN2
XLOC_000630	LOC606724
LOC101930294	SAMD11
SNORA74A	PARVA
SNORA63	XLOC_009474
VTRNA1-3	SMAD7
chr1:024114297-024114238	SNORD95
SNORD10	ENST00000413645
SCARNA13	ENST00000438790

SLC24A3
SNORA65
HCLS1
NINJ2
RETN
MIRLET7BHG
PALMD
SNORD66
PABPN1L
STMN4
SNORD15A
ARHGDIB
SNORA34
SNORA12
PFN1P2
SCARNA11
ADAMTS1
AK124190
VTRNA1-2
chr7:105891330-105891389
MIRLET7BHG
SNORA71B
PEBP4
SNORD26
NLGN1
SNORA64
ST6GALNAC6
LENG9
EAF2
SNORA27
RN7SK
AV738989
SNORA71D
SNORA81
XLOC_007753
ENST00000430756
DIO3
FN1
RNU105A
LINC01208
CRIP2
SNORD83B
LOC142937
SLC35F3
XAGE3
THC2548652
STAC3
SNORA44
LIN7B
CRIP1
SNORD69
KCNIP4
SNORA48
TRPM8
ASCL2
TCONS_l2_00017538
ID2
VAPB
SYCE3
EFR3B
TMEM79
SNORD58A
DSEL
SMAD9
ATXN10
GPR162
LAMC1
SLC39A8
ELMO2
LOC284581
KLKP1
XLOC_012317
TPMT
TCONS_l2_00017189
SNORA11C
THC2538606

NPB
TCONS_l2_00021878
RAI2
INE1
SNORA19
ADAMTS1
FAM189A1
SNORA15
ID3
HTRA1
SNORD16
SNORA11D
SNORA9
SNORA54
SEMA3B-AS1
TAF15
SNORA73A
SNORD27
APOD
SNORA49
XLOC_004528
SRGN
ID1
LINC00599
SNORA71C
NPAS1
ACRC
FGFR3
ENST00000609207
SCARNA14
MAP6D1
FEV
TWIST1
TCEAL2
SNORA5B
SNORD8
chr14:090871996-090871937
AKR1C1
LSMEM1
PMEPA1
SNORA79
SNORA2A
RFPL2
XLOC_000026
CTSF
FSCN1
CCDC19
SH3GL3
LOC285178
SCARNA12
TTI2
SNORA57
PTGFR
RABL2B
SULF2
ND6
METRNL
ZNF112
ENST00000433310
LPXN
FAM222A
chr1:040038784-040038843
XLOC_012847
ENST00000430247
XLOC_000683
ADAMTSL3
SNORA5A
SNORA74B
HLA-DMB
AP1S1
DMKN
SNORA71A
XLOC_002730
SNORD97
SEMA3B-AS1
CRIP1

Genes DOWNREGULATED by WT ERG and not by ERG-K362A

Gene Name	
H2AFJ	C3orf18
FOS	C1QTNF9B-AS1
EGR1	LINC00869
HES1	OXR1
FOSB	HIST2H2BF
TSPY3	DEPDC1B
CCL20	PLA2G4A
RASD1	PTPRK
TSPY10	SACS
LAMA1	XLOC_010707
DUSP1	LOC149351
FAM213A	JADE1
LCN2	DDIT3
RNF103	PIF1
MAGEC2	SLC51A
CYP11A1	ELOVL1
PLA2G2A	OACYLP
THC2577566	PBK
CXCL2	IFIT1
GPX8	MAPK9
CHAC1	ZNF844
CT45A5	ZBTB21
ATF3	SETD7
FAM65B	HMMR
SSX4B	LOC101928559
MMP24	HYAL1
PTPRR	ING3
FGL1	SI
FMR1NB	HIST1H1D
TCONS_l2_00030890	AURKB
chr3:096706792-096706851	RNF145
MAGEA1	PTTG2
TCONS_l2_00028240	RLN1
PI3	ANG
LOX	CEP55
KLF6	HNF4G
MSANTD4	ENST00000451914

C1QTNF9B-AS1
KCNJ3
LOC101060211
SSX7
FCGBP
SLED1
ADH1C
HMGCS2
PDE4D
CDH26
SPINK1
DHRS2
ARG1
PSME2
GPR126
BCHE
BTN3A2
ARG1
ARHGAP28
TRIB1
ATF3
MALAT1
CENPA
DDC
RDM1
FAM65B
LINC01029
FAM72A
LOC650226
LINC00869
SSX2
CNKSR3
MIPEP
MALAT1
ACSM3
TCONS_00030032
SSX3
FUOM
KLF4
SSX4B
NAV3
EPB41L2
H3F3B
MVP
C2orf72
PPP1R15A
SEC24D
chr13:049549271-049549212
LRRC70
LOC388692
CCDC85A
THC2659602
TOX3
LOC145837
chr7:007949226-007949167
TTC29
XLOC_011294
RDH10
SLC10A7
DNAJB9
IGF1
TFF3
FAM83D
DHFR
MIPEP
IER3
HCG4
NUP93
CCNA2
LINC00869
CKLF
PPAP2C
PVT1
ASPM
HOMEZ
EPB41L5
TBC1D4
MEIS1
ANXA4
AURKA

MALAT1
LAMB1
ENST00000454441
HIST1H1C
FAM72D
RNASE4
SHISA3
LAMA1
UGT8
PTTG3P
GPX8
XLOC_011294
IL17C
BHLHE40
REPS2
KCNH8
ELF5
IER3
LINC00869
ENST00000573315
RFX6
C2CD3
ARHGAP28
CCNB1
FAM63A
AUTS2
TRIM68
HMGN5
MLLT3
ARHGAP11A
ACADSB
LOC145837
KIF25
DIAPH3
KLK3
NEAT1
HERPUD1
REPS2
PARPBP
GDF15
TFF3
GAS2
IGF1
ALDH2
chr17:074222655-074222596
IFI35
TCONS_l2_00020391

Gene co-occupied by ERG and EZH2 within 1000 bp

Gene Name		
AASS	ALDH1A3	ALDH1A2
ABCB9	ALDOB	ARSG
ABCC1	ALK	ART3
ABCG1	ALPK2	ASAP1
ABCG2	ALPK3	ASB9
ABHD12	ALPK3	ASCL4
ABHD2	AMER3	ASIC2
ABL1	AMN1	ASIP
AC006946.15	AMOTL1	ASZ1
AC009802.1	AMPD3	ATAD2
AC074212.3	ANGPT1	ATAT1
AC112721.1	ANGPTL3	ATG12
ACACA	ANK3	ATL1
ACAP3	ANKH	ARHGAP28
ACE	ANKIB1	ARHGAP29
ACMSD	ANKRD28	ARHGAP35
ACPL2	ANKRD29	ARHGEF1
ACSBG1	ANKRD34C	ARHGEF10
ACSS1	ANKRD45	ARHGEF3
ACTB	ANKS1B	ARHGEF38
ACTR1A	ANO3	ARID1B
ACTR3	ANO4	ARID5B
ADAM2	ANP32B	ARSG
ADAM29	AP000679.2	ART3
ADAM9	AP000708.1	ASAP1
ADAMTSL3	AP3B1	ASB9
ADARB1	AP3S1	ASCL4
ADCY1	AP5M1	ASIC2
ADNP	APBA1	ASIP
ADRBK2	APIP	ASZ1
AFAP1	APOL5	ATAD2
AFF1	APOLD1	ATAT1
AFF2	APP	ATG12
AFF3	APPBP2	ATL1
AGAP1	ARAP2	ATOH8
AGBL1	ARFIP1	ATP10A
AGBL4	ARHGAP20	ATP11B

AHCYL1
AHNAK
AIM1
AIM1L
AK4
AKAP13
AKAP6
AKAP7
AKR1D1
AKT3
ALDH1A1
ATRX
ATXN3
ARMC8
AUTS2
AVEN
AVPR1A
AXL
B4GALNT1
B4GALT1
B4GALT5
BACH2
BAG2
BAI1
BAI3
BAIAP2L1
BASP1
BATF
BCAP29
BCL2
BCL2L13
BICD1
BMF
BMI1
BMP7
BMPR1A
BMPR2
BNC1
BOC
BRD3
ARHGAP26
ARHGAP28
ARHGAP29
ARHGAP35
ARHGEF1
ARHGEF10
ARHGEF3
ARHGEF38
ARID1B
ARID2
ARID5B
C1orf94
ATXN7L1
C2CD3
C2CD4C
C2orf15
C2orf76
C3orf14
C3orf20
C3orf70
C3orf72
C3orf83
C4orf22
C4orf51
C5
C5orf27
C6
C6orf106
C6orf132
C6orf58
C7orf10
C8orf33
C8orf34
C8orf44-SGK3
C9orf135
C9orf91
CA13
CABP1
CACHD1
CACNA1B
ATP1A2
ATP2A3
ATP2B1
ATP2B4
ATP5G2
ATP6V0E1
ATP6V1E2
ATP6V1G1
ATP8A1
ATP8A2
ATP8B4
C21orf88
CCDC106
CCDC108
CCDC109B
CCDC129
CCDC141
CCDC146
CCDC158
CCDC177
CCDC178
CCDC39
CCDC40
CCDC42B
CCDC57
CCDC60
CCDC67
CCDC68
CCDC77
CCDC91
CCM2L
CCND1
CCSER1
CD14
CD36
CDC14A
CDC14B
CDC23
CDC42EP5
CDH2

BRD4
BRINP1
BRINP2
BRMS1L
BTBD11
BTNL9
BZW1
C10orf11
C10orf76
C11orf35
C11orf80
C12orf40
C12orf55
C12orf79
C15orf26
C17orf67
C18orf25
C1orf112
C1orf168
C1orf21
C1orf222
CBLC
CHGA
CHGB
CHL1
CHMP3
CHN1
CHN2
CHODL
CHRM2
CHRNB2
CHRNB4
CHRND
CHST11
CIT
CLDN11
CLIC1
CLIC5
CLMP
CLPSL1
CACNA1C
CACNA2D1
CACNA2D2
CACNB4
CADM1
CADM2
CADPS
CADPS2
CALCB
CAMKK2
CAMTA1
CANX
CAPN14
CAPSL
CARD11
CASC10
CASP2
CASQ2
CAV1
CAV2
C20orf112
CREG2
CRH
CRHR1
CRIM1
CRISPLD1
CSMD2
CSMD3
CSRP2
CT62
CTC-349C3.1
CTD-3148I10.1
CTDSP1
CTDSPL
CTNNA1
CTNNA2
CTNNA3
CTNNBL1
CTTNBP2NL
CUX1
CDH22
CDH4
CDK14
CDK19
CDK3
CDK6
CDKN1A
CDKN2A
CECR6
CELSR1
CENPO
CEP120
CEP128
CEP192
CEP350
CEP89
CERS6
CES2
CFTR
CAV3
CBFA2T2
DGKI
DHH
DHODH
DHX32
DHX35
DIAPH1
DIO2
DIP2B
DIP2C
DISC1
DISP1
DKKL1
DLG2
DLGAP1
DLGAP4
DLK2
DLX1
DLX4
DMGDH

CLSTN2
CLTC
CMSS1
CMTM4
CMTM8
CNRIP1
CNST
CNTD1
CNTD2
CNTN1
CNTN4
CNTNAP5
COL14A1
COL24A1
COL27A1
COL28A1
COL4A3
COL4A4
COL9A1
COMMD1
COPB1
CORIN
CORO2A
CPAMD8
CPEB4
CPED1
CPLX2
CH25H
CHCHD5
CHD6
CREB5
E2F4
E2F6
EBF1
EBF2
EBNA1BP2
ECE1
EDA
EDC3
EDEM2
CUX2
CXCL13
CXCL6
CXXC4
CYB5A
CYB5R4
CYP26A1
CYP27B1
CYP3A43
CYP7B1
CYTH3
DAAM1
DAB1
DACT1
DAGLA
DAP
DBI
DBNDD2
DCAF11
DCDC1
DCST1
DDI2
DDIT3
DDX60L
DEAF1
CPM
CPNE8
CPNE9
CPQ
CRADD
DGKB
ESPN
ESRRG
ETFA
ETFB
ETNPPL
ETS1
ETV1
ETV4
EVA1A
DNAH12
DNAH7
DNAH8
DNAJB4
DNAJC28
DNAJC6
DNAL1
DNASE2B
DNER
DOCK1
DOCK10
DOCK2
DOCK3
DOCK4
DOCK5
DOCK9
DOK6
DPH6
DPYD
DPYD
DPYSL3
DSC3
DSCAM
DSCR4
DSCR4
DENND1A
DENND3
DEPTOR
DERL1
DESI2
DYNLRB1
FAM3B
FAM49B
FAM65B
FAM78A
FAM89A
FAM9B
FANK1
FARP1
FARP2

EDN3
EEF1A1
EEF1D
EEF2K
EFCAB12
EFHD1
EFR3A
EGFR
EGR1
EIF3H
EIF4EBP1
ELF2
ELL2
ELMO1
ELOVL6
ELOVL7
EMCN
EMD
EMX1
ENOX1
ENOX2
ENTHD1
ENTPD5
EPB41L2
EPB41L4A
EPB41L4A-AS2
EPB41L4B
EPB41L5
EPHA5
EPHA7
EPHB1
EPN2
EPS8
EPSTI1
ERBB2
DSE
DTNA
DUSP18
DUSP19
DYNC1I1
EVI5
EWSR1
EXOC3L1
EXOC4
EXOC5
EXOC6
EXOC6B
EXT1
EYA1
EYA1
EYA2
EZR
F13B
F9
FAF1
FAM101A
FAM105A
FAM107A
FAM107B
FAM120B
FAM129A
FAM129B
FAM134B
FAM13A
FAM149A
FAM150B
FAM154B
FAM155A
FAM159A
FAM162A
FAM163A
FAM172A
FAM174B
FAM188B2
FAM189A1
ERBB4
ERC1
ERC2
ERCC6
ERG
FAT3
FAXDC2
FBRSL1
FBXL13
FBXL17
FBXL17
FBXL7
FBXO41
FBXO46
FBXO9
FBXW11
FCHSD2
FCRLB
FCRLB
FECH
FEZ1
FGD4
FGF12
FGF14
FGF2
FGFR1
FGGY
FHIT
FHOD1
FIBCD1
FIP1L1
FKBP5
FLT4
FMN1
FMNL2
FNBP1L
FNDC3B
FNIP2
FOCAD
FOXA3
FAM189A2
FAM193A
FAM19A1
FAM211A
FAM213A

ERP44
FRS2
FRYL
FSCN2
FSHR
FSIP2
FUT8
FYN
FZD1
GABBR2
GABRB3
GALNT1
GALNT14
GALNTL6
GALR1
GAPVD1
GAREM
GATA6
GATM
GBE1
GCSAM
GDAP1
GDF6
GDNF
GFM1
GFPT2
GGCX
GHR
GHRHR
GLB1
GLB1L2
GLI2
GLI3
GLI4
GLIS3
GLP2R
GLRA3
GLYATL3
GNA12
GNAI1
FAM214A
GPR153
GPR158
GPR179
GPR39
GPR63
GPR65
GPR78
GPR85
GPR98
GPRC5B
GPRIN3
GREB1L
GREM1
GRHL2
GRHL3
GRIA1
GRID1
GRID2
GRIK2
GRIK4
GRIN2B
GRIP1
GRXCR1
GSPT1
GUCY1A2
H3F3B
HAPLN2
HDAC9
HECW1
HECW2
HEPACAM2
HERC3
HERC4
HES2
HEY1
HEY2
HGF
HHAT
HIBCH
FRMD4A
HOMER2
HOXA10
HOXA11
HOXA11
HOXA11
HOXA9
HOXB7
HOXC4
HOXC9
HPSE
HPSE2
HRH3
HS6ST2
HS6ST3
HSPA4L
HSPBAP1
HTR4
HUS1
HYLS1
IGF1R
IGFBP1
IGFBP3
IGFL4
IGSF3
IL10RB
IL19
IL8
ILKAP
IMMP2L
IMP3
INPP5A
INSM2
IQGAP1
IRAK3
IRS1
IRS2
IRX4
ISX
ITGA4

GNAL
GNAQ
GNB1
GNB4
GNG7
FOXB1
FOXN3
FOXO3
FOXP1
FPR1
GPR150
KAT6B
KAZN
KCNAB1
KCNB2
KCND2
KCND3
KCNH5
KCNIP1
KCNJ15
KCNJ6
KCNK13
KCNMA1
KCNMB2
KCNN2
KCNQ1
KCNQ3
KCTD20
KCTD3
KDM4B
KDM4C
KDM6A
KDR
KHDRBS3
KIAA0100
KIAA0319
KIAA0368
KIAA0825
KIAA1024
KIAA1199
HIF3A
HIPK2
HIST1H1D
HK1
HLCS
GOLGA4
GOLM1
GPATCH2
GPR126
GPR128
HNRNPL
KLRC4-KLRK1
KNSTRN
KSR2
LAIR2
LAMC1
LAMP3
LANCL2
LAPTM4B
LARGE
LARP4B
LCLAT1
LCOR
LCORL
LDLRAD4
LECT1
LECT2
LEF1
LEFTY1
LEKR1
LEMD1
LEPR
LEPREL1
LGALS3BP
LGMN
LGR4
LHFP
LHX2
LHX4
LIMS1
ITGA9
ITGB2
ITGB3
ITPR2
JAG1
HMCN2
HMGA2
HMGN4
HMGXB4
HNF4A
KAT6A
LRRK1
LRRTM4
LSAMP
LSM11
LSM14A
LTN1
LURAP1L
LY75
LYPD5
LYPD6B
MACF1
MACROD2
MAGI1
MAGI2
MAL2
MAML2
MAN1A1
MANBA
MAP2K4
MAP2K5
MAP3K19
MAP4
MAP4K5
MAP6
MAPK10
MAPK14
MAPKAP1
MARCH10
MARCH4

KIAA1217
KIAA1244
KIAA1257
KIAA1324
KIAA1377
KIAA1430
KIAA1522
KIAA1614
KIAA2018
KIAA2022
KIF26B
KIF3B
KIRREL3
KITLG
KLF1
JAK1
JHDM1D
JPH4
JTB
KANK1
KLRC3
LINC00908
LIPH
LL22NC03-63E9.3
LMO1
LMO7
LMOD3
LMX1B
LNX1
LOH12CR1
LPHN2
KLHL12
KLHL17
KLHL3
KLHL35
KLHL9
LRP2
LRRC16A
LRRC6
LRRC69
LRRCC1
LRRFIP2
MYLK4
MYO10
MYO16
MYO1B
MYO1D
MYO3B
MYO5B
MYO6
MZF1
N4BP3
NAALAD2
NAALADL2
NAPA
NARG2
NARS2
NAV2
NAV3
NBAS
NCALD
MARK1
MAST4
MAT2A
MB21D2
MBD6
MBNL1
MBTPS1
MC5R
MCC
MCM9
LPHN3
LPP
LPPR1
LRBA
LRP12
MECOM
MECP2
MED12L
MED27
MED30
MEF2A
MEF2C
MEGF6
MEGF9
MEIS1
MEP1A
MERTK
MET
METTL25
METTL6
MFSD6
MGAT5
MGAT5B
MGST1
MIB1
MICAL2
MICU1
MIPOL1
MIR3654
MKLN1
NOG
NOL4
NOS1AP
NOS2
NOSTRIN
NOV
NPAS3
NPBWR1
NPHS1
NPL
NPR2
NPY
NR1I2
NR2F1
NR2F2
NR5A2
NRCAM
NREP
NRG4

MLPH
MME
MMP24
MMP25
MOB3B
MPPED1
MPPED2
MRPL28
MRPL33
MRVI1
MS4A6E
MSH5
MSH6
MSRB3
MSX2
MTA3
MTBP
MTFMT
MTFP1
MTFR1
MCMDC2
MCPH1
MCTP2
ME2
MEAF6
MVB12A
MYBL1
MYBPC1
MYCBP2
MYH15
MYLK
ORC5
OSBPL1A
OSBPL6
OVOL2
OXGR1
OXR1
PACS1
PACSIN2
PAG1
NCAM1
NCKAP1
NCOR1
NDUFAF6
NEDD4L
NEK10
NELL2
NEUROG3
NFATC1
NFIA
NFIB
NFIX
NHEJ1
NID1
NIN
NIPA1
NISCH
NKAIN2
NKAIN3
NKAIN4
MTIF2
MTMR2
MTMR3
MTNR1B
MUSK
NLRP14
NLRP3
NLRP8
NMD3
NMNAT2
NOC2L
PHC2
PHF19
PHLPP1
PHYHIPL
PIGS
PIGV
PIK3AP1
PIK3CD
PIK3R3
NRP2
NRXN1
NRXN2
NRXN3
NT5C2
NT5DC1
NTHL1
NTM
NTN1
NTN4
NTNG1
NTRK2
NUAK1
NUDCD1
NUDT12
NUDT16
NUDT3
NUPR1L
NVL
NWD1
NKG2-E
NKX3-2
NKX6-1
NLGN1
NLGN4Y
ONECUT2
OPA3
OPCML
OPHN1
OPN4
OPRK1
PREX1
PREX2
PRICKLE1
PRICKLE2
PRKAR2B
PRKCE
PRKCH
PRKD1
PRKD3

PALLD
PALM2
PALM2-AKAP2
PAM
PAMR1
PAPPA2
PAPSS1
PARD3
PARK7
PARN
PAX2
PAX5
PAX6
PCNX
PCSK2
PCSK5
PCYT1B
PDE10A
PDE11A
PDE4B
PDE4D
PDE5A
PDE6A
PDE9A
PDE9A
PDE9A
PDGFRA
PDIA5
PDLIM5
PDLIM7
NXPE3
OC90
OGFOD2
OGG1
OLFM1
PFKFB1
PGAP1
PGAP3
PGLYRP2
PHACTR3
PIN4
PIP5KL1
PITPNM2
PIWIL1
PKP4
PLA2G5
PLCB1
PLCL1
PLCXD2
PLD1
PLEKHB2
PLEKHG1
PLEKHG4B
PLEKHM3
PLOD2
PLXNA4
PML
POLA1
POLE
POM121C
POM121L2
POU6F2
PPARG
PPFIA2
PPFIBP1
PPFIBP2
PPIC
PPM1H
PPP1R16B
PPP1R42
PDZD2
PEG10
PER2
PEX14
PEX2
PPP6R2
PPP6R3
PRAME
PRDM1
PRDM16
PRKG1
PRKG2
PRKRIP1
PRKX
PROM1
PRR15L
PSD3
PSMA5
PTCRA
PTGIS
PTGR1
PTGS1
PTP4A3
PTPRA
PTPRB
PTPRG
PTPRJ
PTPRJ
PTPRM
PTPRN2
PTPRO
PTPRQ
PTPRT
PTPRU
PTTG1IP
PUM2
PUSL1
PXDNL
PXMP2
PXN
PPP2R2B
PPP2R5A
PPP3CB
PPP4R1
PPP4R4
RAB20
RAB21
RAB30
RAB31
RAB32

PHACTR4
RAB3B
RAB3C
RAB4A
RAB8B
RABGAP1
RABL3
RAD51B
RAD52
RAET1E
RALGAPA2
RALYL
RANBP3L
RAP1GAP2
RAPGEF4
RARB
RASAL2
RASGRF1
RASSF8
RBFOX1
RBFOX3
RBM18
RBM47
RBMS1
RBMS3
RCAN2
RCN1
RECK
RELA
RELN
RERE
RERG
RFESD
RFTN2
RFX2
RFX3
RGMA
RHBDD3
RHOBTB1
RHOBTB3
PRDM8
RNF157
RNF215
RNF38
RNGTT
RNLS
ROCK1
ROR1
RORA
RORB
ROS1
RP11-1102P16.1
RP11-127H5.1
RP11-169F17.1
RP11-210M15.2
RP11-215A19.2
RP11-219B4.5
RP11-234B24.6
RP11-298I3.5
RP11-307N16.6
RP11-362K2.2
RP11-383H13.1
RP11-403P17.5
RP11-81K2.1
RP11-849H4.2
RP1-228P16.5
RP1-27O5.3
RP1-4G17.5
RPA3
RPA3-AS1
RPH3AL
RPL17-C18orf32
RPL18
RPS6KA2
RPTOR
RTN1
RUNX1T1
RUNX2
RXFP3
RYK
RAB39A
SCGN
SCN3B
SCN8A
SCOC
SCUBE1
SDAD1
SDK1
SEC22C
SEC24D
SEC61A2
SELV
SEMA3C
SEMA4B
SEPP1
SERPINE2
SERTAD4
SETD3
SETD7
SETD8
SFI1
SGCD
SGCE
SGIP1
SGSM1
SH2B2
SH2D6
SH3D19
SH3GL2
SH3PXD2B
SH3RF1
SH3RF2
SH3RF3
SH3TC2
SHANK2
SHFM1
SHISA8
SHOX2
SHROOM3
SIK3

PYGB
QPCT
R3HDM2
RAB11FIP5
RAB1A
RIN2
RNASE11
RNF121
RNF138
RNF145
RNF150
SLC22A4
SLC22A6
SLC24A3
SLC25A13
SLC25A33
SLC25A36
SLC26A3
SLC29A2
SLC2A13
SLC2A3
SLC2A5
SLC30A8
SLC35B4
SLC35D3
SLC35F2
SLC35F4
SLC35F6
SLC36A1
SLC37A2
SLC38A1
SLC38A11
SLC38A2
SLC38A4
SLC43A1
SLC45A4
SLC6A1
SLC7A8
SLC8A1
SLC8A2
RHOQ
RHPN2
RIMBP2
RIMS1
RIMS2
SBF2
SBSPON
SC5D
SCAI
SCAPER
SCARB2
SOGA2
SOGA3
SORBS2
SORCS2
SORCS3
SORL1
SOS2
SOST
SOX6
SPATA6L
SPEF2
SPHK2
SPIDR
SPIRE1
SPOCK1
SPOCK3
SPRED2
SPTB
SRFBP1
SRGAP1
SRPK2
SRRM3
SSBP4
SSH2
SSPN
ST18
ST6GAL1
ST6GALNAC2
ST7
RYR3
S100A11
SAMD3
SASH1
SATB1
SLC17A2
SLC1A1
SLC22A10
SLC22A15
SLC22A2
SLC22A3
SUPT3H
SUSD1
SUSD5
SV2B
SVEP1
SYBU
SYMPK
SYN3
SYNE2
SYNRG
SYT1
SYT5
TACC2
TAF15
TANC2
TBC1D1
TBC1D1
TBC1D14
TBC1D22B
TBC1D2B
TBC1D30
TBC1D4
TBC1D8
TBC1D9
TBCE
TBCEL
TBPL1
TBXAS1
TCF20

SLC9A5
SLC9A9
SLCO1C1
SLCO2A1
SLCO3A1
SLCO5A1
SLFN13
SMARCD3
SMC6
SMOX
SIK3
SIPA1L2
SIPA1L3
SLC15A5
SLC17A1
SNTG2
SNX15
SNX16
SNX25
SNX33
SOGA1
TIAM1
TIGD5
TIGD6
TIMD4
TLE1
TLE3
TLE4
TLL2
TLN2
TLX1NB
TM2D1
TM6SF1
TMC6
TMC8
TMCC2
TMCC3
TMEM100
TMEM108
TMEM117
ST8SIA1
ST8SIA6
STC2
STEAP2
STEAP4
STIL
STK3
STK32A
STK39
STK4
SMURF1
SMYD3
SNAP25
SNAP91
SND1
STYK1
SUCO
SUFU
SULF1
SULF2
SULT2B1
TP53TG5
TPBG
TPD52
TPK1
TPM1
TPRA1
TPRG1
TPST1
TRABD2B
TRAF3IP2
TRAK1
TRANK1
TRAPPC9
TRHDE
TRIM36
TRIM8
TRIO
TRMT1L
TRPC7
TCF7
TCFL5
TCHH
TCTN2
TEAD2
TENM2
TESC
TESK2
TFEB
TFEC
STK40
STOM
STON2
STOX2
STXBP6
THBD
THOC5
THRAP3
THRB
THSD4
THSD7A
UGT2B28
UNC13B
UNC5A
UNC5B
UNC5C
UNC79
UPK3B
USP39
USP42
UST
UTP6
UTRN
VAMP8
VAT1L
VAV1
VAV3
VDAC1
VEGFC
VEPH1

TMEM125
TMEM179
TMEM181
TMEM204
TMEM229A
TMEM229B
TMEM233
TMEM241
TMEM245
TMEM260
TMEM5
TMEM57
TMEM63C
TMEM71
TMEM74
TMEM86A
TMOD3
TMPRSS11F
TMPRSS2
TMTC1
TFPI
TG
TGFA
TGFBR3
THAP4
TNFRSF9
TNFSF10
TNIK
TNS3
TOX
TP53BP2
XPOT
XXYLT1
XYLT1
YTHDF1
ZBTB1
ZBTB16
ZBTB44
ZCCHC7
ZDHHC9
TRPM1
TRPM3
TRPM8
TRPS1
TRPV4
TSG101
TSGA10
TSKU
TSNAX-DISC1
TSPAN18
TSPAN31
TSPAN8
TTC23
TTC7A
TTI1
TTK
TTPA
TUB
TXK
WWC3
TMTC2
TMX4
TNFAIP8
TNFAIP8L3
TNFRSF11B
UBE2I
UBE2R2
UBE3C
UBR1
UBR3
UGT1A1
ZNF343
ZNF385B
ZNF462
ZNF516
ZNF563
ZNF608
ZNF627
ZNF704
ZNF804B
VPS13B
VPS13C
VPS13D
VPS37B
VRK2
VRK3
VSTM2A
VTI1A
VWA5A
VWA8
VWC2L
VWDE
WDFY3
WDR86
WIBG
WNK2
WNK4
WNT5B
WSCD1
WSCD2
WWOX
WWP1
TXNDC16
TXNRD1
UBA2
UBAC1
UBE2E1
UBE2H
XKR6
XKR7
XPNPEP3

ZEB2
ZFAND3
ZFHX3
ZHX2
ZIC3
ZMYND8
ZNF114
ZNF12
ZNF135
ZNF18
ZNF214
ZNF236
ZNF24
ZNF334
ZNF341
ZNF808
ZNRF2
ZPLD1
ZSCAN20
ZSCAN5A
WWC1
WWC2

Results

ERG is methylated in ERG fusion positive cells

In understanding the mechanism of ERG induced oncogenesis, different evidences suggested that EZH2 could have a relevant role in ERG-mediated cancer progression. Our group and others have reported that EZH2 is induced at mRNA and protein levels by the TMPRSS2-ERG gene fusion which occurs frequently in prostate tumors, and that ERG and EZH2 are recruited to diverse, selected gene promoters and enhancers in human cell lines and human prostate tumors (Kunderfranco, Mello-Grand et al. 2010; Yu, Mani et al. 2010). However, the underlining mechanisms and the role of EZH2 in primary prostate cancers remain unclear. EZH2 is a methyltransferase protein, which exhibits histone methyl-transferase activity with specificity to histone H3K27 (Cao, Wang et al. 2002). However, recent findings have shown that EZH2 could methylate also non-histone proteins, recognizing a histone-like sequence, called "R-K-S" motif, in target proteins (Lee, Lee et al. 2012). Starting from this notion, we searched this specific motif among all the family members of the ETS transcription factors and discovered that ERG protein harbours this specific "R-K-S" motif centered at lysine 362 (Figure 18A). Alignment of the full ERG amino acid sequences derived from various species showed that this motif was evolutionarily conserved among higher eukaryotes, further underlining the relevance of this sequence (Figure 18B). Interestingly, the "R-K-S" motif was contained in only other two ETS members, FLI1 and FEV, which share high homology with ERG (Figure 18C). These observations prompted us to hypothesise that the histone like sequence contained in ERG protein could serve as an acceptor site for methylation by EZH2. To test this, we performed immunoprecipitation experiments of ERG in ERG translocation positive cells, VCaP, with an anti-ERG antibody, followed by immunoblotting using a pan-methyl lysine antibody, able to recognize proteins methylated on lysine residues. Interestingly, we found that a substantial fraction of ERG was methylated in VCaP cells (Figure 18D).

A

MIQTVPDPAAHIKEALSVVSEDQSLFECAYGTPHLAKTEMTASSSSDYGQTSKMSPRVPQQDWLSQPPAR

VTIKMECNPSQVNGSRNSPDECSVAKGGKMVGSPDTVGMNYGSYMEEKHMPPPNMTTNERRVIVPADPTL

WSTDHVRQWLEWAVKEYGLPDVNILLFQNIDGKELCKMTKDDFQRLTPSYNADILLSHLHYLRETPLPHL

TSDDVDKALQNSPRLMHARNTGGAAFIFPNTSVYPEATQRITTRPDLPYEPPRRSAWTGHGHPTPQSKAA

QPSPSTVPKTEDQRPQLDPYQILGPTSSRLANPGSGQIQLWQFLLELLSDSSNSSCITWEGTNGEFKMTD

PDEVARRWGE**RKS**KPNMNYDKLSRALRYYYDKNIMTKVHGKRYAYKFDFHGIAQALQPHPPESSLYKYP

SDLPYMGSYHAHPQKMNFVAPHPPALPVTSSSFFAAPNPYWNSPTGGIYPNTRLPTSHMPSHLGTYY

B

Human (P11380-3)	PDEVARRWGERKSKPNMNYDKLSRAL 376
Bovine (A6QLR0-1)	PDEVARRWGERKSKPNMNYDKLSRAL 345
Mouse (P81270-1)	PDEVARRWGERKSKPNMNYDKLSRAL 376
Chicken (Q90837-1)	PDEVARRWGERKSKPNMNYDKLSRAL 368
King cobra (V8NS51-1)	PDEVARRWGERKSKPNMNYDKLSRAL 273
Xenopus (Q9W700-1)	PDEVARRWGERKSKPNMNYDKLSRAL 375
Salmon (B5X1W7-1)	PDEVARRWGERKSKPNMNYDKLSRAL 368
Zebrafish (Q5PR65-1)	PDEVARRWGERKSKPNMNYDKLSRAL 316
Lytechinus (Q01414-1)	PDEVARRWGERKSKPNMNYDKLSRAL 62
	**************************

C

ERG (P11308-3)	LELLSDS-SNSSCITWE-GTNGEFKMTDP--DEVARRWGERKSKPNMNYDKLSRALRYY
FLI1(Q01543)	LELLSDS-ANASCITWE-GTNGEFKMTDP--DEVARRWGERKSKPNMNYDKLSRALRYY
FEV (Q99581)	LELLADR-ANAGCIAWE-GGHGEFKLTDP--DEVARRWGERKSKPNMNYDKLSRALRYY

D

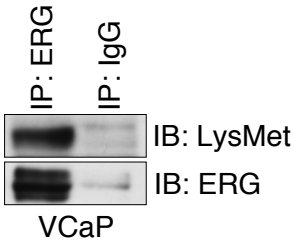

Figure 18. **ERG contains a "R-K-S" motif and is methylated in VCaP cells.** (**A**) ERG protein sequence (P11308-3) with the "R-K-S" motif underlined in red. (**B**) Sequence alignment of ERG domain containing R-K-S motif from diverse species. (**C**) Alignment of ETS binding site of the ERG subfamily members. (**D**) ERG immunoprecipitation (IP) with anti-ERG antibody followed by immunoblotting with anti-methyl-lysine antibody (IB: LysMet). Immunoprecipitation with IgG antibody was used as negative control.

ERG methylation occurs at a specific site of the protein and is EZH2 dependent

To determine whether methylation occurred in the "R-K-S" motif, supporting lysine 362 (K362) as a key residue for ERG methylation, we generated an ERG mutant construct in which the lysine 362 was replaced by alanine (ERG-K362A). Exogenous expression of wild type ERG (WT-ERG) and ERG-K362A mutant vectors in VCaP cells, followed by immunoprecipitation with an antibody against the HA-tag of the plasmids, showed reduced methylation of the ERG-K362A mutant construct compared to WT-ERG, confirming that K362 was the main methylation site (Figure 19).

To facilitate studies on ERG methylation, we generated a polyclonal antibody that specifically recognized methylated ERG at residue K362 (mERG Ab). In order to verify the specificity of the antibody, we took advantage of the peptide competition assay. To this end, the antibody was incubated with the methylated competitor peptide (M-peptide) or with the same peptide without any modifications (C-peptide), and then used for protein recognition. Immunoblotting showed that the M-peptide was able to neutralize the mERG antibody, while C-peptide was not (Figure 20A), confirming the specificity of the antibody for the methylated lysine 362 of ERG. We obtained similar results by performing immunofluorescence with mERG antibody and the competitor peptides in VCaP cells (Figure 20B). Furthermore, immunofluorescence also showed that ERG and mERG had similar intranuclear distribution, and both co-localized with EZH2 (Figure 21).

Importantly, mERG was detected by immunoblotting in lysates of five different ERG fusion positive primary tumors, providing direct evidences that ERG methylation occurred in human clinical samples (Figure 22).

To determine the role of EZH2 in ERG methylation, we targeted EZH2 genetically, by siRNA-mediated knockdown, and pharmacologically, with the pharmacological inhibitor deazaneplanocin (DZNep).

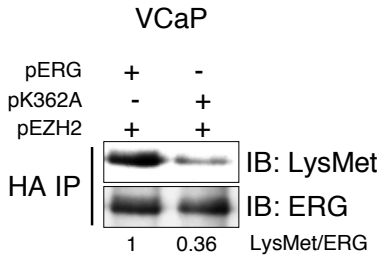

Figure 19. **ERG is methylated at lysine 362.** Wild type ERG (pERG) and ERG-K362A mutant (pK362A) constructs were transfected in VCaP cells along with EZH2 (pEZH2) and after 24h were immunoprecipitated using an anti-HA antibody (HA IP). Immunoblotting was performed with anti-ERG and anti-methyl-lysine antibodies. Densitometry values of methylated/total ERG (LysMet/ERG) ratio are shown.

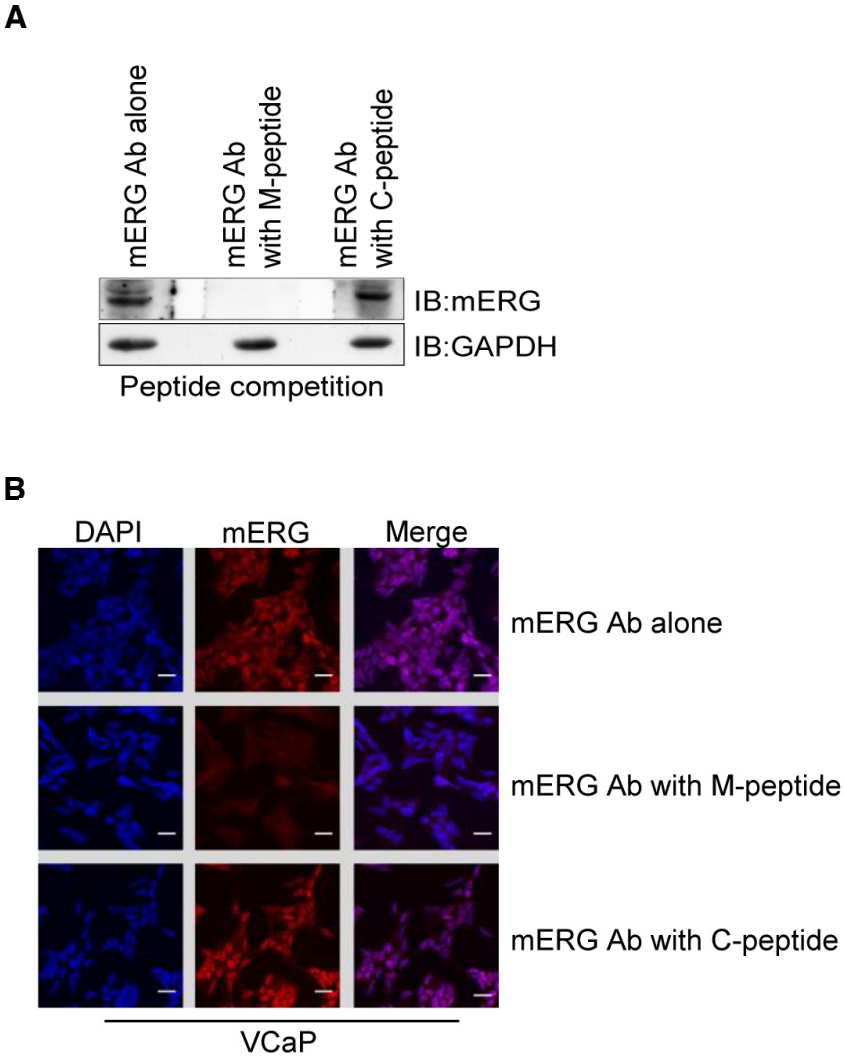

Figure 20. **Specificity of m-ERG antibody.** (**A**) Detection of methylated ERG (mERG) in VCaP cells by immunoblotting with anti-mERG antibody alone or in competition with methylated (M-peptide) and non-methylated (C-peptide) peptides. (**B**) Detection of mERG in VCaP cells by immunofluorescence microscopy with anti-mERG antibody pre-incubated with the specific competitor peptides. Scale bar = 20μm.

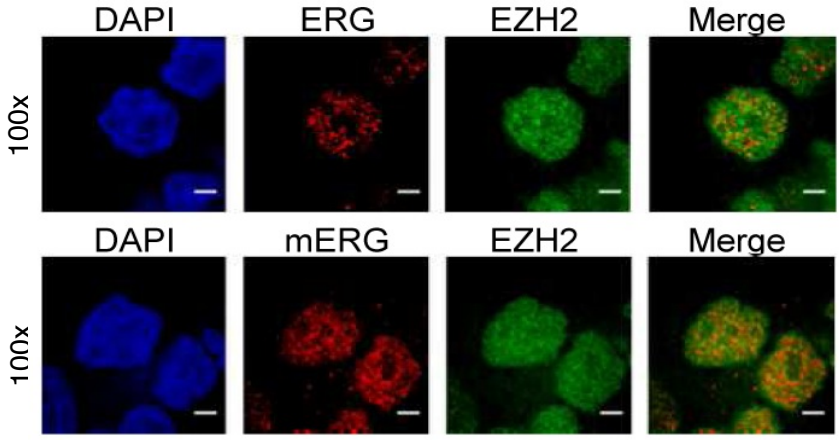

Figure 21. **ERG and EZH2 intranuclear co-localization.** Detection of ERG, EZH2 and mERG in VCaP cells by immunofluorescence microscopy. Scale bar =100 μm.

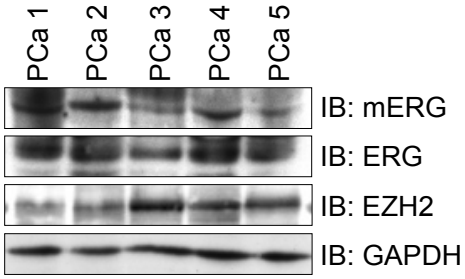

Figure 22. **ERG is methylated in prostate tumors.** Immunoblotting analysis of mERG, ERG and EZH2 in five ERG positive human prostate cancer samples (PCa).

Genetic EZH2 inhibition by siRNA (Figure 23) and pharmacological ablation by DZNep treatment (Figure 24) markedly reduced the level of methylated ERG detected by using the anti-methyl-lysine or the anti-mERG antibody, without affecting cell viability.

Furthermore, ectopically expressed WT-ERG was methylated in ERG-negative immortalized prostate epithelial RWPE1 cells, while the ERG-K362A mutant was not (Figure 25, *left panel*). Concomitant expression of EZH2 significantly increased methylation of WT-ERG but was ineffective on ERG-K362A, sustaining a direct link between EZH2 and K362 methylation (Figure 25, *middle* and *right panels*).

Collectively, these data established for the first time that ERG is methylated at lysine 362 by EZH2 in prostate cancer cells.

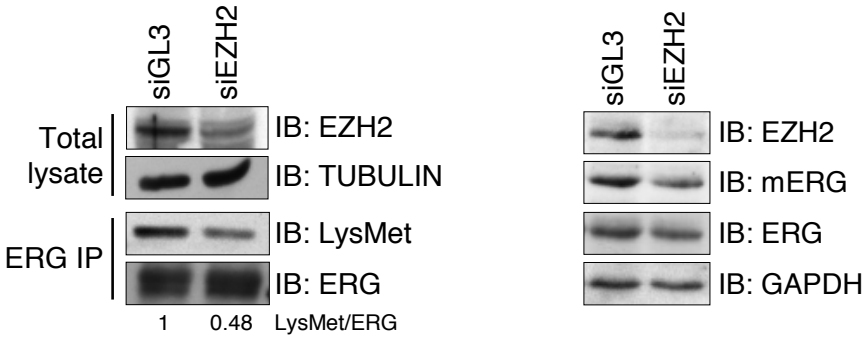

Figure 23. **ERG methylation is reduced upon EZH2 knockdown.** IP of ERG in VCaP cells transfected with control (siGL3) or EZH2 directed siRNAs (siEZH2) (*left panel*). Densitometry values of methylated/total ERG (LysMet/ERG) ratio are shown. On the right, detection of mERG, ERG and EZH2 by immunoblotting in VCaP cells upon EZH2 knockdown as described above. Lysates were collected 48h after transfection.

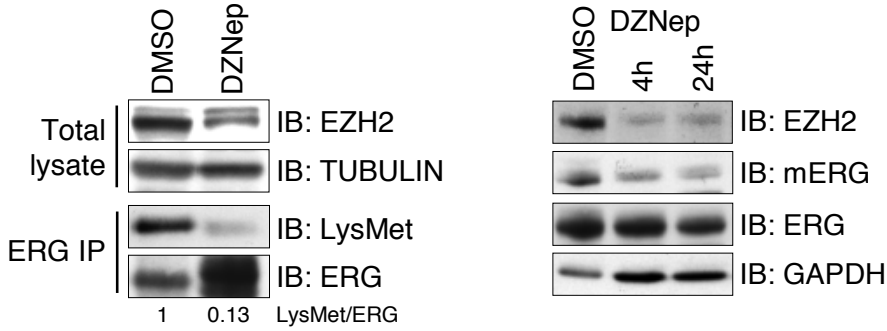

Figure 24. **ERG methylation is reduced upon DZNep treatment.** IP of ERG in VCaP cells treated with DZNep (10μM) for 72h (*left panel*). Densitometry values of methylated/total ERG (LysMet/ERG) ratio are shown. On the right, detection of mERG, ERG and EZH2 by immunoblotting in VCaP cells treated with DMSO (control) or DZNep (10μM) at indicated time.

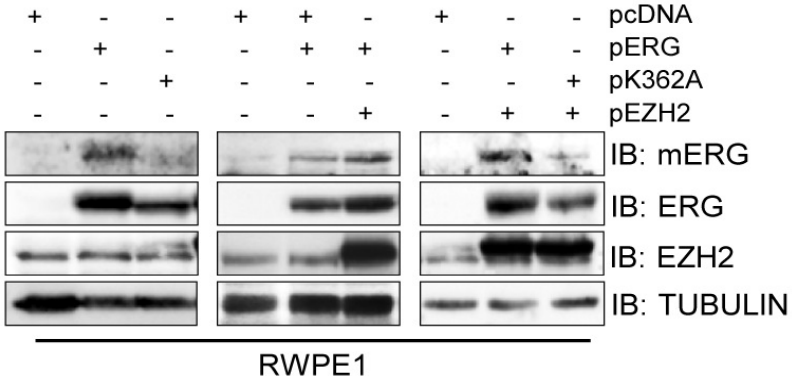

Figure 25. **ERG-K362A is not methylated in RWPE1 cells.** Immunoblot analysis of mERG and ERG in RWPE1 cells transiently transfected with the indicated plasmids. Lysates were collected 24h after transfection.

ERG and EZH2 interact in prostate cancer cells

These findings raised the intriguing possibility that EZH2 could interact with ERG to catalyse K362 methylation. To explore this possibility, we performed co-immunoprecipitation experiments (Co-IP) with an anti-ERG or an anti-EZH2 antibody in VCaP cells, which endogenously express ERG at high levels. Immunoprecipitation with the anti-EZH2 antibody, but not the control antibody (IP: IgG), led to the co-precipitation of ERG (Figure 26). However, immunoprecipitation with the anti-ERG antibody did not lead to the co-precipitation of EZH2 although the antibody efficiently pulled down ERG (Figure 26). We considered the possibility that the presence of EZH2 protein could mask or compromise the binding of the anti-ERG antibody, which is directed to an epitope mapping within an internal region of ERG of human origin.

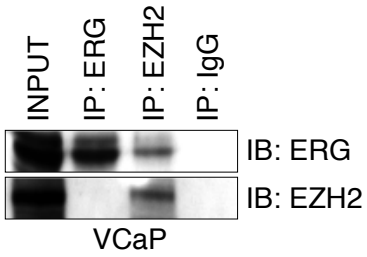

Figure 26**. ERG and EZH2 interact in VCaP cells.** Co-immunoprecipitation (Co-IP) of ERG and EZH2 in VCaP cells with ERG and EZH2 specific antibodies, and IgG as negative control, followed by immunoblotting with the indicated antibodies. INPUT: total lysate.

To solve this issue, we experimentally overexpressed ha-tagged ERG expression vector in PC3 cells, which do not express endogenous ERG, and performed Co-IP experiments 24h from transfection using in parallel anti-HA, anti-ERG and anti-EZH2 antibodies. As shown in figure 27, ERG protein was detected with the anti-ERG antibody in the EZH2-immunoprecipitate, confirming that ERG co-precipitated with EZH2. Importantly, EZH2 protein was detected in the HA-immunoprecipitate, revealing that EZH2 co-precipitated with the ha-tagged ERG. The anti-ERG antibody

was unable to co-immunoprecipitate EZH2 despite its ability to pull-down ERG. Taken together, these data confirmed ERG and EZH2 interaction in both prostate cell types.

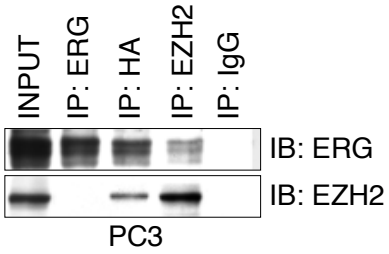

Figure 27**. Exogenous ERG interacts with EZH2 in PC3 cells.** Co-IP of ERG and EZH2 in PC3 cells transiently transfected with ha-tagged ERG expression vector. Lysates were collected and used for Co-IP 24h after transfection.

Because ERG-EZH2 interaction was prominent in prostate cancer cells, we performed additional Co-IP experiments to determine whether that association occurred also in ERG positive human prostate tumors. Protein lysates derived from three ERG positive clinical samples were interrogated by reciprocal Co-IP experiments using anti-ERG and anti-EZH2 antibodies. Importantly, we found a detectable interaction in all tumor samples tested (Figure 28). Collectively, these data demonstrate for the first time that ERG and EZH2 interact also in human prostate tumors.

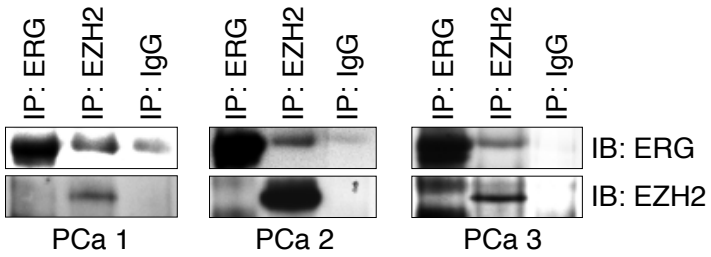

Figure 28. **ERG and EZH2 interact in prostate cancers.** Co-IP of ERG and EZH2 in ERG positive prostate cancers (PCa) followed by immunoblotting with ERG and EZH2 antibodies. Some EZH2 non-specific bands appear in the ERG immunoprecipitation of sample PCa 3, as the correct band is the one in EZH2 IP.

Identification of ERG domain(s) involved in the interaction with EZH2

In order to better define the region of ERG involved in the interaction with EZH2, we generated multiple ha-tagged ERG truncated expression vectors (Table 5 on page 71 and figure 29). Ha-ΔC-ERG lacks 88 amino acids located at the C-terminal region but still retains both pointed (PNT) and ETS domain; ha-P-I-ERG lacks 168 amino acids at the C-terminal region including the ETS domain; ha-P-ERG lacks 278 amino acids at the C-terminal region but still keeps the pointed domain; lastly ha-N-ERG lacks both ETS and PNT domains. We also used the N-terminal truncated ERG2 isoform, which lacks the first 18 N-terminal amino acids, 5 amino acids in the PNT domain and 24 amino acids transcribed from exon a72. It still retains both pointed (PNT) and ETS domain. We then expressed full-length ERG, N-terminal truncated ERG2 or the truncated constructs of ERG in PC3 cells and checked their expression with the anti-ERG and anti-HA antibodies. As shown in figure 30, the expression of full-length ERG and the truncated forms, namely ERG2, ha-ΔC-ERG, ha-P-I-ERG, ha-P-ERG and ha-N-ERG was comparable, while the expression of the shorter construct, ha-N-ERG, which has a molecular weight of 15 kDa, was reduced due to lower efficiency of transfection.

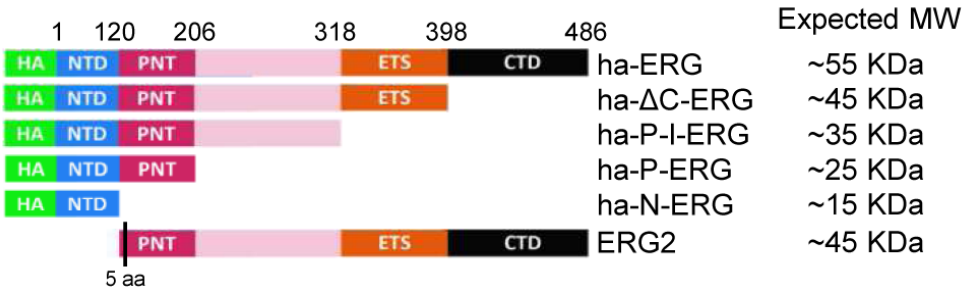

Figure 29. **ERG truncated constructs.** Diagram of truncated ERG constructs generated and the retained domains. Expected molecular weight (MW) is also reported. NTD=N-terminal domain; PNT=pointed domain; ETS=ETS domain; CTD=C-terminal domain. HA=hemagglutinin tag.

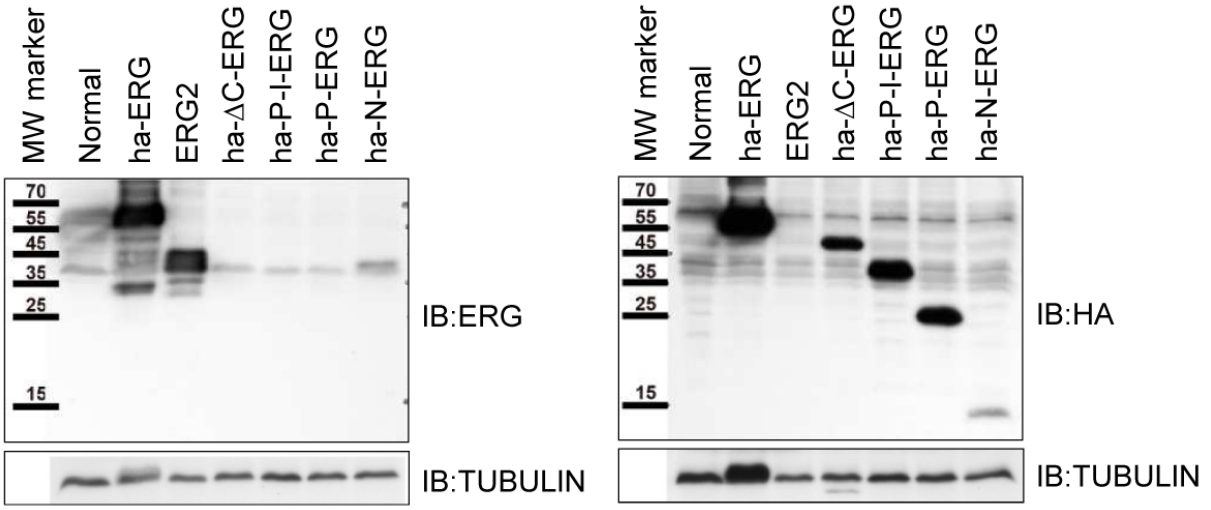

Figure 30. **ERG constructs immunodetection.** Immunodetection of the indicated ERG constructs using anti-ERG (*left panel*) and anti-HA (*right panel*) antibodies. 24h after transfection PC3 cells were healthy and were processed for protein extraction.

Next, we performed Co-IP experiments in PC3 cells transiently transfected with ERG truncated vectors using in parallel anti-HA, anti-ERG and anti-EZH2 antibodies. As shown in figure 31, immunoprecipitation with the anti-EZH2 antibody revealed that the N-terminal truncated-ERG2 did not co-precipitate with EZH2. Immunoprecipitation with the anti-HA antibody was performed as a negative control, since the N-terminal truncated ERG2 construct has not the ha-tag. These data indicated that the region responsible for ERG binding to EZH2 was present in the N-terminal region of ERG. Indeed, all the other constructs retaining the N-terminal domain exhibited a detectable interaction with EZH2, indicating that the major domains responsible for ERG binding to EZH2 were present in that specific region of ERG (Figure 32). Notably, in the case of ha-N-ERG (Figure 32), we could detect EZH2 in the ha-ERG-immunoprecipitate, while we could not detect ha-N-ERG in the EZH2-immunoprecipitate. We consider the possibility that some technical problems concerning the low molecular weight and the low level of expression of this ERG construct could affect its detection.

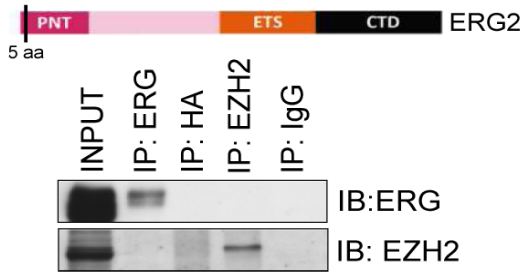

Figure 31. **ERG2 does not interact with EZH2.** Binding of N-terminal truncated ERG2 to endogenous EZH2 was assessed by Co-IP experiments in PC3 transiently transfected. Lysates were prepared for Co-IP 24h after transfection.

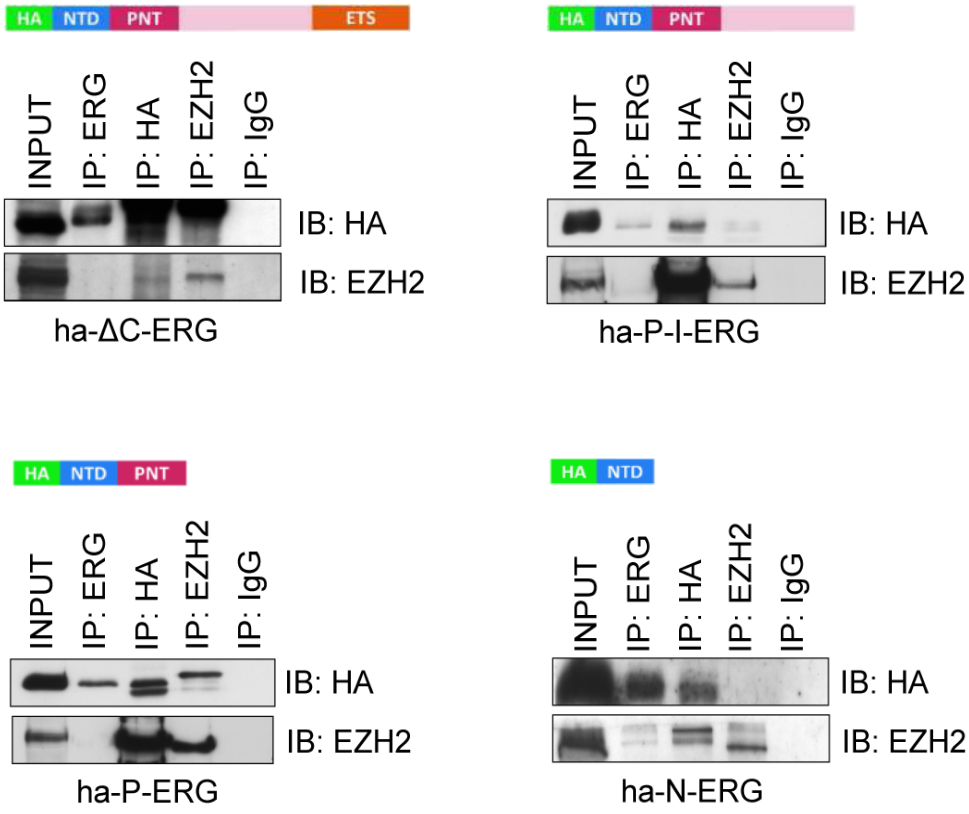

Figure 32**. Evaluation of the ERG domain involved in the interaction with EZH2.** Binding of ha-ΔC-ERG, ha-P-I-ERG, ha-P-ERG and ha-N-ERG to endogenous EZH2 assessed by Co-IP experiments in PC3 cells transiently transfected with the ERG constructs. Cells have been lysated 24h after transfection for Co-IP.

To further prove that the interaction occurred in the N-terminal region of ERG, we generated a his-tagged ERG construct lacking the N-terminal portion of the protein (his-ΔN-ERG). Histidine pull-down and immunoprecipitation with anti-EZH2 and anti-ERG antibodies, following transient transfection in PC3 cells, showed

that the ΔN-ERG construct was unable to bind EZH2, confirming that the N-terminal region of ERG is essential for the interaction with EZH2 (Figure 33).

Importantly, performing Histidine pull-down in VCaP cells upon transient overexpression of the his-tagged ΔN-ERG mutant, we found that the construct was not methylated (Figure 34), suggesting that the interaction was also essential for ERG methylation.

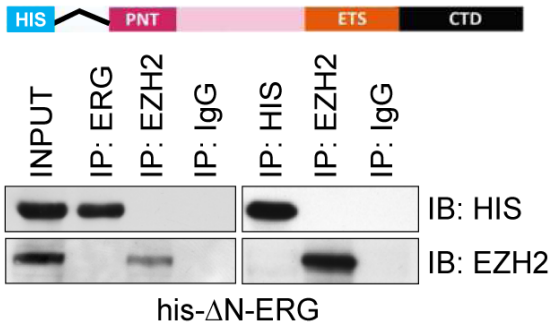

Figure 33. **The ΔN-ERG construct does not interact with EZH2.** Binding of his-ΔN-ERG3 to endogenous EZH2 assessed by Co-IP and Histidine pull-down (IP: HIS) in PC3 cells transiently transfected. Cells have been lysated 24h after transfection.

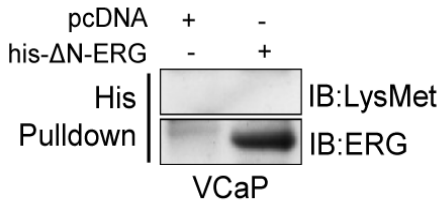

Figure 34. **The ΔN-ERG construct is not methylated.** Methylation of his-ΔN-ERG construct evaluated by Histidine pull-down followed by immunoblot with a pan-methyl lysine antibody in VCaP cells transiently transfected. Cells have been harvested and lysated 24h after transfection.

Identification of EZH2 domain(s) involved in the interaction with ERG

With a similar approach, we defined the minimal EZH2 region responsible for the interaction with ERG. To map this region, we generated different EZH2 truncated expression vectors (Table 5 and figure 35). Myc-EZH2-ΔSET lacks 141 amino acids located at the C-terminal region that represents the SET catalytic domain of the protein; myc-EZH2-ΔCXC lacks 243 amino acids at the C-terminal region including the SET domain and a region rich of cysteins; lastly myc-EZH2-1-340 is a fragment which retains only 340 amino acids at the N-terminal region that correspond to the domain of interaction between EZH2 and the DNA methyltransferases 1, 3A and 3B (DNMT1, DNMT3A-B), and the PRC2 component EED.

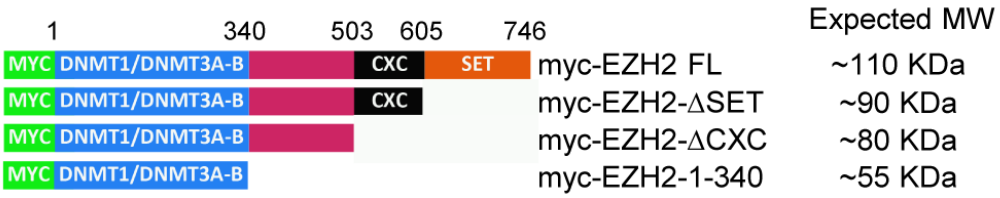

Figure 35. **EZH2 truncated constructs.** Diagram of truncated EZH2 constructs generated and the retained domains. Expected molecular weight (MW) is also reported. DNMT1/DNMT3A-B=region of binding for DNMT1 and DNMT3A-B proteins; CXC=cysteines rich domain; SET=SET catalytic domain. MYC=myc tag;

We then expressed full-length EZH2 or the truncated forms in PC3 cells and checked their expression with the anti-EZH2 and the anti-MYC antibodies. As shown in figure 36, the expression of full-length myc-EZH2 and the truncated forms, namely myc-EZH2-ΔSET, myc-EZH2-ΔCXC and myc-EZH2-1-340, is comparable. Therefore, we co-expressed ha-tagged ERG construct along with the myc-tagged full-length or truncated EZH2 constructs in PC3 cells. Next, we collected lysates 24h after transfection and performed Co-IP experiments using anti-HA, anti-EZH2 and anti-MYC antibodies. Immunoprecipitation with the anti-HA antibody and immunoblotting with the anti-EZH2 antibody revealed that the myc-EZH2-ΔSET and

the myc-EZH2-ΔCXC constructs exhibited detectable interaction with ERG, while the myc-EZH2-1-340 fragment was unable to immunoprecipitate ERG (Figure 37).

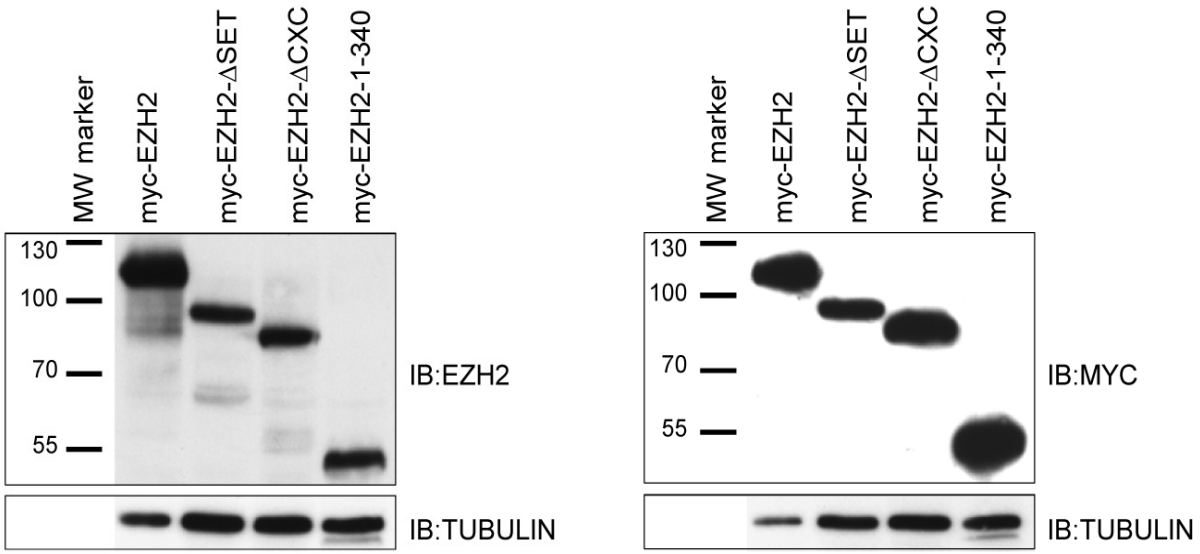

Figure 36. **EZH2 constructs immunodetection.** Immunodetection of the indicated EZH2 constructs using anti-EZH2 (*left panel*) and anti-Myc (*right panel*) antibodies. PC3 cells have been lysated and analysed 24h after transfection.

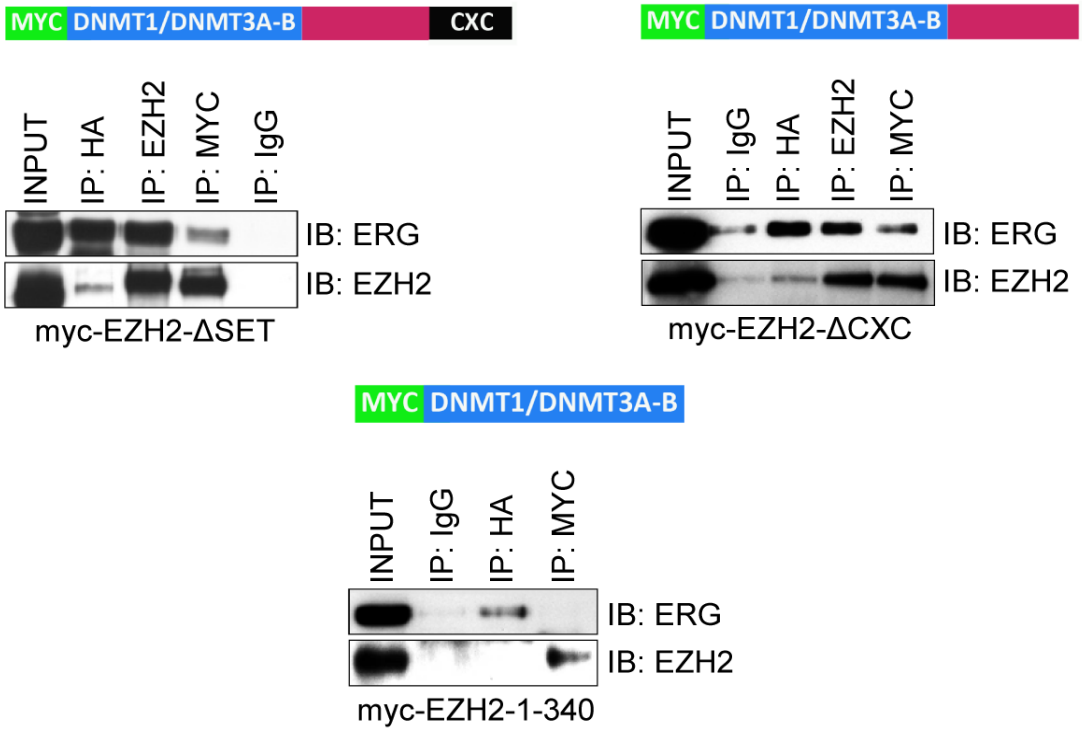

Figure 37. **Evaluation of the EZH2 domain involved in the interaction with ERG.** Binding of myc-EZH2-ΔSET, myc-EZH2-ΔCXC and myc-EZH2-1-340 to ha-ERG assessed by Co-IP experiments in PC3 cells transiently transfected. Cells have been lysated for Co-IP 24h after transfection.

Taken together, these data indicated that the SET domain and the CXC region of EZH2 are dispensable for binding to ERG, while the ERG interacting domain was within the region from amino acids 340 to 503.

EZH2 enhances ERG transcriptional activity and the interaction is necessary for this process

We next addressed the functional relevance of the interaction and ERG methylation. We hypothesized that EZH2 by interacting with ERG could mediate ERG methylation and affect ERG transcriptional activity. To test this hypothesis, we took advantage of an ETS promoter reporter, containing an ETS responsive element, and evaluated the effect of ERG and EZH2 on the activity of this promoter in the ERG-negative LNCaP and RWPE1 cells. Interestingly, we observed that concomitant expression of ERG and wild type EZH2 enhanced the induction of the ETS responsive reporter in LNCaP cells, whereas the EZH2-ΔSET mutant, lacking methyltransferase activity, failed to do so (Figure 38A). Consistently, knockdown of EZH2 abolished the induction of the ETS reporter mediated by ERG (Figure 38B), indicating that ERG and EZH2 cooperatively activated ETS targets. In RWPE1 cells, concomitant expression of wild type EZH2 but not EZH2-ΔSET increased ERG-induced ETS reporter activity (Figure 38C), underlining that EZH2 significantly increased ERG transcriptional activity and that the EZH2 methyltransferase activity was involved in this process. Furthermore, the ΔN-ERG mutant, unable to interact with EZH2, failed to activate the ETS promoter reporter and did not cooperate with EZH2 in enhancing the luciferase activity (Figure 39). Taken together, these data strongly indicated that EZH2 promoted the trans-activating function of ERG and both direct interaction and EZH2 catalytic activity were instrumental in this process.

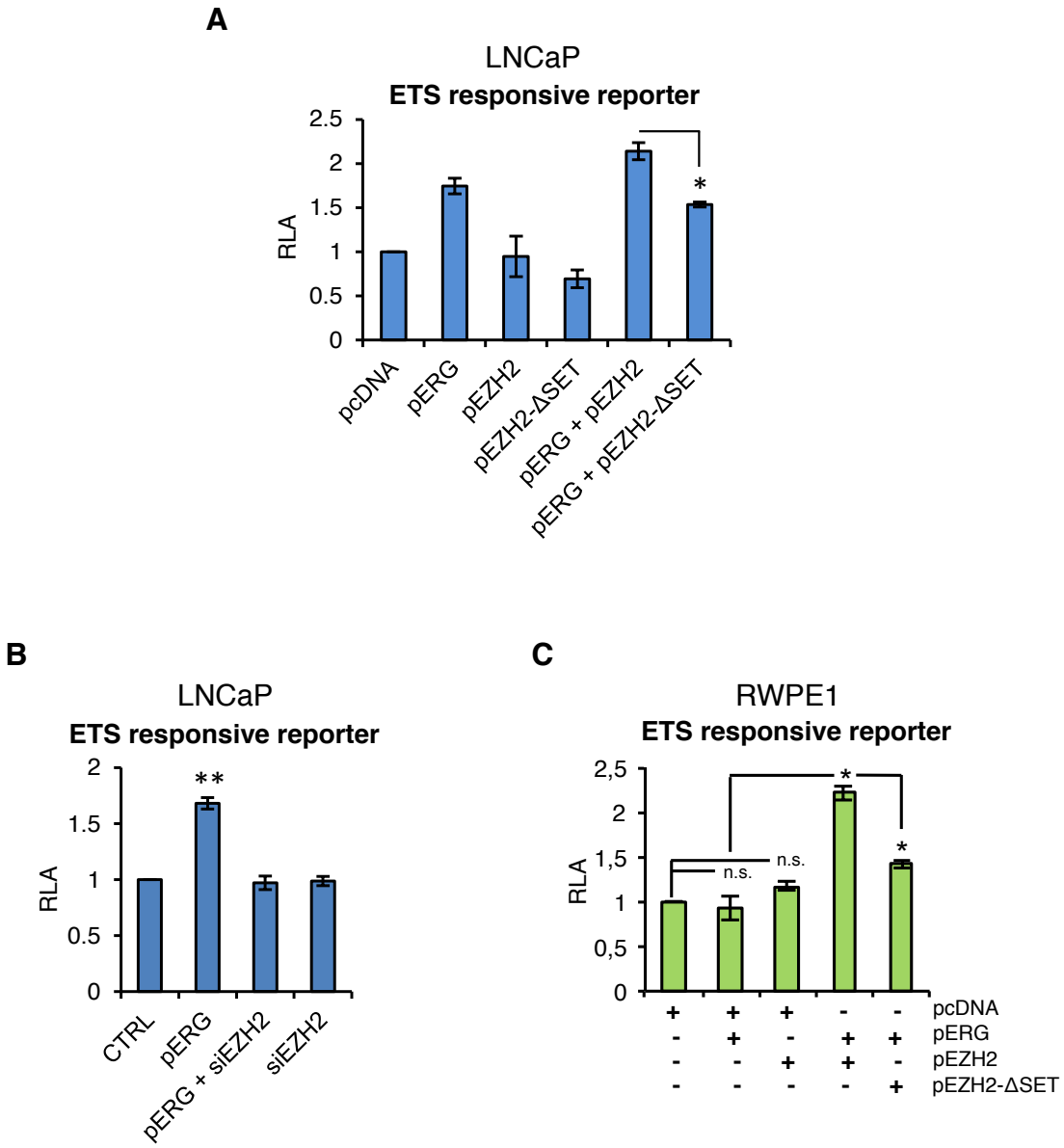

Figure 38**. EZH2 promotes the trans-activating function of ERG.** (**A**) Activity of ETS responsive reporter in LNCaP cells transfected with the indicated expression vectors. (**B**) ETS responsive reporter activity in LNCaP cells with ERG overexpression and/or EZH2 knockdown. (**C**) ETS responsive reporter activity in RWPE1 cells transfected with the indicated vectors including WT-EZH2 and EZH2-ΔSET. Luciferase reporter activity was measured after 24h, and results are expressed as the ratio of luciferase activity to Renilla and then represented as Relative Luciferase Activity (RLA) as fold change to pcDNA or control (CTRL= pcDNA+siGL3). * $p<0.05$; ** $p<0.01$; n.s. not significant.

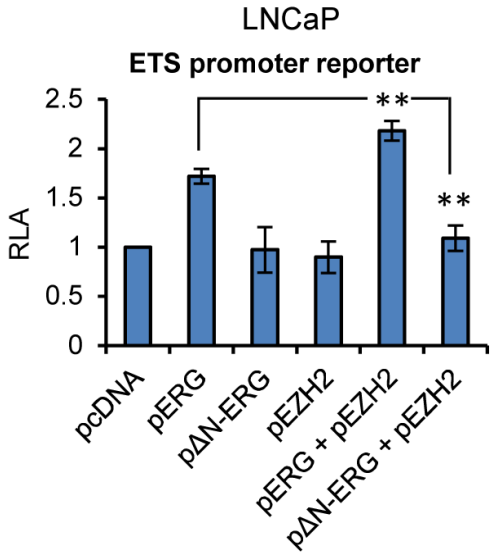

Figure 39**. ERG-EZH2 interaction is necessary for ERG activity.** ETS responsive reporter activity in LNCaP cells transfected with the indicated vectors including WT-ERG and ΔN-ERG. Luciferase reporter activity was measured after 24h, and results are expressed as the ratio of luciferase activity to Renilla and then represented as Relative Luciferase Activity (RLA) as fold change to pcDNA. ** $p<0.01$.

ERG and EZH2 cooperate to activate IL-6 expression

Next, to dissect the role of ERG-EZH2 connection on native promoters, we began by evaluating IL-6 gene, which is frequently overexpressed in prostate tumors and has an important role in prostate carcinogenesis (Culig and Puhr 2012). Moreover, IL-6 was recently reported to be under the control of EZH2 in breast cancer cells (Lee, Li et al. 2011). Thus, we hypothesized that it could be a target of ERG-EZH2 in VCaP cells. In keeping with this, we identified a highly scored ETS binding site (EBS) on the IL-6 promoter, and consequently we assessed the occupancy of ERG and EZH2 around this site by chromatin immunoprecipitation (ChIP). Using a set of primers spanning the promoter around the putative EBS, either proteins were found to be highly enriched on IL-6 promoter (Figure 40, *left panel*), along with accumulation of active (H3Ac) compared to repressive (H3K27me3) histone marks in ERG-expressing LNCaP (LNCaP ERG) compared to control LNCaP cells (Figure 40, *right panel*). Consistently, ERG expression increased IL-6 transcrip-

tion and promoter activity, and EZH2 knockdown following ERG overexpression prevented IL-6 induction, indicating that ERG and EZH2 cooperatively induced the gene (Figure 41).

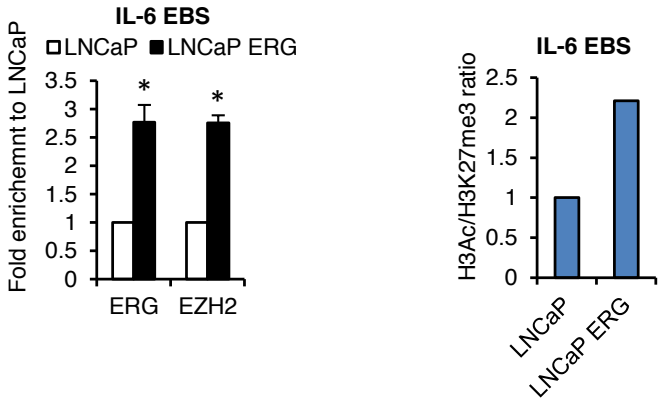

Figure 40**. ERG and EZH2 occupancy on IL-6 promoter in LNCaP cells.** ERG and EZH2 occupancy on IL-6 promoter at the ETS binding site (EBS) in LNCaP and LNCaP ERG cells determined by chromatin immunoprecipitation (ChIP) (*left panel*). Results are expressed as the ratio of immunoprecipitated DNA to Input DNA and then represented as fold change to LNCaP cells. * p<0.05. On the right, histone 3 acetylation (H3Ac) and histone 3 lysine 27 tri-methylation (H3K27me3) occupancy on IL-6 promoter evaluated by ChIP. Data are shown as H3Ac/H3K27me3 ratio normalized to control LNCaP cells.

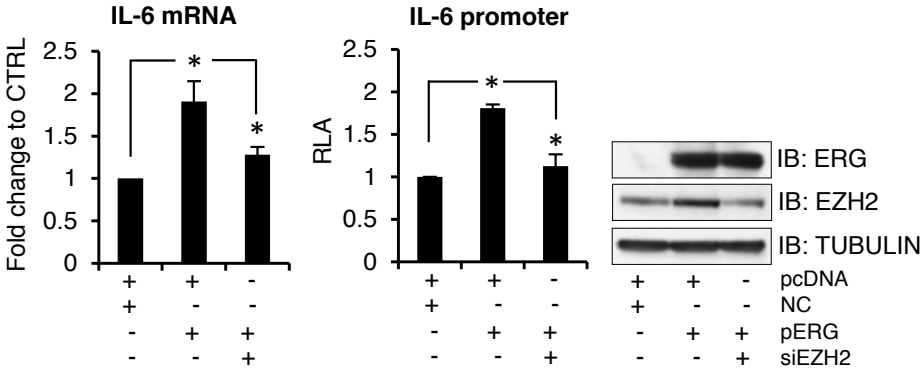

Figure 41**. ERG and EZH2 cooperate in IL-6 induction.** qRT-PCR analysis of IL-6 mRNA (*left panel*) and IL-6 promoter activity (*middle panel*) in LNCaP cells with ERG overexpression and EZH2 knockdown. Total RNA and luciferase reporter activity were measured 48h after transfection. Expression of the indicated proteins was verified by immunoblotting (*right panel*). * p<0.05.

Furthermore, while ERG and EZH2 cooperated to induce IL-6 transcription, the EZH2-ΔSET mutant did not (Figure 42), pointing the relevance of EZH2 catalytic function.

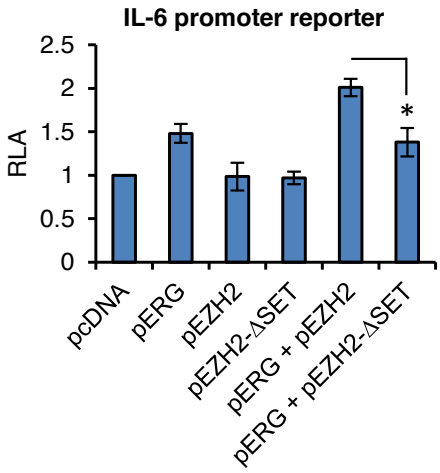

Figure 42. **EZH2 catalytic function is relevant for sustaining IL-6 expression.** IL-6 promoter reporter activity in LNCaP cells transfected with the indicated expression vectors. Luciferase reporter activity was measured 24h after transfection and results are expressed as the ratio of luciferase activity to Renilla and then represented as Relative Luciferase Activity (RLA) as fold change to pcDNA. * p<0.05.

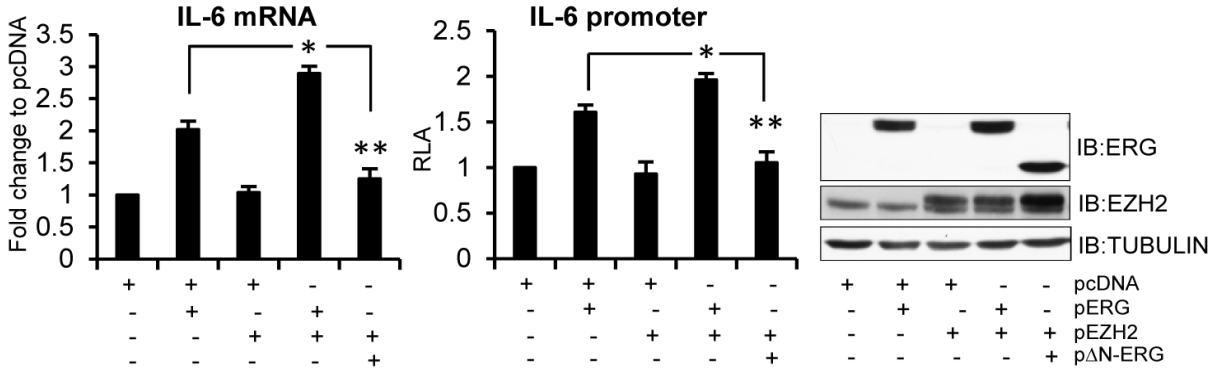

Figure 43. **ERG-EZH2 interaction is necessary for ERG-mediated IL-6 induction.** IL-6 mRNA determined by qRT-PCR analysis (*left panel*) and IL-6 promoter activity by luciferase reporter assay (*middle panel*) in LNCaP cells transfected with the indicated plasmids. Total RNA and luciferase reporter activity were measured 24h after transfection. Expression of the indicated proteins was verified by immunoblotting (*right panel*). * p<0.05; ** p<0.01.

To further demonstrate that ERG-EZH2 interaction was crucial for their cooperation, we took advantage of the ΔN-ERG construct unable to bind to EZH2. As shown in figure 43, the ΔN-ERG construct could not induce IL-6 transcription and synergize with EZH2, supporting the relevance of ERG-EZH2 interaction for the gene transcriptional enhancement.

ERG and EZH2 occupied the IL-6 promoter also in VCaP cells (Figure 44), and

co-recruitment of ERG and EZH2 was confirmed by ChIP-reChIP experiments, performing first ChIP with an antibody against ERG or EZH2, and observing reciprocal and significant enrichment of EZH2 and ERG respectively on the EBS of IL-6 promoter (Figure 45).

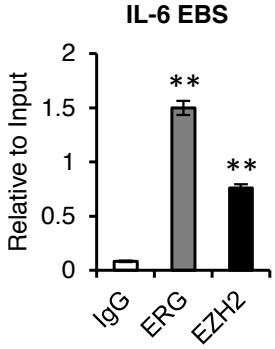

Figure 44. **ERG and EZH2 occupancy on IL-6 promoter in VCaP cells.** ChIP analysis of ERG and EZH2 occupancy around the ETS binding site (EBS) of the IL-6 promoter in VCaP cells. ** p<0.01.

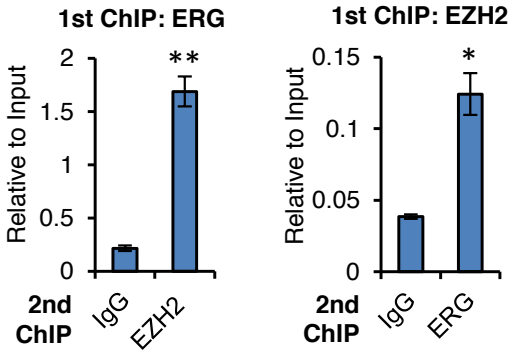

Figure 45. **ERG and EZH2 co-occupy IL-6 promoter in VCaP cells.** Re-ChIP assay was performed to assess co-localization of ERG and EZH2 on IL-6 promoter. First ChIP and second ChIP antibodies were indicated as the chart title and X axis labels, respectively. Quantification of binding was represented as the ratio of immunoprecipitated DNA during second ChIP to Input DNA following first ChIP. * p<0.05; ** p<0.01.

A significant decrease in IL-6 expression was observed following ERG and EZH2 knockdown in VCaP cells (Figure 46, *left panel*) with parallel changes in the IL-6 promoter activity upon combined and single knockdown of ERG and EZH2 (Figure 46, *middle panel*). Consistently, knockdown of both ERG and EZH2 in VCaP cells led to accumulation of repressive (H3K27me3) histone marks on the IL-6 promoter, (Figure 47), in line with the trans-activating function of the ERG-EZH2 complex.

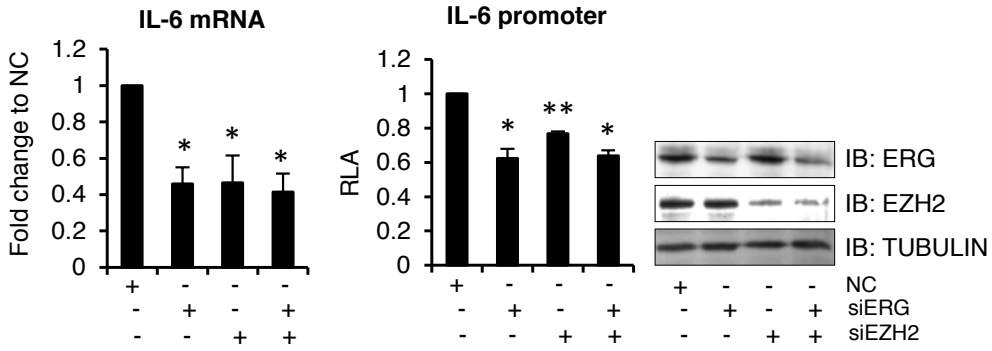

Figure 46. **ERG and EZH2 sustain IL-6 expression in VCaP cells.** qRT-PCR analysis of IL-6 mRNA (*left panel*) and IL-6 promoter activity (*middle panel*) in VaP cells upon ERG and EZH2 depletion. Total RNA and luciferase reporter activity were measured 48h after transfection. Immunoblotting analysis of the indicated proteins is shown on the right panel. * p<0.05; ** p<0.01.

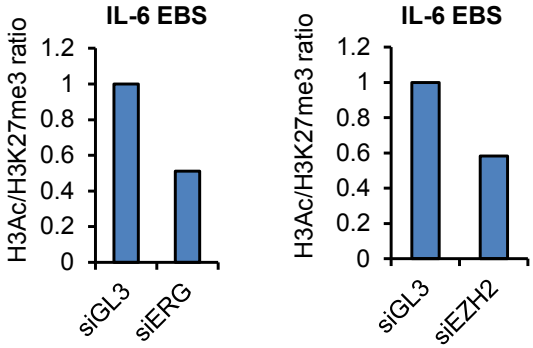

Figure 47**. Histone marks changes in VCaP cells upon ERG and EZH2 knockdown.** Histone 3 acetylation (H3Ac) and histone 3 lysine 27 tri-methylation (H3K27me3) occupancy on the IL-6 promoter in VCaP cells upon ERG (*left panel*) and EZH2 (*right panel*) depletion shown as H3Ac/H3K27me3 ratio normalized to control (siGL3) VCaP cells.

ERG methylation enhances ERG transcriptional activity

To further examine the consequences of K362 methylation on ERG function, we compared the activity of WT-ERG and ERG-K362A mutant after transient expression in LNCaP cells. ChIP experiments revealed that both WT-ERG and ERG-K362A bound to IL-6 promoter, although ERG-K362A exhibited significantly weaker binding to the promoter (Figure 48). Importantly, ERG-K362A was less effective than WT-ERG in inducing IL-6 mRNA and promoter activity (Figure 49). Furthermore, ERG-K362A did not cooperate with EZH2 to activate IL-6 transcription (Figure 49).

Thus, despite of its reduced but still present binding on IL-6 promoter, the methylation defective ERG-K362A mutant had reduced trans-activating ability. Indeed, it was unable to modulate gene expression and to synergize with EZH2, strongly supporting the relevance of EZH2-induced ERG methylation for ERG activity.

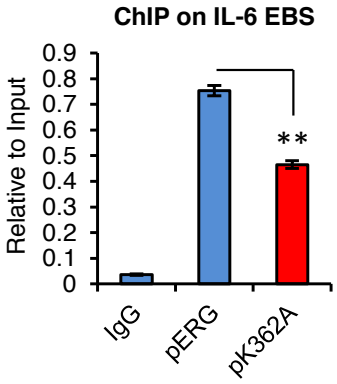

Figure 48**. ERG-K362A binding to IL-6 promoter.** ERG occupancy on IL-6 promoter was evaluated by ChIP in LNCaP cells transfected with wild type ERG (pERG) or ERG-K362A mutant (pK362A). ** p<0.01.

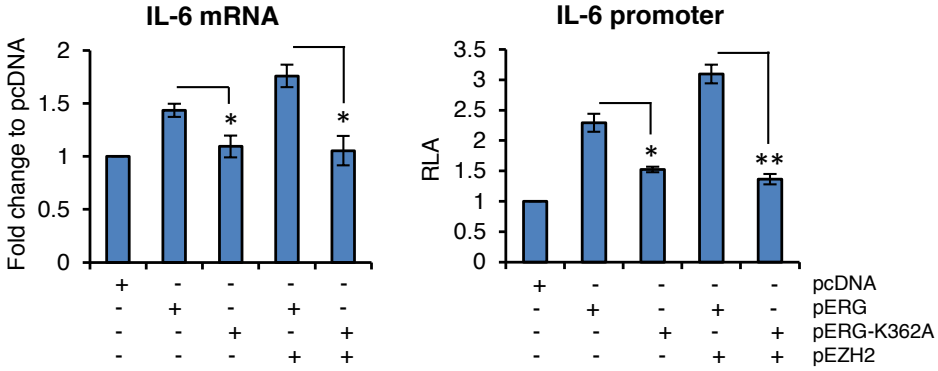

Figure 49**. ERG-K362A is unable to cooperate with EZH2 to induce IL-6 transcription.** qRT-PCR analysis of IL-6 mRNA (*left panel*) and IL-6 promoter activity (*right panel*) in LNCaP cells transiently transfected with the indicated plasmids. Total RNA and luciferase reporter activity were analyzed 24h after transfection. * p<0.05; ** p<0.01.

In order to understand whether ERG and EZH2 formed both activating and repressive complexes on distinct promoters, we examined the expression of Nkx 3.1, an androgen-regulated gene expressed in prostate epithelial cells that we previously

reported to be epigenetically repressed by ERG, as a consequence of EZH2-induced H3K27 methylation (Kunderfranco, Mello-Grand et al. 2010). Consistently with our previous findings, ERG cooperated with EZH2 in repressing Nkx 3.1 expression, as knockdown of EZH2 prevented Nkx 3.1 repression by ERG in LNCaP cells upon ERG overexpression (Figure 50A).

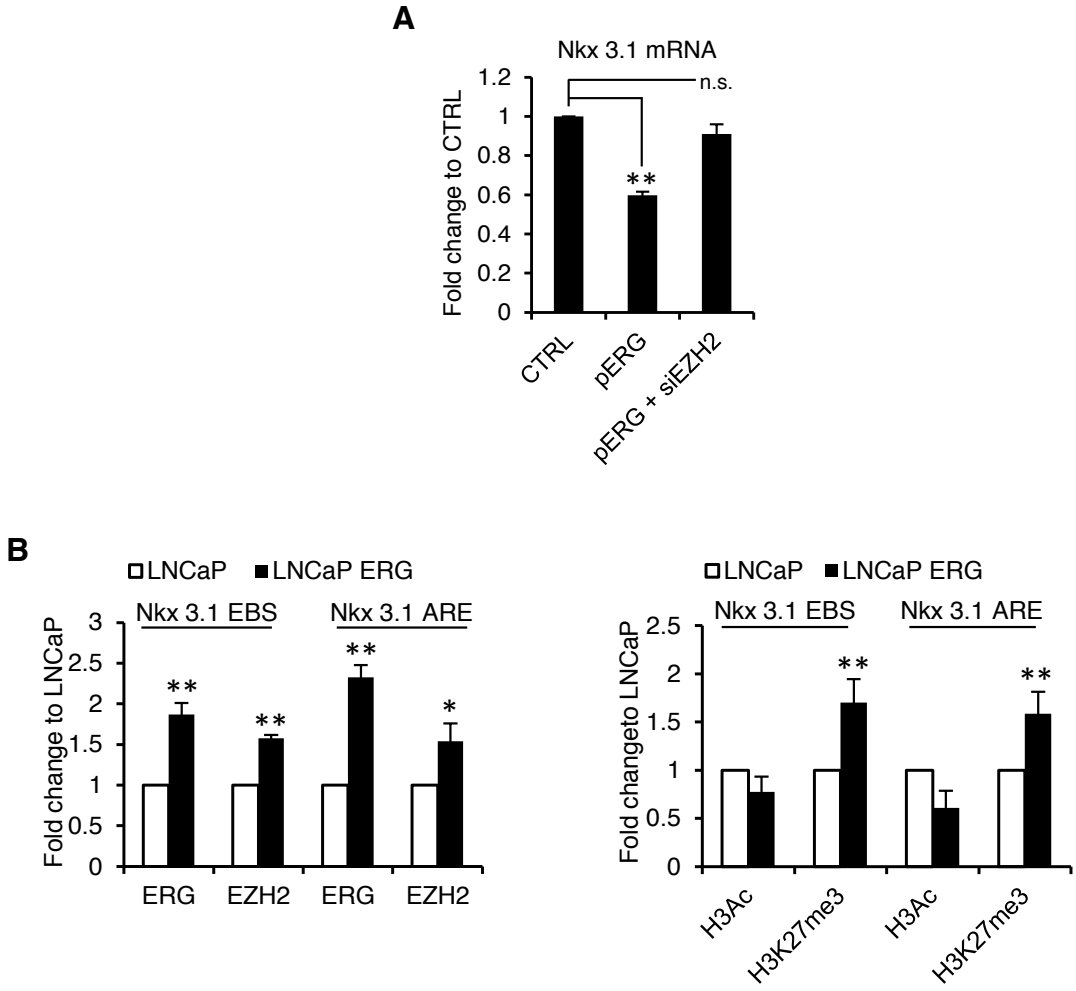

Figure 50. **Nkx 3.1 expression is affected by ERG and EZH2.** (**A**) Nkx 3.1 mRNA evaluated by qRT-PCR in LNCaP cells 48h after ERG overexpression and EZH2 knockdown. (CTRL=pcDNA+siGL3). (**B**) ERG and EZH2 occupancy (*left panel*), and histone 3 acetylation (H3Ac) and lysine 27 tri-methylation (H3K27me3) occupancy (*right panel*) on Nkx 3.1 promoter evaluated by ChIP in the region encompassing the ETS binding site (EBS) and the androgen responsive element (ARE) in LNCaP control and upon ERG overexpression. Results are expressed as the ratio of immunoprecipitated DNA to Input DNA and represented as fold change to LNCaP control. * $p<0.05$; ** $p<0.01$; n.s. not significant.

Moreover, both ERG and EZH2 proteins occupied Nkx 3.1 promoter in a previously identified EBS (Kunderfranco, Mello-Grand et al. 2010) and in a reported androgen responsive element (ARE) (Yamane, Toumazou et al. 2006) (Figure 50B, *left panel*). This corresponded to accumulation of repressive (H3K27me3) histone marks on the promoter in LNCaP ERG compared to LNCaP cells (Figure 50B, *right panel*). Interestingly, the ERG-K362A mutant exhibited reduced binding to the Nkx 3.1 promoter (Figure 51) and was less effective than WT-ERG in repressing Nkx 3.1 (Figure 52), indicating that K362 methylation enhanced also trans-repression function of ERG. Taken together, these findings suggested that ERG and EZH2 could form both activating and repressive complexes on distinct promoters.

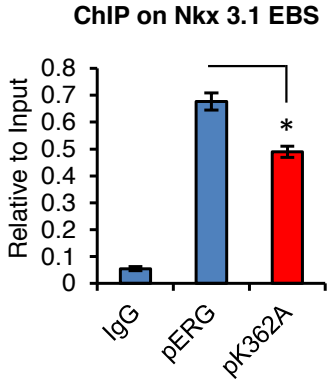

Figure 51**. ERG-K362A binding to Nkx 3.1 promoter is weaker than wild type ERG.** ERG occupancy on Nkx 3.1 promoter was evaluated by ChIP in LNCaP cells transfected with wild type ERG (pERG) or ERG-K362A mutant (pK362A). * p<0.05.

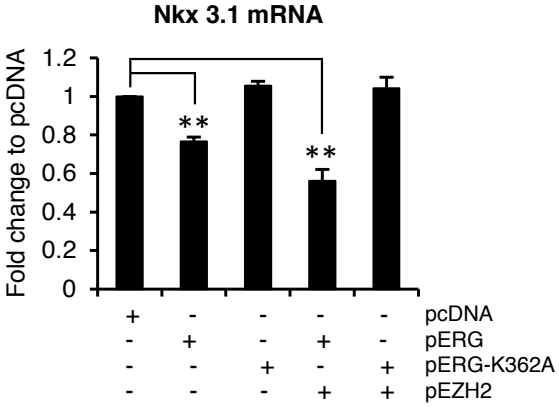

Figure 52**. ERG-K362A is unable to cooperate with EZH2 to repress Nkx 3.1 transcription.** qRT-PCR analysis of Nkx 3.1 mRNA in LNCaP cells transiently transfected with the indicated plasmids. Total RNA was analyzed 24h after transfection. ** p<0.01.

To better characterize activating and repressive complexes, we examined whether the presence of SUZ12, a well-known member of the PRC2 repressive complex together with EZH2, could discriminate the diverse complexes. Interestingly, in VCaP cells enrichment of SUZ12 was present only on Nkx 3.1 promoter and absent on IL-6 promoter, despite similar promoter occupancy of ERG and EZH2 (Figure 53), suggesting that SUZ12 recruitment was solely associated with ERG gene repression. Moreover, knockdown of SUZ12 prevented ERG-induced repression of Nkx 3.1 while did not affect IL-6 trans-activation in LNCaP upon ERG overexpression (Figure 54).

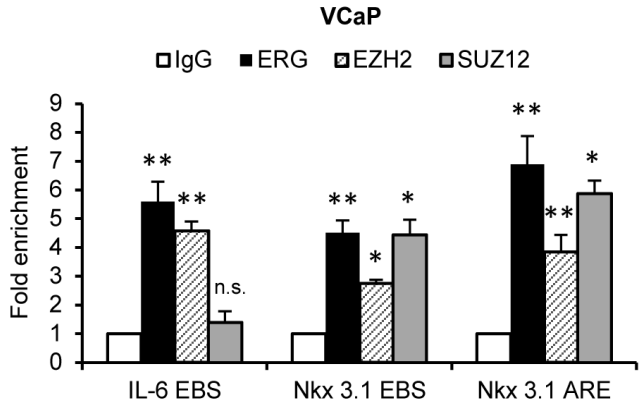

Figure 53. **SUZ12 occupancy in VCaP cells is restricted to repressed genes.** ERG, EZH2 and SUZ12 occupancy on IL-6 and Nkx 3.1 promoters evaluated by ChIP in VCaP cells. * p<0.05; ** p<0.01; n.s. not significant.

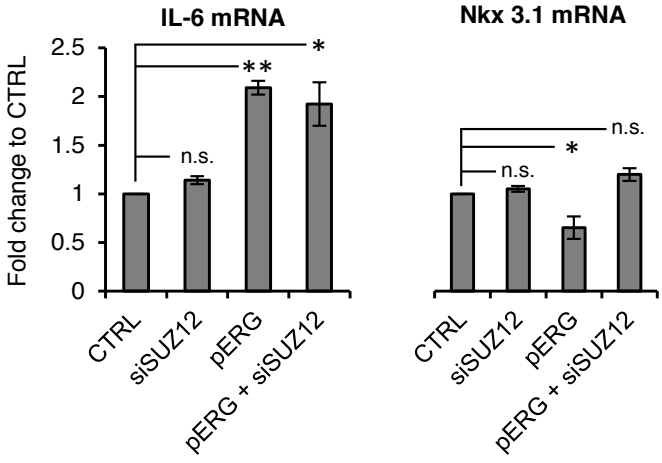

Figure 54. **SUZ12 depletion affects ERG transcriptional repression.** qRT-PCR analysis of IL-6 and Nkx 3.1 mRNA in LNCaP cells 48h after transfection with the indicated plasmids and siRNAs. Results are expressed as the ratio of IL-6 and Nkx 3.1 mRNA to β-actin, then represented as fold change to control (CTRL=pcDNA+siGL3). * p<0.05; ** p<0.01; n.s. not significant.

In support of this mechanism and consistently with the formation of distinct complexes, ChIP-reChIP experiments showed co-localisation of SUZ12, ERG and EZH2 on Nkx 3.1 promoter (Figure 55). However, neither ERG nor EZH2 interacted with SUZ12 on IL-6 promoter (Figure 55). Collectively, these data confirmed that ERG and EZH2 formed canonical PRC2-dependent repressive complexes in presence of SUZ12 and, in parallel, non-canonical PRC2-independent trans-activating complexes without SUZ12 presence.

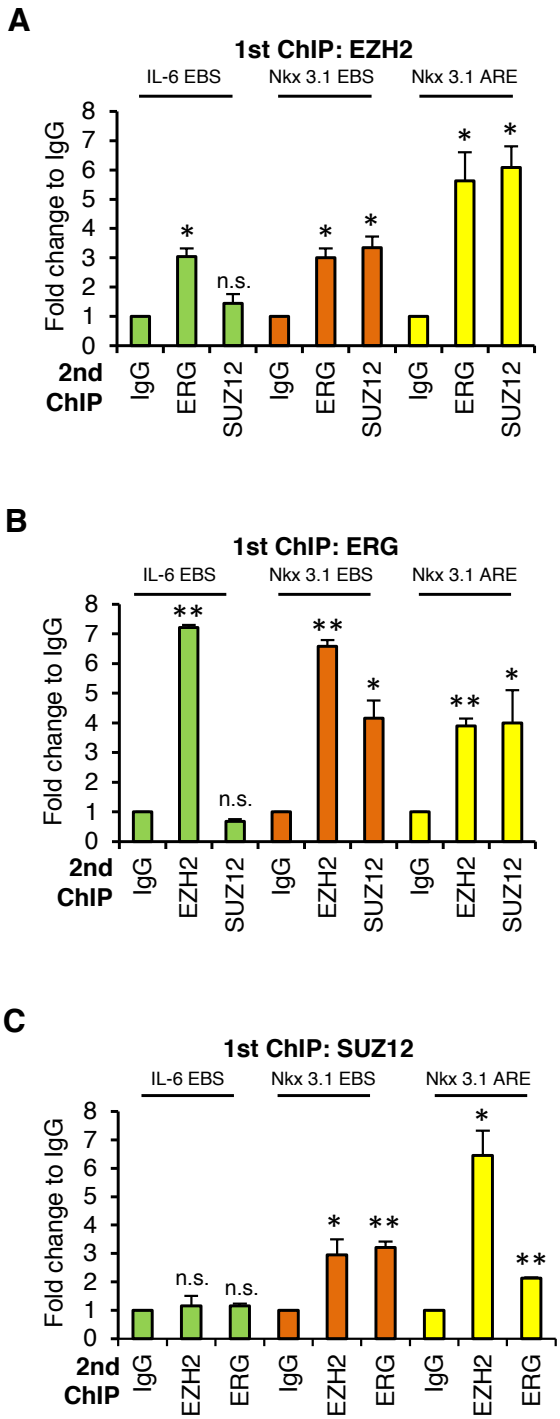

Figure 55. **ERG, EZH2 and SUZ12 co-occupancy in VCaP cells.** Re-ChIP assay was performed to assess co-localization of EZH2, ERG and SUZ12 on IL-6 and Nkx 3.1 promoters. First ChIP and second ChIP antibodies were indicated as the chart title and X axis labels, respectively. Quantification of binding was represented as fold enrichment relative to IgG second ChIP. * $p<0.05$; ** $p<0.01$; n.s. not significant.

Functional characterization of ERG methylation

Our data indicated that the transcriptional functions of ERG were affected by K362 methylation. To assess the functional relevance of ERG methylation, we established stable ERG-K362A expressing LNCaP cells. Through ERG immuno-precipitation, we confirmed abrogation of ERG methylation in this cell line, while the positivity to ERG was observed (Figure 56). Then, to globally assess the impact of ERG methylation on transcription, we compared gene expression profiles of control, WT-ERG and ERG-K362A expressing LNCaP cells. Both WT-ERG and ERG-K362A induced significant changes in the transcriptional program compared to control ERG-negative LNCaP EV cells. However, the transcriptional changes in both activated and repressed genes were significantly smaller for ERG-K362A than WT-ERG (Figure 57). Thus, impairing methylation reduced the overall transcriptional activity of ERG.

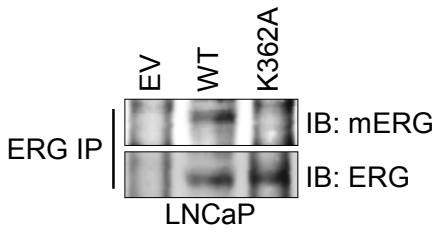

Figure 56. **ERG-K362 is not methylated.** IP of WT-ERG (WT) and ERG-K362A mutant (K362A) in LNCaP cells with stable overexpression followed by immunoblotting with mERG and ERG antibodies.

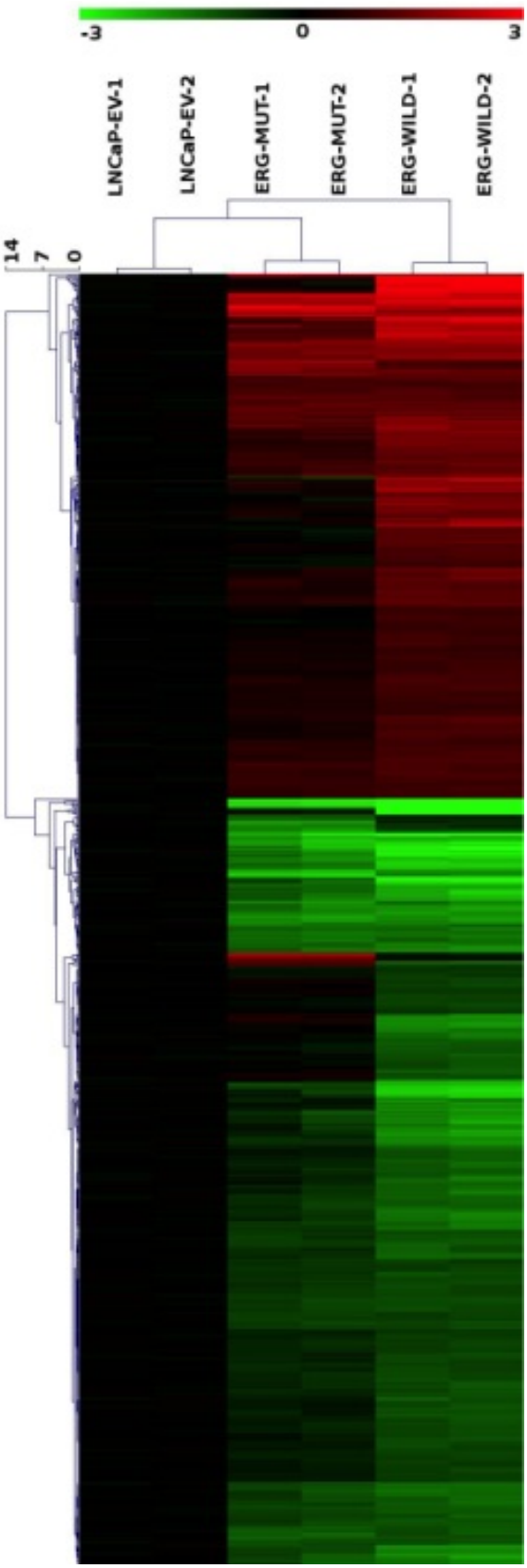

Figure 57. **K362 methylation enhances ERG transcriptional activity.** Heat Map showing transcripts significantly modulated by WT-ERG and ERG-K362A expression vectors compared to control (LNCaP EV). Scale bar shows LogRatio range, red color indicates up-regulation and green down-regulation.

We extracted a list of genes that were more significantly modulated by WT-ERG compared to ERG-K362A, defining a subset of potentially methylation-dependent ERG (mERG) targets. These putative mERG targets were significantly enriched in ERG positive compared to ERG negative primary prostate tumors (Figure 58). Interestingly, functional annotation of mERG targets using MetaCore pathway analysis revealed among the up-regulated genes enrichment of pathways (e.g., ECM remodelling, TGF-β induced EMT) related to tumor progression and metastatic spread (Figure 59).

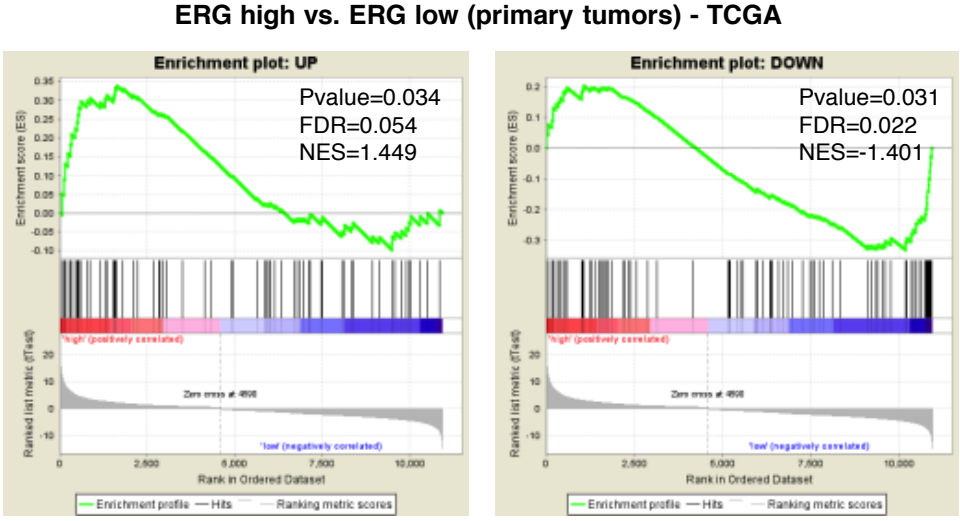

Figure 58. **Methylation sensitive genes are significantly enriched in primary prostate tumors with ERG elevation (ERG high).** Gene set enrichment analysis (GSEA) showing in the TCGA dataset of primary prostate tumors using the lists of methylation-dependent genes (up-regulated and down-regulated) and comparing ERG high versus ERG low expressing tumors. P value, false discovery rate (FDR) and normalized enrichment score (NES) are indicated.

In line with this finding, the methylation-defective ERG-K362A mutant was less capable of promoting migration in the *in vitro* scratch/wound healing assay (Figure 60), survival in anoikis (Figure 61) and anchorage-independent growth (Figure 62) compared to WT-ERG when expressed in LNCaP cells.

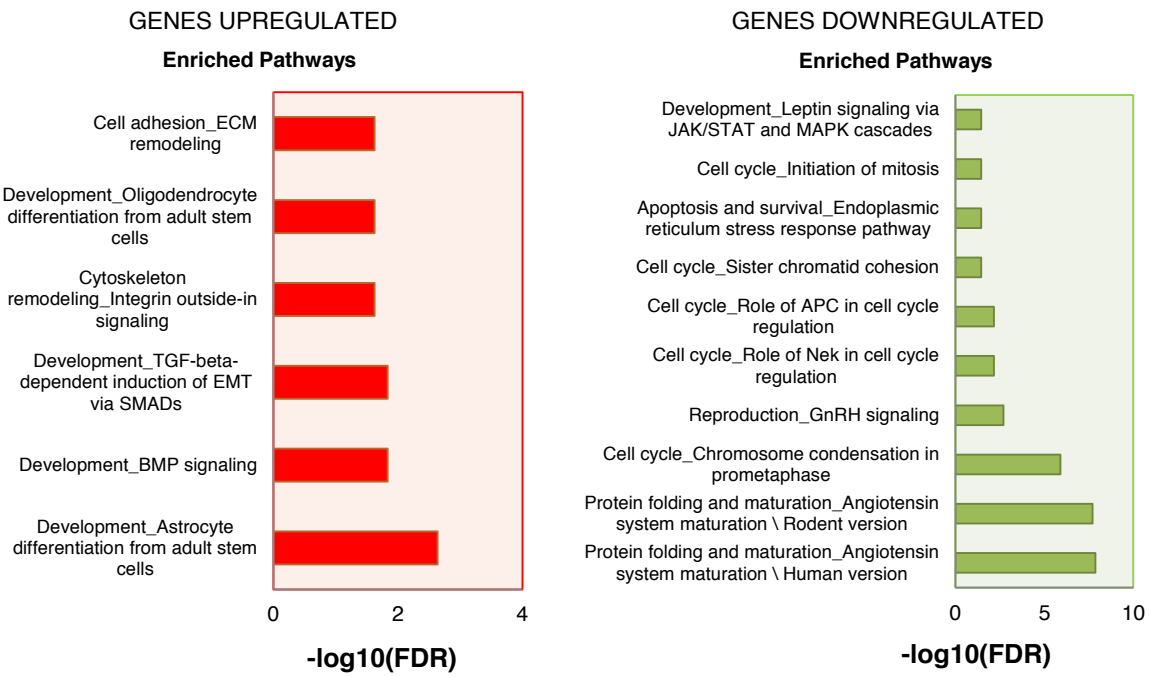

Figure 59. **Functional characterization of methylation-dependent ERG target genes.** MetaCore analysis of the genes more significantly modulated (up-regulated genes on the left; down-regulated genes on the right) by WT-ERG compared to ERG-K362A showing the main pathways in which they are involved.

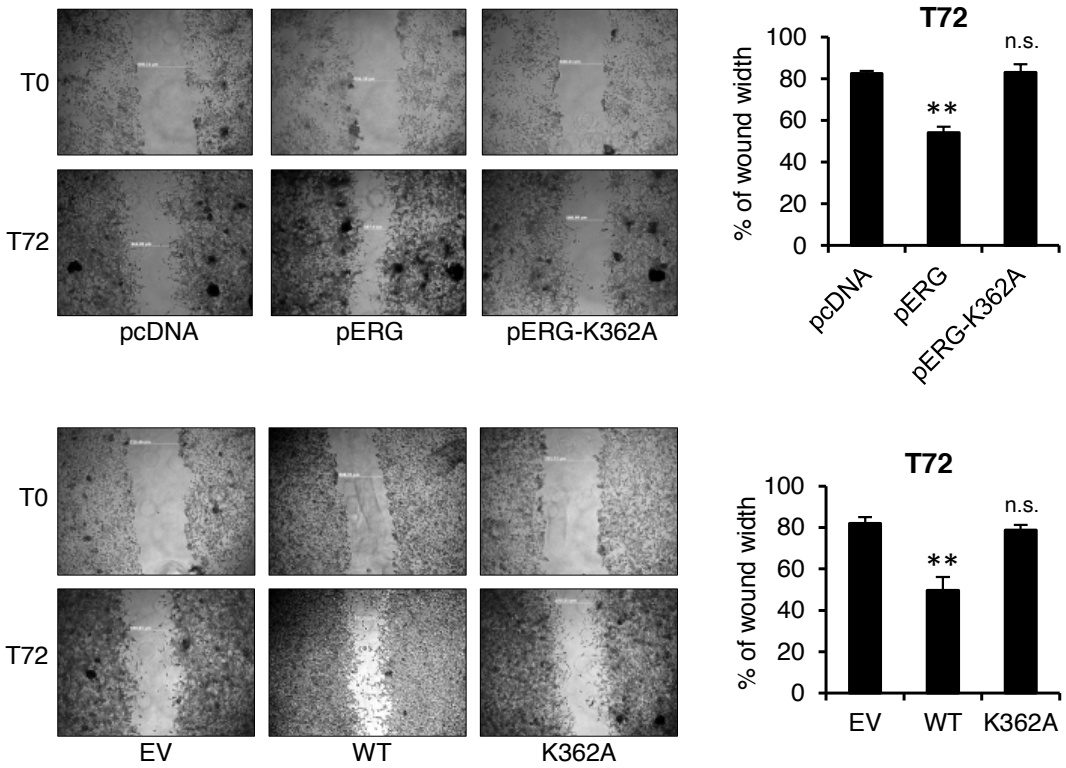

Figure 60. **ERG-K362A mutant shows attenuated capability to migrate.** Cell migration assessed by wound healing assay in LNCaP cells transiently (*upper panel*) or stably (*bottom panel*) expressing WT-ERG or ERG-K362A. Pictures have been taken at time 0 and 72h following the scratch. Differences in wound width shown as percentage relative to T0 are reported on the right. ** $p<0.01$; n.s. not significant.

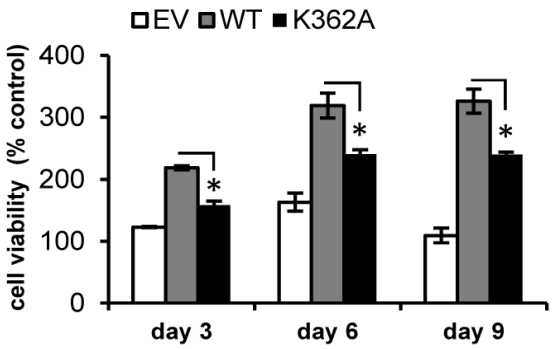

Figure 61. **ERG-K362A mutant confers less resistance to anoikis.** Survival in anoikis measured in LNCaP cells stably expressing WT-ERG or ERG-K362A. Cell viability at the indicated time points is presented as percentage relative to day 0. * $p<0.05$.

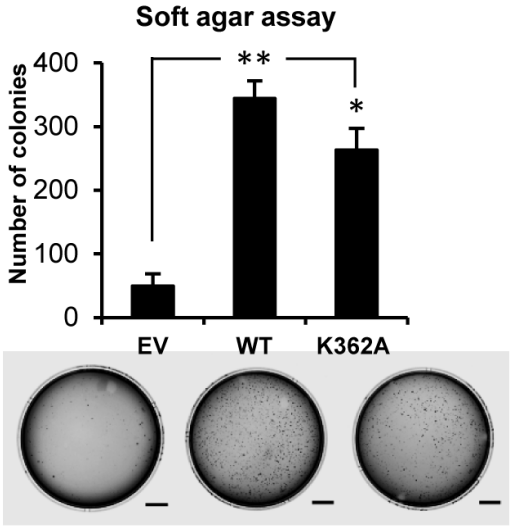

Figure 62. **ERG-K362A mutant confers less capability to grow in anchorage-independent conditions.** Colony formation in soft agar of LNCaP cells stably expressing WT-ERG or ERG-K362A. Representative images are shown at the bottom. * $p<0.05$; ** $p<0.01$. Scale bar = 10 mm.

Reciprocal co-localisation of ERG and EZH2 on the human genome

Methylation and interaction with EZH2 modulated ERG-induced global reprogramming of the prostate cancer transcriptome. Therefore, we sought to define the extent and distribution of ERG and EZH2 complexes in the genome of VCaP cells exploring available ChIP-sequencing datasets, derived from binding events of both proteins in VCaP cell line (Chng, Chang et al. 2012). Reads from EZH2, ERG and Input were mapped to the hg19 human genome assembly and only uniquely mapped reads were kept. Using MACS software, we elicited 14,780 peaks from EZH2 and 48,274 peaks from ERG. Peaks were annotated with our software (peak-tool) using all regions of the gencode-v19 database. The presence of peaks in gene-promoters, gene-bodies and their distances to the TSSs were reported by the tool. Next, we considered ERG-EZH2 co-localized binding regions by selecting ERG peaks that had a proximal EZH2 peak in a window up to 1kb. This analysis revealed a co-recruitment of ERG and EZH2 at 3,614 annotated sites in several regions (promoter, intergenic, intron and exon regions) of VCaP genome (Figure 63).

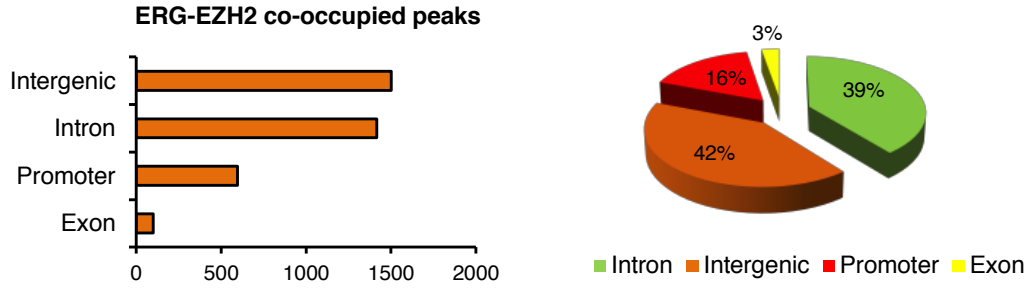

Figure 63. **Genome-wide co-occupancy of ERG and EZH2 in VCaP cells within 1kb.** Distribution of ERG-EZH2 co-occupied sites in VCaP genome, shown as number of annotated sites (*left panel*) and relative percentage (*right panel*) in intergenic, intron, promoter and exon regions.

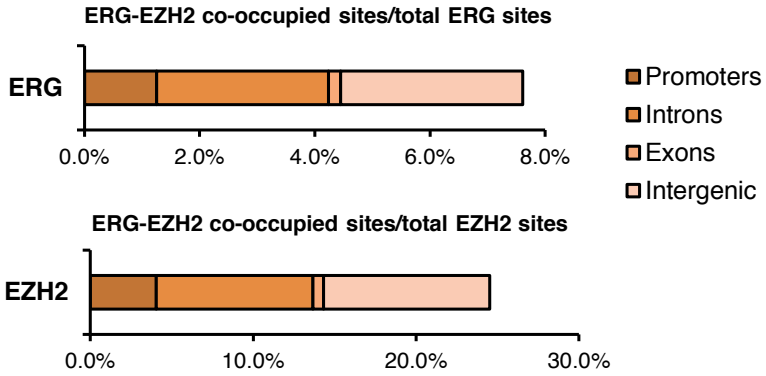

Figure 64**. Distribution of co-occupied regions compared to total annotated sites.** Representation of the percentage of ERG-EZH2 co-occupied regions compared to the total ERG (*top*) and total EZH2 (*bottom*) annotated sites.

We observed that co-recruitment occurred at 24.5% and 7.6% of the total EZH2 and ERG total sites, respectively (Figure 64), suggesting that ERG-EZH2 interaction affects more significantly EZH2 occupancy on the genome and likely drives EZH2 to non-canonical locations.

Interestingly, *de novo* motif analysis revealed that ERG-proximal EZH2 peaks (≤ 1-kb window; n=3,442) were enriched of a canonical ERG sequence motif (Figure 65), whereas ERG-distal EZH2 peaks (>1-kb window; n=11,339) were devoid of any specific binding motif.

Figure 65**. Motif analysis of ERG-proximal EZH2 peaks.** The closely canonical ERG motif revealed by *de novo* motif enrichment search of the ERG-proximal EZH2 peaks.

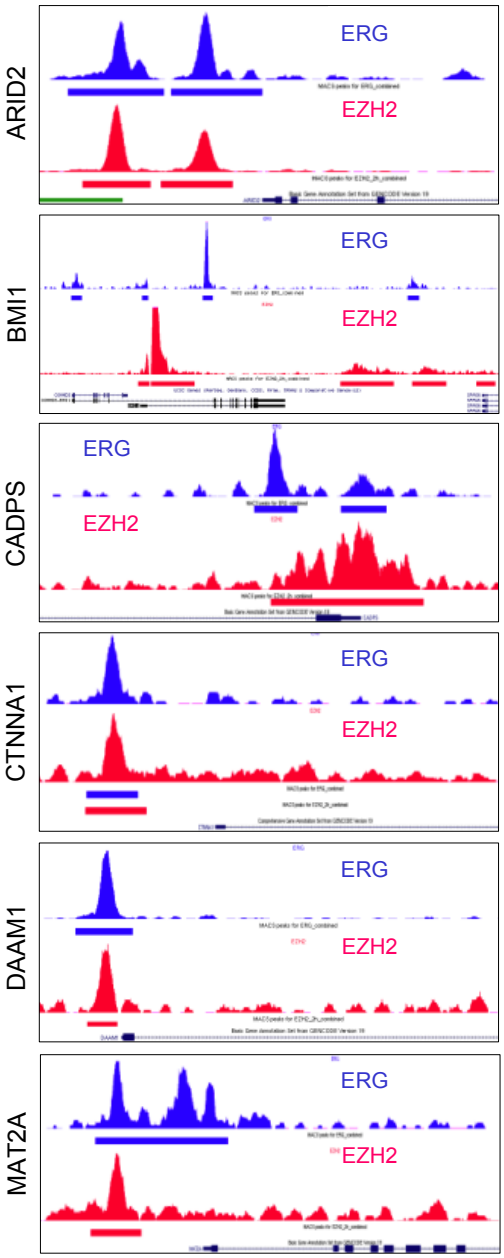

Figure 66. **ERG-EZH2 co-localization on selected gene promoters.** Representative ChIP-seq profiles of gene promoters with ERG (*blue*) and EZH2 (*red*) co-localized peaks in VCaP cells.

To validate these findings, we selected a set of genes with co-localized ERG-EZH2 peaks in their promoter regions and actively transcribed by ERG in VCaP cells (Gupta, Iljin et al. 2010) (Figure 66). ChIP-reChIP and qPCR with gene-specific primers encompassing the predicted binding sites confirmed ERG and EZH2 co-occupancy on all the selected promoters (Figure 67). Consistent with trans-activation

by ERG and EZH2, transcription of these genes was reduced upon ERG and EZH2 knockdown (Figure 68), indicating that both ERG and EZH2 activated transcription of these target genes in prostate cancer cells VCaP.

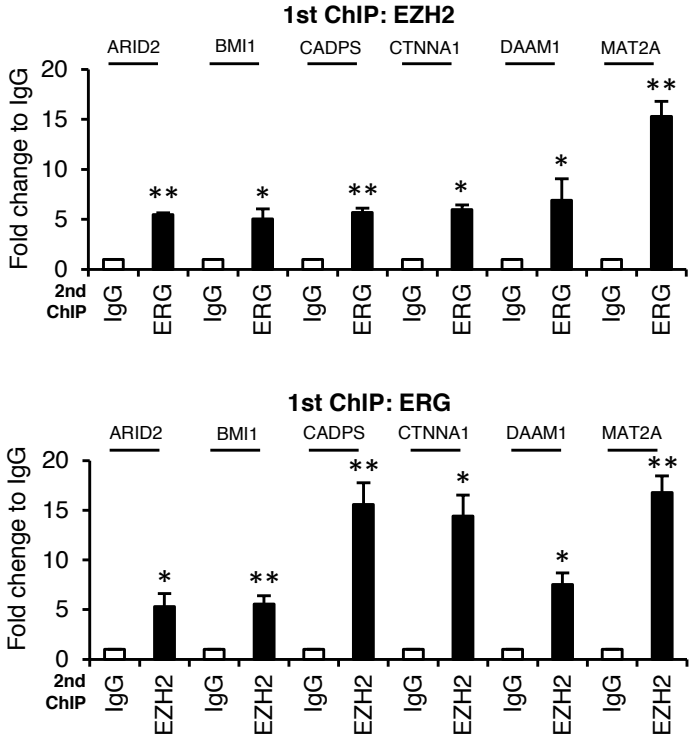

Figure 67. **Validation of ERG-EZH2 co-occupancy on selected genes in VCaP cells.** Re-ChIP analysis of ERG and EZH2 co-localized regions in VCaP cells. First ChIP and second ChIP antibodies were indicated as the chart title and X axis labels, respectively. Quantification of binding was represented as fold enrichment relative to IgG second ChIP. * $p<0.05$; ** $p<0.01$.

To understand the relevance of ERG-EZH2 co-occupied genes, we examined their expression in a cohort of prostate cancer patients with known ERG fusion and expression status (Sboner, Demichelis et al. 2010). Among the co-occupied genes we extracted a signature of 118 genes significantly deregulated between ERG fusion positive and negative tumors (75 up and 43 down; t-test p-value <0.05) (Figure 69). Interestingly, this list acted as a classifier gene signature able to recognize ERG positive tumors in other prostate cancer datasets (Taylor, Schultz et al. 2010; Grasso, Wu et al. 2012) (Figure 70).

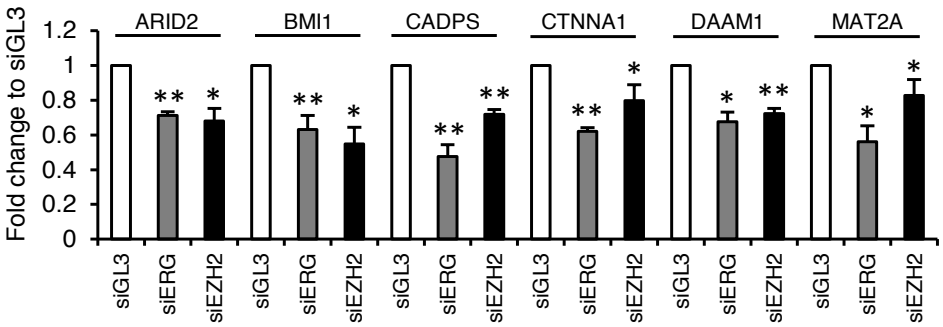

Figure 68. **Expression of the selected genes upon ERG and EZH2 depletion in VCaP cells.** mRNA level of selected co-occupied genes evaluated by qRT-PCR analysis 48h after ERG and EZH2 knockdown in VCaP cells. * p<0.05; ** p<0.01.

Deregulated expression of these genes suggested that they might drive initiation and progression of prostate cancer. Consistently, we found that a set of classifier genes (41 genes, 22 up and 19 down) had prognostic impact. A prognostic risk index gene signature derived by combining the expression values of the classifier genes was highly predictive of reduced overall survival in primary prostate cancer patients (Figure 71).

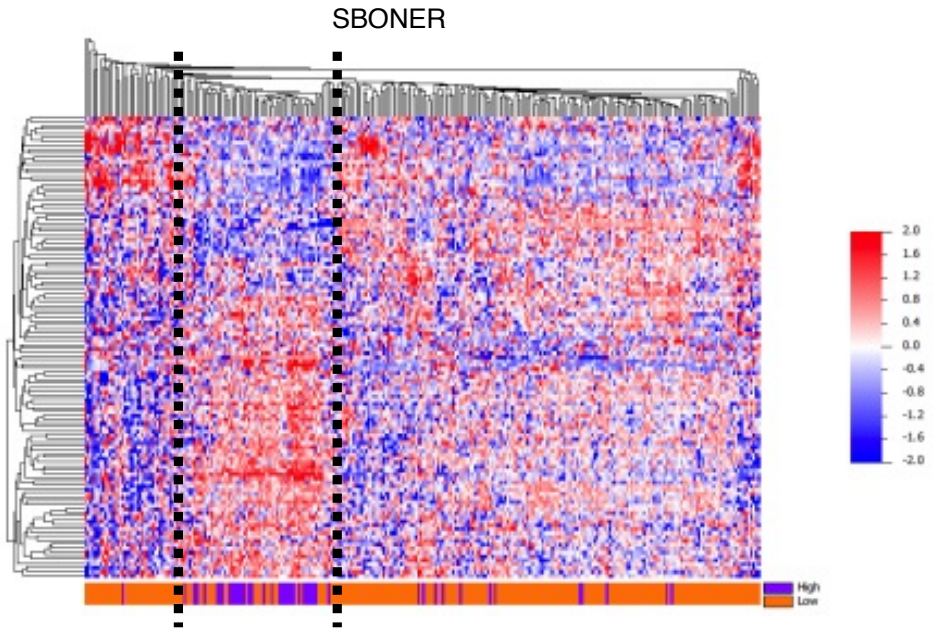

Figure 69. **Sboner dataset.** Heat Map showing expression of ERG-EZH2 co-localized gene signature in the Sboner prostate cancer dataset. Dashed lines highlight the significant deregulation (p value<0.05) in ERG fusion positive (*purple*) versus fusion negative tumors (*orange*).

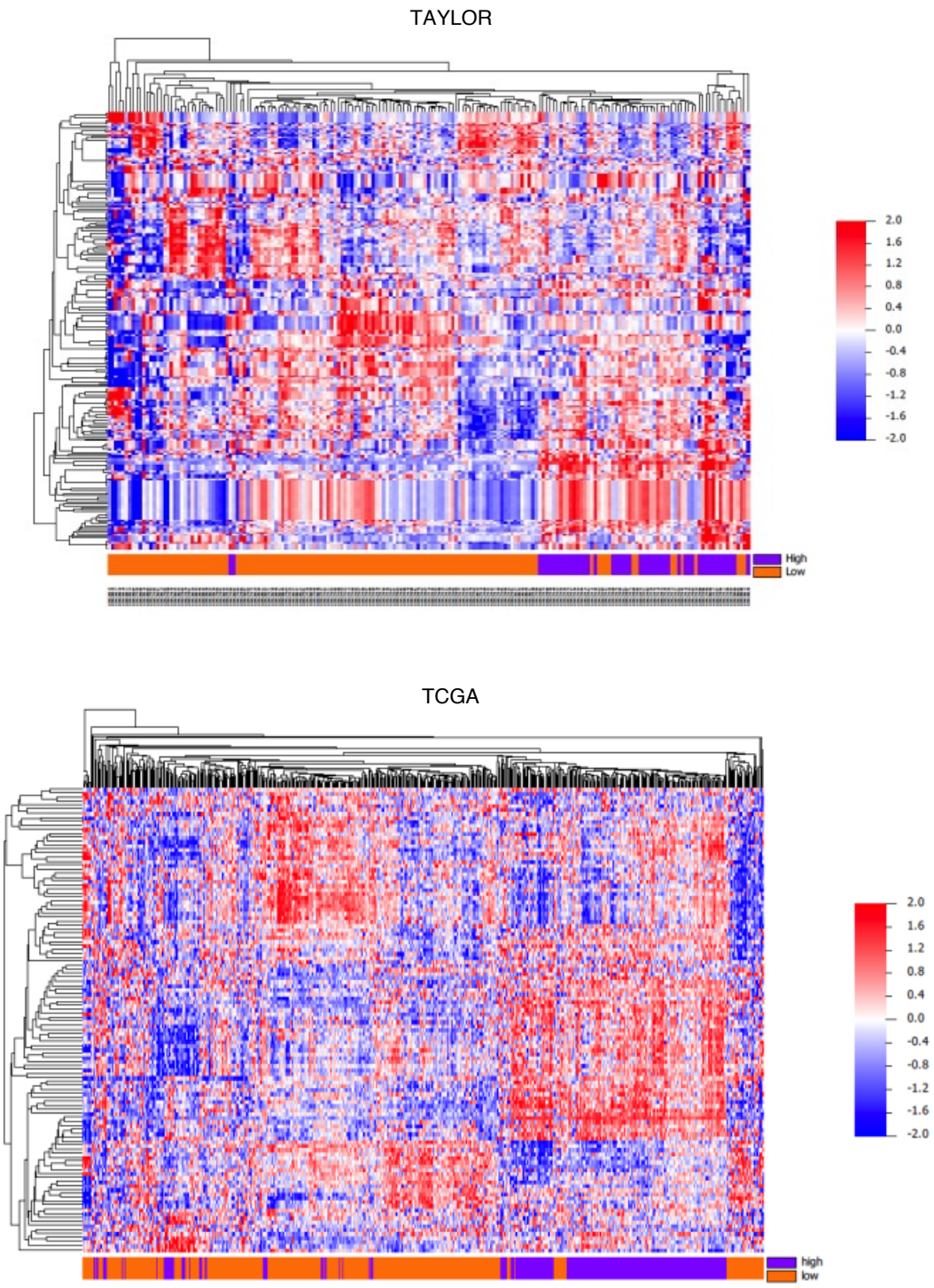

Figure 70. **ERG and EZH2 co-regulated genes are deregulated in ERG positive tumors.** Heat Maps using the co-regulated gene signature extracted from Sboner dataset (see methods) and applied in Taylor (*top*) and TCGA (*bottom*) datasets. Bar shows grouping of ERG high (*purple*) and the ERG low (*orange*) prostate tumors.

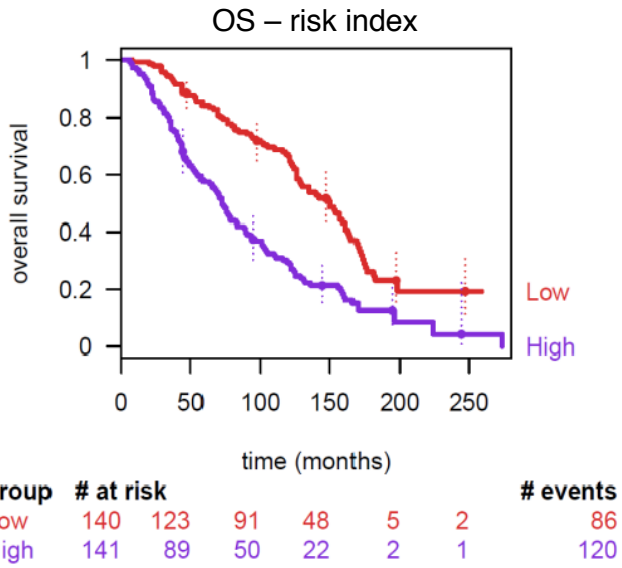

Figure 71. **Genes co-regulated by ERG-EZH2 predict adverse prognosis.** Kaplan-Meier plot using ERG-EZH2 co-regulated genes extracted from the Sboner dataset. A prognostic risk index was calculated and dichotomized in high and low risk by taking the median as threshold.

ERG methylation is enhanced by loss of PTEN

In the past years, it has become evident that ERG overexpression is sufficient to induce prostatic intra-epithelial neoplasia (PIN). However, it is still uncertain if ERG is sufficient to drive progression to carcinoma (King, Xu et al. 2009; Zong, Xin et al. 2009; Chen, Chi et al. 2013). Our findings indicated that ERG interaction with EZH2 and methylation had a relevant impact on ERG driven reprogramming of prostate cancer cell transcriptome. Therefore, we reasoned that factors capable of influencing ERG methylation could enhance the oncogenic properties of ERG and promote tumor progression. On the other hand, agents capable of blocking this interaction could represent an effective strategy against ERG fusion positive tumors.

ERG gene fusion and PTEN loss are found concomitantly in a substantial fraction of prostate cancers and are associated with poor clinical outcome (Carver, Tran et al. 2009; King, Xu et al. 2009). Furthermore, PTEN loss cooperates with ERG to induce progression from non-invasive to locally invasive tumors in mouse models

(Carver, Tran et al. 2009; Chen, Chi et al. 2013). We hypothesized that PTEN loss could enhance EZH2-induced ERG methylation likely by activating the PI3K/AKT pathway. Indeed, PTEN loss activates AKT, which induces phosphorylation of EZH2 at serine 21 (S21) and promotes PRC2-independent activity and methylation of non-histone proteins by EZH2 (Cha, Zhou et al. 2005; Xu, Wu et al. 2012; Kim, Kim et al. 2013). In keeping with this hypothesis, we examined the level of ERG and mERG in NCI-H660 cells that harbor the TMPRSS2-ERG rearrangement but, unlike VCaP cells, are PTEN null. NCI-H660 cells exhibited higher mERG despite the lower level of total ERG and higher phospho AKT (p-AKT), in line with the PTEN depletion, compared to VCaP cells (Figure 72, *left panel*). Consistent with the AKT activation, we also found increased positivity for pS21 EZH2 in NCI-H660 compared to VCaP cells (Figure 72, *right panel*). Increased activity of AKT in PTEN null NCI-H660 cells, therefore, could enhance EZH2-induced methylation of ERG. Accordingly, treatment of VCaP cells with the AKT inhibitor MK-2206 markedly reduced ERG methylation (Figure 73) indicating a link between AKT activation and ERG methylation.

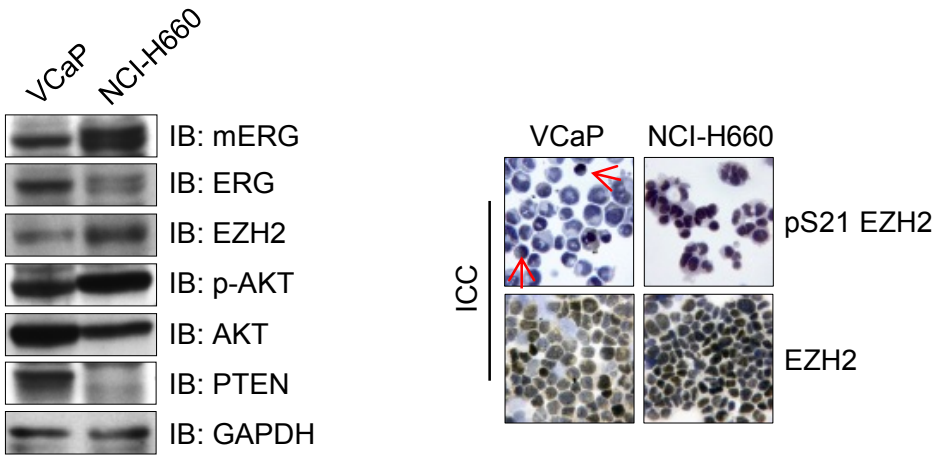

Figure 72. **Comparison between VCaP and NCI-H660 cell lines.** Immunoblot analysis of mERG, EZH2, AKT and PTEN in VCaP and NCI-H660 cells (*left panel*). EZH2 and pS21 EZH2 evaluated by immunocytochemistry (ICC) in VCaP and NCI-H660 cells (*right panel*). Red arrows indicate some positive nuclei.

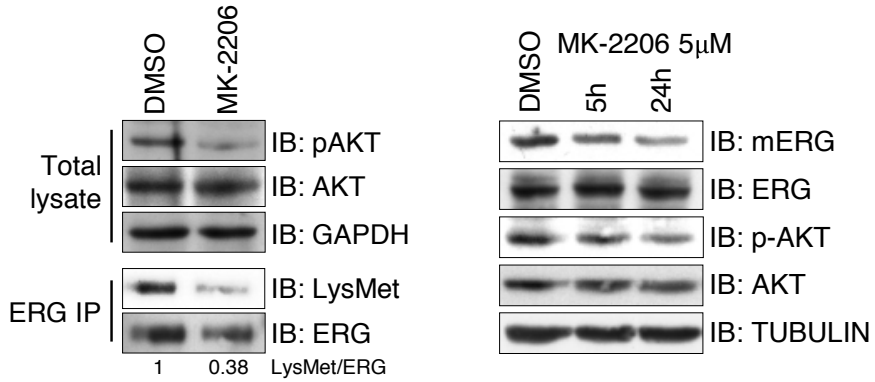

Figure 73. **p-AKT inhibition reduces ERG methylation.** IP of ERG in MK-2206 treated VCaP cells, followed by immunoblot with a pan-methyl lysine antibody (*left panel)*. Healthy cells have been harvested after 5 hours of treatment with 5μM of the drug. Densitometry values of methylated/total ERG (LysMet/ERG) ratio are shown**.** On the right, immunoblot analysis of pAKT, AKT and mERG in VCaP cells treated with MK-2206 (5μM) for 5 and 24h. After 24h cells were still alive and healthy.

To test directly whether PTEN depletion could activate AKT and lead to ERG methylation, we knocked down PTEN in VCaP cells. Consistent with this hypothesis, PTEN depletion significantly increased ERG methylation (Figure 74), suggesting that PTEN/AKT pathway could be involved in modulating ERG methylation status. Next, to further elucidate the role of PTEN loss, we established PTEN stable knockdown in VCaP cells. VCaP cells with stable PTEN depletion (VCaP shPTEN) exhibited higher mERG along with increased p-AKT (Figure 75, *left panel*) and pS21 EZH2 (Figure 75, *right panel*) compared to control VCAP-EV cells. Concomitantly, the expression of ERG-EZH2 co-occupied targets increased in VCaP-shPTEN (Figure 76).

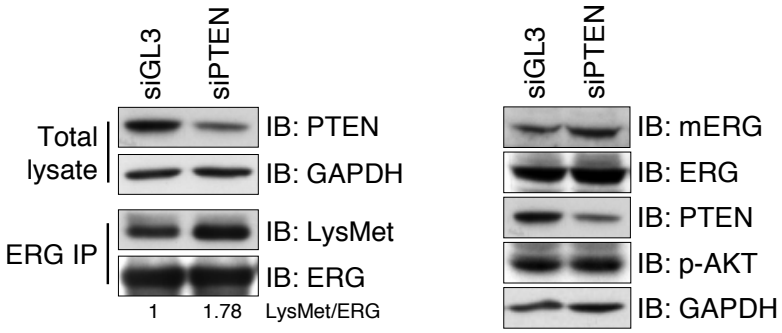

Figure 74. **PTEN loss enhances ERG methylation.** IP of ERG in VCaP cells transfected with control (siGL3) or PTEN (siPTEN) directed siRNAs (*left panel*). Densitometry values of methylated/total ERG (LysMet/ERG) ratio are indicated. On the right, detection of mERG, ERG and EZH2 by immunoblotting in VCaP cells upon PTEN knockdown. Lysates were collected and processed 48h after transfection.

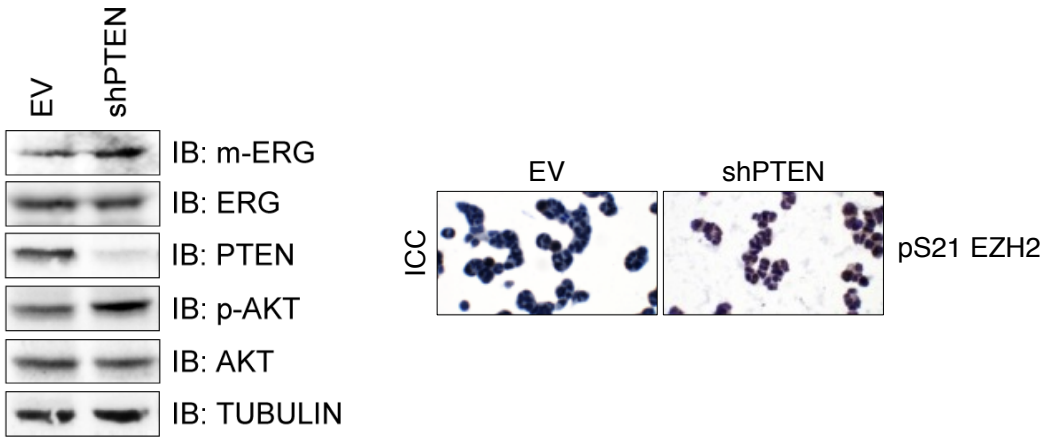

Figure 75. **PTEN depletion enhances ERG methylation and EZH2 phosphorylation at serine 21.** Immunoblot analysis of PTEN, mERG and p-AKT in control (EV) and stable PTEN knockdown (shPTEN) VCaP cells (*left panel*). On the right, pS21 EZH2 evaluated by immunocytochemistry (ICC) in VCaP EV and VCaP shPTEN.

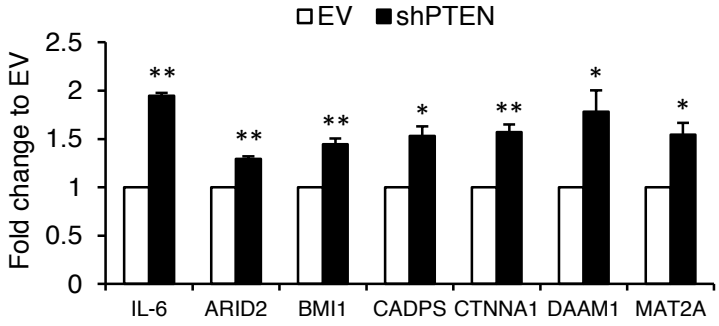

Figure 76. **PTEN depletion enhances ERG-EZH2 co-occupied genes expression.** mRNA analysis by qRT-PCR of ERG-EZH2 co-occupied genes in VCaP EV and VCaP shPTEN. * $p<0.05$; ** $p<0.01$.

Taken together, these data suggested that loss of PTEN could be an important event enhancing ERG methylation and provide for the first time a molecular support for the frequent association of ERG fusion with PTEN loss in prostate tumors.

Collectively, these experimental data reveal a novel interaction between EZH2 and ERG which enables the transforming potential of ERG and sets the basis for tumor progression in the context of ERG fusion positive tumors. EZH2-induced ERG methylation is at the center of cross-talks between ERG and other key oncogenic pathways, like PTEN/PI3K/AKT, that affect activity of EZH2 and promote ERG methylation.

Discussion

Deregulated expression of ETS factors due to chromosomal rearrangements is a very frequent event in prostate cancer. Above all, TMPRSS2-ERG fusion has been identified in approximately 50% of prostate cancers, and observed in more than 90% of prostate tumors with ETS-family gene rearrangements (Tomlins, Rhodes et al. 2005; Tomlins, Laxman et al. 2007; Kumar-Sinha, Tomlins et al. 2008). In recent years, it has become clear that the aberrant expression of ERG can produce profound phenotypes, indicating that a change in ERG activity has a tremendous impact on prostate epithelium. However, many of the pathways and mechanisms through which ERG exerts its oncogenic role are still to be defined.

In a previous study, confirmed and enlarged by other investigators, we showed the presence of a cross-talk between ETS transcription factors and epigenetic effectors, and we demonstrated how altered expression of ERG leads to the induction of the key PcG protein EZH2, which in turn mediates epigenetic silencing of several genes (Kunderfranco, Mello-Grand et al. 2010; Yu, Mani et al. 2010). Starting from these evidences, we examined in depth the relationship between ERG and EZH2, and with the present study we show that EZH2 fulfils a very important role in mediating ERG transcriptional activity directly interacting with it and determining its non-histone methylation.

In the last years, many reports have revealed that several protein lysine methyltransferases, like EZH2, can also regulate the methylation of non-histone proteins. Lysine methylation has recently emerged as an important post-translation modification that can profoundly affect the function of diverse non-histone proteins, including transcription factors. Indeed, there are several examples of transcription factors and chromatin regulatory proteins that are methylated by histone-modifying enzymes, showing that lysine methylation may be important not only in epigenetic regulation of gene expression, but also in the regulation of cellular signal transduction pathways (Stark, Wang et al. 2011; Hamamoto, Saloura et al. 2015). In this study, we demonstrated that EZH2 determines non-histone methylation of ERG

protein at lysine 362 in both prostate cancer cells and prostate primary tumors, and that the physical interaction between the two proteins is instrumental in this process. Our results revealed that EZH2 interacting with ERG significantly enhances ERG activity and cooperates with it in its transcriptional reprogramming. As supporting evidences we found that ERG-induced activation or repression was lost upon concomitant EZH2 depletion or when the interaction with EZH2 was compromised, underlining the functional relevance of that interaction in ERG transcriptional activity. Generating different ERG and EZH2 truncated constructs, we could characterize the regions involved in the interaction, and taking advantage of the ERG construct unable to interact with EZH2 we proved that the interaction is fundamental for mediating ERG methylation and transcriptional activity. Intriguingly, considering the entire TMPRSS2-ERG hybrid transcripts identified and characterized in prostate cancers, it appears that the transcripts most frequently found in ERG fusion positive tumors contain both the methylation and the EZH2 interacting domain herein described. Consistently, fusion variants devoid of the interacting domain appear to be extremely rare in prostate tumors, further supporting the relevance of EZH2 binding for ERG-mediated prostate carcinogenesis (Clark, Merson et al. 2007).

The ERG co-regulatory networks have been matter of discussion since long time. It has been known that ERG, working together with several oncogenic co-repressors, such as HDACs and polycomb proteins like EZH2, could directly modulate the transcriptional profile of AR, impeding epithelial differentiation and contributing to prostate cancer progression (Chng et al, 2012). It has also been shown that ERG is able to disrupt AR signalling and differentiation program, inhibiting AR activity, and potentiating EZH2-mediated dedifferentiation and repressive epigenetic programs (Yu et al., 2010). On one hand, our results confirm EZH2 as an ERG co-operator in genes silencing by mediating histone methylation on the promoters of repressed genes. In this scenario, the interaction is necessary to recruit EZH2 on selected ERG target genes, where EZH2 can act as a canonical gene silencer enhan-

cing the trans-repression function of ERG. On the other hand, our data demonstrate that EZH2 together with ERG could form on distinct promoters both repressive and activating complexes, sustaining the novel and recently identified activating function of EZH2. Notably, we found that the presence of another PcG protein, SUZ12, discriminates these complexes, and that EZH2 is able to cooperate in ERG-induced transcription, functioning without any other PRC2 component. Indeed, SUZ12 depletion does not affect the expression of activated genes, as EZH2 knockdown does, while it prevented ERG-induced repression, demonstrating that its recruitment is solely associated with ERG-mediated gene repression. These findings are consistent with other studies that reported the capability of EZH2 to function in a non-canonical manner and independently from the PRC2 (Lee, Li et al. 2011; Xu, Wu et al. 2012). However, while we supported the novel EZH2 activating function independent of H3K27 methylation in prostate cancer cells, with this study we also provide new insights in ERG-mediated oncogenesis, demonstrating that the non-canonical function of EZH2 has a significant impact on ERG transcriptional activity and prostate cancer progression.

Given that EZH2 affects the transcriptional activity of ERG, our data also support a relevant role of EZH2-mediated ERG methylation in enhancing ERG transcriptional and oncogenic properties. We observed that ERG presents a robust signature of induced and repressed genes, and that this signature is significantly affected when ERG could not be methylated. Intriguingly, we found that the genes more affected by the loss of methylation, defined as methylation-dependent, were significantly enriched in ERG positive compared to ERG negative primary prostate tumors. These data corroborate that ERG methylation is a crucial event important for mediating its transcriptional activity. Moreover, these methylation-dependent genes appear to be important in conferring metastatic properties, suggesting that ERG methylation is necessary to enhance transcription of selected genes relevant in determining tumorigenesis and cancer progression. Importantly, we demonstrated

by ChIP experiments that ERG-K362A mutant is still able to occupy promoter regions, although with a weaker binding, sustaining methylation as a critical modification that affects ERG activity independently of its promoter occupancy.

By analysing ChIP-sequencing dataset of VCaP cells, we discovered that ERG and EZH2 co-occupied several regions in the human genome, including promoter, intron, exon and intergenic regions. This finding supported a role for ERG-EZH2 interaction in the global reprogramming of the prostate cancer transcriptome. Interestingly, when we segregated the total EZH2 peaks into those that were proximal to ERG peaks in a 1kb window, and those distal to ERG peaks, we found a closely canonical ERG motif in several ERG-proximal EZH2 peaks, while similar analysis of the ERG-distal EZH2 peaks did not reveal any relevant binding site motif. Moreover, the percentage of co-occupied regions in respect to the total EZH2 annotated sites was higher compared to that one in respect to ERG total sites, suggesting that ERG likely drives EZH2 to non-canonical selected location, affecting its occupancy. Relevantly, among the identified ERG-EZH2 co-occupied genes, we found a list of genes significantly deregulated between ERG fusion positive and negative prostate tumors, showing that ERG-EZH2 co-occupied genes can be used to molecularly distinguish ERG positive prostate cancers from fusion negative tumors. Moreover, among these genes we found a set of classifier genes with a high prognostic impact, indicating that ERG-EZH2 target genes could also provide information about the outcome of the disease.

Although it is evident that ERG possesses oncogenic properties, it has been much less clear how it promotes prostate cancer progression. Importantly, it has been emerging that the TMPRSS2-ERG translocation is insufficient to initiate prostate neoplasia and that cooperating oncogenic lesions are required. A well-established event that cooperates with ERG up-regulation in leading to prostate cancer progression is loss of PTEN. Several studies supported PTEN loss as a “second hit” that makes ERG tumorigenesis more invasive and penetrant (Carver, Tran et al. 2009;

King, Xu et al. 2009). Intriguingly, it has been recently reported that ERG-induced transcriptome changes were more enriched in amplitude in a background with PTEN deficiency (Chen, Chi et al. 2013). However, the mechanism by which deprivation of PTEN increases ERG activity remains unclear. In this study, we proved that loss of PTEN, as well as p-AKT deregulation, is a key event in modulating ERG methylation. As supporting evidences, we found that transient depletion of PTEN increased ERG methylation in VCaP cells, while pharmacological inhibition of p-AKT reduced the amount of methylated ERG. These findings help to explain the synergistic oncogenic activation mediated by ERG overexpression and PTEN deprivation. From a mechanistic point of view, we sustain that p-AKT activation mediated by loss of PTEN could be the critical connection step, responsible for inducing EZH2 phosphorylation and subsequent ERG methylation. EZH2 possesses diverse residues that could be modified, and its phosphorylation status is fundamental in directing and modulating its enzymatic activity (Zeng, Chen et al. 2011). In 2005, Cha et al. reported that EZH2 could be phosphorylated at serine 21 (S21) by p-AKT, and that post-translational modification suppressed its canonical methyltransferase activity, by impeding EZH2 binding to histone H3. At a later stage, Xu et al. demonstrated in 2012 that phosphorylation of EZH2 at S21 could switch its activity from a Polycomb repressor to a transcriptional coactivator independent of the PRC2 complex, pointing this modification as a crucial event in EZH2 non-canonical H3K27 methylation function. Interestingly, comparing VCaP cells with a more tumorigenic cell line, NCI-H660, that is TMPRSS2-ERG fusion positive but AR negative and PTEN null, we observed increased levels of p-AKT, methylated ERG, and pS21 EZH2 in the more aggressive cell line. These data prompted us to verify a mechanism through which loss of PTEN could enhance ERG oncogenesis by inducing p-AKT and EZH2 phosphorylation. In line with this, PTEN depletion in VCaP cells led to an increase of pS21 EZH2 and ERG methylation, supporting the connection between these two pathways. Furthermore, several ERG-

EZH2 co-occupied genes were up-regulated upon PTEN depletion, sustaining the enhancement of ERG activity in response to PTEN deprivation and increased methylation. Importantly, these findings might explain the weak tumorigenic properties of ERG in early stages of carcinogenesis, and the need of cooperation with other oncogenic events. Our work provides for the first time a mechanistic insight for the frequent cooperation between ERG and loss of PTEN, and opens new perspectives to the identification of other mechanisms able to link these two pathways or enhance ERG activity.

Collectively, this work provides new insights regarding ERG activity, and it tries to find an explanation about the incapability of ERG alone to drive malignancy. Here we propose ERG methylation as a critical modification in ERG tumors, a modification that could be promoted or enhanced by several mechanisms, such as interaction with EZH2 or PTEN loss, and be a driver event for prostate cancer progression (Figure 77). Importantly, these findings provide a broadly relevant mechanism for tumor progression, and define a therapeutically actionable pathway that could have a broad impact on the management of ERG fusion positive prostate cancers. Treatment with DZNep alone or in combination with other drugs able to inhibit EZH2 or AKT activity, decreasing in turn ERG methylation, could be a novel and valid approach to treat ERG positive patients who concomitantly present high levels of EZH2 expression or PTEN deficiency.

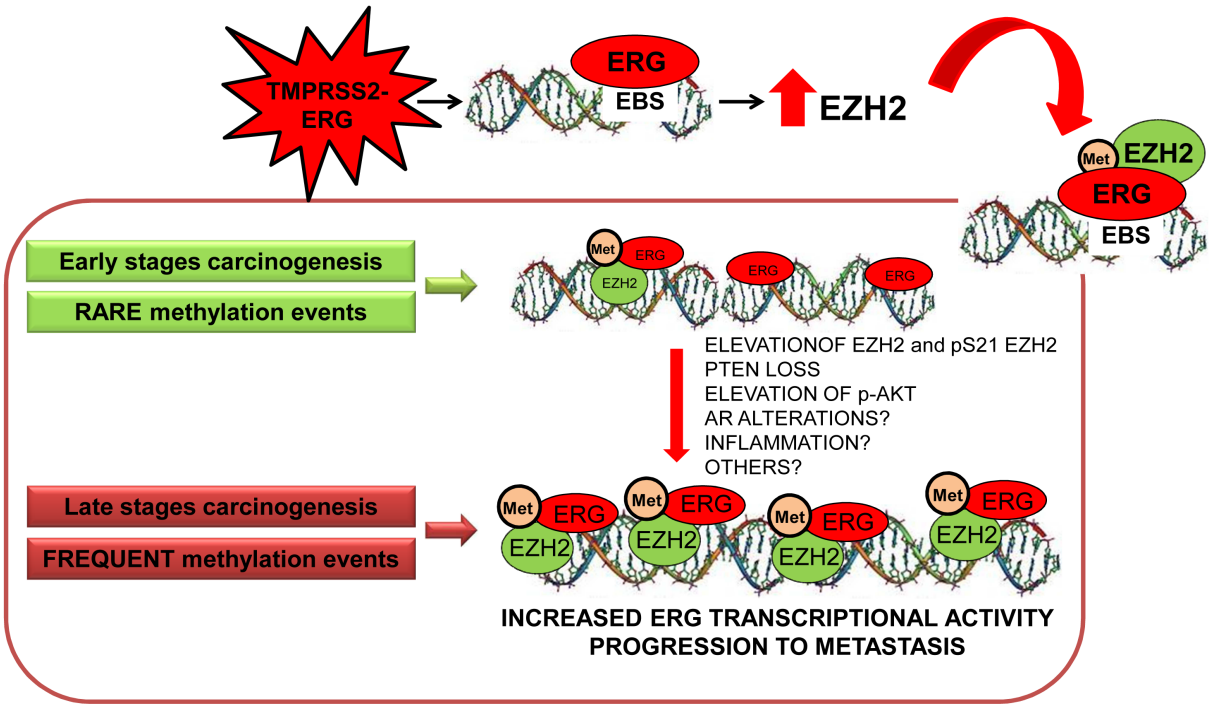

Figure 77. **Schematic model of the novel findings identified.** TMPRSS2-ERG fusion leads to androgen-dependent robust induction of ERG protein, which in turn activates several ETS target genes including EZH2. EZH2 interacts with and methylates ERG, enhancing its transcriptional activity. At early stages of carcinogenesis, only a small fraction of ERG is methylated. However, when other events occur, such as PTEN loss, increase of EZH2 phosphorylation at S21, and other hits to be discovered, ERG methylation increases, leading to enhanced ERG transcriptional activity and prostate cancer progression.

Ongoing & Future Directions

From the present study, ERG methylation appears to be a critical modification of ERG transcriptional and oncogenic activity, which could be promoted or enhanced by several mechanisms. Considering that loss of PTEN increases ERG transcriptional deregulation, it would be important to evaluate the impact of PTEN loss on the malignant phenotype of ERG positive cancer cells by *in vitro* and *in vivo* experiments. Performing some preliminary experiments, we have already observed increased colony formation in soft agar conditions by VCaP-shPTEN cells compared to normal VCaP, suggesting that the increase of ERG methylation could enhance tumorigenesis. Further studies with this cell model, such as mouse tail vein injections or Chicken Chorioallantoic Membrane (CAM) assay, are needed to better understand if VCaP-shPTEN cells also present increased tumorigenic and metastatic capabilities *in vivo* due to an increase of ERG methylation.

The link that we uncovered between EZH2-induced methylation and oncogenic functions of ERG suggests that interfering with this process could provide an effective strategy to be exploited for treatment of ERG positive tumors. Indeed, pharmacological inhibition of EZH2 by DZNep drug directly interferes with ERG methylation, causing its reduction. Considering this notion, it would also be important to assess the effects of EZH2 inhibition on ERG transcriptional and oncogenic activity, by ChIP experiments and functional assays, in order to evaluate the pharmacological effects on ERG functions. Moreover, it would be interesting to evaluate the capability of diverse EZH2 inhibitors to reduce tumorigenic and metastatic capability *in vivo*, and to verify if this approach could be a more valid strategy in the PTEN loss model. All these future studies will help to better characterize the importance of ERG methylation, and discovering the trigger mechanisms at the base of this modification could be a significant priority in the near future, leading to novel therapeutic strategies able to reverse ERG methylation and disrupt the ERG co-regulatory network.

References

Abate-Shen, C. and M. M. Shen (2000). "Molecular genetics of prostate cancer." Genes Dev **14**(19): 2410-2434.

Abate-Shen, C., M. M. Shen, et al. (2008). "Integrating differentiation and cancer: the Nkx3.1 homeobox gene in prostate organogenesis and carcinogenesis." Differentiation **76**(6): 717-727.

Agarkar, V. B., N. D. Babayeva, et al. (2010). "Crystal structure of mouse Elf3 C-terminal DNA-binding domain in complex with type II TGF-beta receptor promoter DNA." J Mol Biol **397**(1): 278-289.

Albino, D., N. Longoni, et al. (2012). "ESE3/EHF controls epithelial cell differentiation and its loss leads to prostate tumors with mesenchymal and stem-like features." Cancer Res **72**(11): 2889-2900.

Alimonti, A., C. Nardella, et al. (2010). "A novel type of cellular senescence that can be enhanced in mouse models and human tumor xenografts to suppress prostate tumorigenesis." J Clin Invest **120**(3): 681-693.

Alipov, G., T. Nakayama, et al. (2005). "Overexpression of Ets-1 proto-oncogene in latent and clinical prostatic carcinomas." Histopathology **46**(2): 202-208.

Ananthanarayanan, V., R. J. Deaton, et al. (2005). "Alpha-methylacyl-CoA racemase (AMACR) expression in normal prostatic glands and high-grade prostatic intraepithelial neoplasia (HGPIN): association with diagnosis of prostate cancer." Prostate **63**(4): 341-346.

Arber, S., D. R. Ladle, et al. (2000). "ETS gene Er81 controls the formation of functional connections between group Ia sensory afferents and motor neurons." Cell **101**(5): 485-498.

Asatiani, E., W. X. Huang, et al. (2005). "Deletion, methylation, and expression of the NKX3.1 suppressor gene in primary human prostate cancer." Cancer Res **65**(4): 1164-1173.

Athanasiou, M., G. Mavrothalassitis, et al. (2000). "FLI-1 is a suppressor of erythroid differentiation in human hematopoietic cells." Leukemia **14**(3): 439-445.

Baca, S. C., D. Prandi, et al. (2013). "Punctuated evolution of prostate cancer genomes." Cell **153**(3): 666-677.

Baldus, C. D., S. Liyanarachchi, et al. (2004). "Acute myeloid leukemia with complex karyotypes and abnormal chromosome 21: Amplification discloses overexpression of APP, ETS2, and ERG genes." Proc Natl Acad Sci U S A **101**(11): 3915-3920.

Barbieri, C. E., S. C. Baca, et al. (2012). "Exome sequencing identifies recurrent SPOP, FOXA1 and MED12 mutations in prostate cancer." Nat Genet **44**(6): 685-689.

Barbieri, C. E. and S. A. Tomlins (2014). "The prostate cancer genome: perspectives and potential." Urol Oncol **32**(1): 53 e15-22.

Bastus, N. C., L. K. Boyd, et al. (2010). "Androgen-induced TMPRSS2:ERG fusion in nonmalignant prostate epithelial cells." Cancer Res **70**(23): 9544-9548.

Baylin, S. B., M. Makos, et al. (1991). "Abnormal patterns of DNA methylation in human neoplasia: potential consequences for tumor progression." Cancer Cells **3**(10): 383-390.

Berezovska, O. P., A. B. Glinskii, et al. (2006). "Essential role for activation of the Polycomb group (PcG) protein chromatin silencing pathway in metastatic prostate cancer." Cell Cycle **5**(16): 1886-1901.

Berger, M. F., M. S. Lawrence, et al. (2011). "The genomic complexity of primary human prostate cancer." Nature **470**(7333): 214-220.

Bertram, J., J. W. Peacock, et al. (2006). "Loss of PTEN is associated with progression to androgen independence." Prostate **66**(9): 895-902.

Bhatia-Gaur, R., A. A. Donjacour, et al. (1999). "Roles for Nkx3.1 in prostate development and cancer." Genes Dev **13**(8): 966-977.

Birdsey, G. M., N. H. Dryden, et al. (2008). "Transcription factor Erg regulates angiogenesis and endothelial apoptosis through VE-cadherin." Blood **111**(7): 3498-3506.

Birdsey, G. M., N. H. Dryden, et al. (2012). "The transcription factor Erg regulates expression of histone deacetylase 6 and multiple pathways involved in endothelial cell migration and angiogenesis." Blood **119**(3): 894-903.

Bowen, C. and E. P. Gelmann (2010). "NKX3.1 activates cellular response to DNA damage." Cancer Res **70**(8): 3089-3097.

Boyd, L. K., X. Mao, et al. (2012). "The complexity of prostate cancer: genomic alterations and heterogeneity." Nat Rev Urol **9**(11): 652-664.

Bray, M., J. Driscoll, et al. (2000). "Treatment of lethal Ebola virus infection in mice with a single dose of an S-adenosyl-L-homocysteine hydrolase inhibitor." Antiviral Res **45**(2): 135-147.

Bryant, R. J., N. A. Cross, et al. (2007). "EZH2 promotes proliferation and invasiveness of prostate cancer cells." Prostate **67**(5): 547-556.

Cangemi, R., A. Mensah, et al. (2008). "Reduced expression and tumor suppressor function of the ETS transcription factor ESE-3 in prostate cancer." Oncogene **27**(20): 2877-2885.

Cao, R., L. Wang, et al. (2002). "Role of histone H3 lysine 27 methylation in Polycomb-group silencing." Science **298**(5595): 1039-1043.

Carbone, G. M., E. McGuffie, et al. (2004). "DNA binding and antigene activity of a daunomycin-conjugated triplex-forming oligonucleotide targeting the P2 promoter of the human c-myc gene." Nucleic Acids Res **32**(8): 2396-2410.

Carnero, A., C. Blanco-Aparicio, et al. (2008). "The PTEN/PI3K/AKT signalling pathway in cancer, therapeutic implications." Curr Cancer Drug Targets **8**(3): 187-198.

Carson, J. A., R. A. Fillmore, et al. (2000). "The smooth muscle gamma-actin gene promoter is a molecular target for the mouse bagpipe homologue, mNkx3-1, and serum response factor." J Biol Chem **275**(50): 39061-39072.

Carver, B. S., C. Chapinski, et al. (2011). "Reciprocal feedback regulation of PI3K and androgen receptor signaling in PTEN-deficient prostate cancer." Cancer Cell **19**(5): 575-586.

Carver, B. S., J. Tran, et al. (2009). "Aberrant ERG expression cooperates with loss of PTEN to promote cancer progression in the prostate." Nat Genet **41**(5): 619-624.

Catron, K. M., N. Iler, et al. (1993). "Nucleotides flanking a conserved TAAT core dictate the DNA binding specificity of three murine homeodomain proteins." Mol Cell Biol **13**(4): 2354-2365.

Center, M. M., A. Jemal, et al. (2012). "International variation in prostate cancer incidence and mortality rates." Eur Urol **61**(6): 1079-1092.

Cha, T. L., B. P. Zhou, et al. (2005). "Akt-mediated phosphorylation of EZH2 suppresses methylation of lysine 27 in histone H3." Science **310**(5746): 306-310.

Chae, H., M. Kim, et al. (2010). "B lymphoblastic leukemia with ETV6 amplification." Cancer Genet Cytogenet **203**(2): 284-287.

Chen, Y., P. Chi, et al. (2013). "ETS factors reprogram the androgen receptor cistrome and prime prostate tumorigenesis in response to PTEN loss." Nat Med **19**(8): 1023-1029.

Chen, Z., L. C. Trotman, et al. (2005). "Crucial role of p53-dependent cellular senescence in suppression of Pten-deficient tumorigenesis." Nature **436**(7051): 725-730.

Chng, K. R., C. W. Chang, et al. (2012). "A transcriptional repressor co-regulatory network governing androgen response in prostate cancers." EMBO J **31**(12): 2810-2823.

Chu, I. M., L. Hengst, et al. (2008). "The Cdk inhibitor p27 in human cancer: prognostic potential and relevance to anticancer therapy." Nat Rev Cancer **8**(4): 253-267.

Ciau-Uitz, A., L. Wang, et al. (2013). "ETS transcription factors in hematopoietic stem cell development." Blood Cells Mol Dis **51**(4): 248-255.

Clark, J., S. Merson, et al. (2007). "Diversity of TMPRSS2-ERG fusion transcripts in the human prostate." Oncogene **26**(18): 2667-2673.

Clausen, P. A., M. Athanasiou, et al. (1997). "ETS-1 induces increased expression of erythroid markers in the pluripotent erythroleukemic cell lines K562 and HEL." Leukemia **11**(8): 1224-1233.

Cooper, C. D., J. A. Newman, et al. (2014). "Recent advances in the structural molecular biology of Ets transcription factors: interactions, interfaces and inhibition." Biochem Soc Trans **42**(1): 130-138.

Cooper, C. S. and C. S. Foster (2009). "Concepts of epigenetics in prostate cancer development." Br J Cancer **100**(2): 240-245.

Culig, Z. and M. Puhr (2012). "Interleukin-6: a multifunctional targetable cytokine in human prostate cancer." Mol Cell Endocrinol **360**(1-2): 52-58.

Cunha, G. R. and B. Lung (1978). "The possible influence of temporal factors in androgenic responsiveness of urogenital tissue recombinants from wild-type and androgen-insensitive (Tfm) mice." J Exp Zool **205**(2): 181-193.

De Velasco, M. A. and H. Uemura (2012). "Preclinical Remodeling of Human Prostate Cancer through the PTEN/AKT Pathway." Adv Urol **2012**: 419348.

DeKoter, R. P. and H. Singh (2000). "Regulation of B lymphocyte and macrophage development by graded expression of PU.1." Science **288**(5470): 1439-1441.

Donaldson, L. W., J. M. Petersen, et al. (1996). "Solution structure of the ETS domain from murine Ets-1: a winged helix-turn-helix DNA binding motif." EMBO J **15**(1): 125-134.

Dong, J. T. (2006). "Prevalent mutations in prostate cancer." J Cell Biochem **97**(3): 433-447.

Eguchi, M., M. Eguchi-Ishimae, et al. (1999). "Fusion of ETV6 to neurotrophin-3 receptor TRKC in acute myeloid leukemia with t(12;15)(p13;q25)." Blood **93**(4): 1355-1363.

Ellwood-Yen, K., T. G. Graeber, et al. (2003). "Myc-driven murine prostate cancer shares molecular features with human prostate tumors." Cancer Cell **4**(3): 223-238.

Farnham, P. J. (2009). "Insights from genomic profiling of transcription factors." Nat Rev Genet **10**(9): 605-616.

Feldman, B. J. and D. Feldman (2001). "The development of androgen-independent prostate cancer." Nat Rev Cancer **1**(1): 34-45.

Flavin, R., S. Peluso, et al. (2010). "Fatty acid synthase as a potential therapeutic target in cancer." Future Oncol **6**(4): 551-562.

Frank, S. B. and C. K. Miranti (2013). "Disruption of prostate epithelial differentiation pathways and prostate cancer development." Front Oncol **3**: 273.

Gambarotta, G., C. Boccaccio, et al. (1996). "Ets up-regulates MET transcription." Oncogene **13**(9): 1911-1917.

Gao, H., X. Ouyang, et al. (2006). "Emergence of androgen independence at early stages of prostate cancer progression in Nkx3.1; Pten mice." Cancer Res **66**(16): 7929-7933.

Garcia, D. R., A. M. Arancibia, et al. (2013). "Intrachromosomal amplification of chromosome 21 (iAMP21) detected by ETV6/RUNX1 FISH screening in childhood acute lymphoblastic leukemia: a case report." Rev Bras Hematol Hemoter **35**(5): 369-371.

Gavrilov, D., O. Kenzior, et al. (2001). "Expression of urokinase plasminogen activator and receptor in conjunction with the ets family and AP-1 complex transcription factors in high grade prostate cancers." Eur J Cancer **37**(8): 1033-1040.

Gelmann, E. P. (2003). "Searching for the gatekeeper oncogene of prostate cancer." Crit Rev Oncol Hematol **46 Suppl**: S11-20.

Gelmann, E. P., D. J. Steadman, et al. (2002). "Occurrence of NKX3.1 C154T polymorphism in men with and without prostate cancer and studies of its effect on protein function." Cancer Res **62**(9): 2654-2659.

Geng, C., B. He, et al. (2013). "Prostate cancer-associated mutations in speckle-type POZ protein (SPOP) regulate steroid receptor coactivator 3 protein turnover." Proc Natl Acad Sci U S A **110**(17): 6997-7002.

Ghosh, S., M. Basu, et al. (2012). "ETS-1 protein regulates vascular endothelial growth factor-induced matrix metalloproteinase-9 and matrix metalloproteinase-13 expression in human ovarian carcinoma cell line SKOV-3." J Biol Chem **287**(18): 15001-15015.

Gleason, D. F. and G. T. Mellinger (1974). "Prediction of prognosis for prostatic adenocarcinoma by combined histological grading and clinical staging." J Urol **111**(1): 58-64.

Golabek, T., J. Powroznik, et al. (2015). "The impact of nutrition in urogenital cancers." Arch Med Sci **11**(2): 411-418.

Golub, T. R., G. F. Barker, et al. (1994). "Fusion of PDGF receptor beta to a novel ets-like gene, tel, in chronic myelomonocytic leukemia with t(5;12) chromosomal translocation." Cell **77**(2): 307-316.

Golub, T. R., A. Goga, et al. (1996). "Oligomerization of the ABL tyrosine kinase by the Ets protein TEL in human leukemia." Mol Cell Biol **16**(8): 4107-4116.

Gonnissen, A., S. Isebaert, et al. (2013). "Hedgehog signaling in prostate cancer and its therapeutic implication." Int J Mol Sci **14**(7): 13979-14007.

Grasso, C. S., Y. M. Wu, et al. (2012). "The mutational landscape of lethal castration-resistant prostate cancer." Nature **487**(7406): 239-243.

Green, S. M., H. J. Coyne, 3rd, et al. (2010). "DNA binding by the ETS protein TEL (ETV6) is regulated by autoinhibition and self-association." J Biol Chem **285**(24): 18496-18504.

Gu, X., L. F. Zerbini, et al. (2007). "Reduced PDEF expression increases invasion and expression of mesenchymal genes in prostate cancer cells." Cancer Res **67**(9): 4219-4226.

Gupta, S., K. Iljin, et al. (2010). "FZD4 as a mediator of ERG oncogene-induced WNT signaling and epithelial-to-mesenchymal transition in human prostate cancer cells." Cancer Res **70**(17): 6735-6745.

Haffner, M. C., M. J. Aryee, et al. (2010). "Androgen-induced TOP2B-mediated double-strand breaks and prostate cancer gene rearrangements." Nat Genet **42**(8): 668-675.

Hamamoto, R., V. Saloura, et al. (2015). "Critical roles of non-histone protein lysine methylation in human tumorigenesis." Nat Rev Cancer **15**(2): 110-124.

Han, R., M. Pacifici, et al. (2015). "Endothelial Erg expression is required for embryogenesis and vascular integrity." Organogenesis: 0.

Harris, W. P., E. A. Mostaghel, et al. (2009). "Androgen deprivation therapy: progress in understanding mechanisms of resistance and optimizing androgen depletion." Nat Clin Pract Urol **6**(2): 76-85.

Harrow, J., A. Frankish, et al. (2012). "GENCODE: the reference human genome annotation for The ENCODE Project." Genome Res **22**(9): 1760-1774.

Hart, A., F. Melet, et al. (2000). "Fli-1 is required for murine vascular and megakaryocytic development and is hemizygously deleted in patients with thrombocytopenia." Immunity **13**(2): 167-177.

Hassler, M. and T. J. Richmond (2001). "The B-box dominates SAP-1-SRF interactions in the structure of the ternary complex." EMBO J **20**(12): 3018-3028.

He, A., X. Shen, et al. (2012). "PRC2 directly methylates GATA4 and represses its transcriptional activity." Genes Dev **26**(1): 37-42.

Heemers, H. V. and D. J. Tindall (2007). "Androgen receptor (AR) coregulators: a diversity of functions converging on and regulating the AR transcriptional complex." Endocr Rev **28**(7): 778-808.

Henrique, R. and C. Jeronimo (2004). "Molecular detection of prostate cancer: a role for GSTP1 hypermethylation." Eur Urol **46**(5): 660-669; discussion 669.

Heo, S. H., Y. J. Choi, et al. (2010). "Expression profiling of ETS and MMP factors in VEGF-activated endothelial cells: role of MMP-10 in VEGF-induced angiogenesis." J Cell Physiol **224**(3): 734-742.

Holder, S. L. and S. A. Abdulkadir (2014). "PIM1 kinase as a target in prostate cancer: roles in tumorigenesis, castration resistance, and docetaxel resistance." Curr Cancer Drug Targets **14**(2): 105-114.

Hollenhorst, P. C., L. P. McIntosh, et al. (2011). "Genomic and biochemical insights into the specificity of ETS transcription factors." Annu Rev Biochem **80**: 437-471.

Holt, S. K., E. M. Kwon, et al. (2010). "Association of hepsin gene variants with prostate cancer risk and prognosis." Prostate **70**(9): 1012-1019.

Holterman, C. E., A. Franovic, et al. (2010). "ETS-1 oncogenic activity mediated by transforming growth factor alpha." Cancer Res **70**(2): 730-740.

Hu, Y., A. Dobi, et al. (2008). "Delineation of TMPRSS2-ERG splice variants in prostate cancer." Clin Cancer Res **14**(15): 4719-4725.

Ichikawa, H., K. Shimizu, et al. (1994). "An RNA-binding protein gene, TLS/FUS, is fused to ERG in human myeloid leukemia with t(16;21) chromosomal translocation." Cancer Res **54**(11): 2865-2868.

Iljin, K., M. Wolf, et al. (2006). "TMPRSS2 fusions with oncogenic ETS factors in prostate cancer involve unbalanced genomic rearrangements and are associated with HDAC1 and epigenetic reprogramming." Cancer Res **66**(21): 10242-10246.

Janknecht, R. (2005). "EWS-ETS oncoproteins: the linchpins of Ewing tumors." Gene **363**: 1-14.

Jenkins, R. B., J. Qian, et al. (1997). "Detection of c-myc oncogene amplification and chromosomal anomalies in metastatic prostatic carcinoma by fluorescence in situ hybridization." Cancer Res **57**(3): 524-531.

Jenuwein, T. and C. D. Allis (2001). "Translating the histone code." Science **293**(5532): 1074-1080.

Jiang, N., S. Zhu, et al. (2013). "A-methylacyl-CoA racemase (AMACR) and prostate-cancer risk: a meta-analysis of 4,385 participants." PLoS One **8**(10): e74386.

Kanaya, T., K. Hase, et al. (2012). "The Ets transcription factor Spi-B is essential for the differentiation of intestinal microfold cells." Nat Immunol **13**(8): 729-736.

Kang, H. S., M. L. Nelson, et al. (2008). "Identification and structural characterization of a CBP/p300-binding domain from the ETS family transcription factor GABP alpha." J Mol Biol **377**(3): 636-646.

Kar, A. and A. Gutierrez-Hartmann (2013). "Molecular mechanisms of ETS transcription factor-mediated tumorigenesis." Crit Rev Biochem Mol Biol **48**(6): 522-543.

Karantanos, T., P. G. Corn, et al. (2013). "Prostate cancer progression after androgen deprivation therapy: mechanisms of castrate resistance and novel therapeutic approaches." Oncogene **32**(49): 5501-5511.

Karhadkar, S. S., G. S. Bova, et al. (2004). "Hedgehog signalling in prostate regeneration, neoplasia and metastasis." Nature **431**(7009): 707-712.

Kim, C. A., M. L. Phillips, et al. (2001). "Polymerization of the SAM domain of TEL in leukemogenesis and transcriptional repression." EMBO J **20**(15): 4173-4182.

Kim, E., M. Kim, et al. (2013). "Phosphorylation of EZH2 activates STAT3 signaling via STAT3 methylation and promotes tumorigenicity of glioblastoma stem-like cells." Cancer Cell **23**(6): 839-852.

Kim, J., I. E. Eltoum, et al. (2009). "Interactions between cells with distinct mutations in c-MYC and Pten in prostate cancer." PLoS Genet **5**(7): e1000542.

Kim, J., M. Roh, et al. (2012). "A mouse model of heterogeneous, c-MYC-initiated prostate cancer with loss of Pten and p53." Oncogene **31**(3): 322-332.

Kim, M. J., R. Bhatia-Gaur, et al. (2002). "Nkx3.1 mutant mice recapitulate early stages of prostate carcinogenesis." Cancer Res **62**(11): 2999-3004.

Kim, M. J., R. D. Cardiff, et al. (2002). "Cooperativity of Nkx3.1 and Pten loss of function in a mouse model of prostate carcinogenesis." Proc Natl Acad Sci U S A **99**(5): 2884-2889.

Kim, Y. and M. Nirenberg (1989). "Drosophila NK-homeobox genes." Proc Natl Acad Sci U S A **86**(20): 7716-7720.

King, J. C., J. Xu, et al. (2009). "Cooperativity of TMPRSS2-ERG with PI3-kinase pathway activation in prostate oncogenesis." Nat Genet **41**(5): 524-526.

Kleer, C. G., Q. Cao, et al. (2003). "EZH2 is a marker of aggressive breast cancer and promotes neoplastic transformation of breast epithelial cells." Proc Natl Acad Sci U S A **100**(20): 11606-11611.

Klezovitch, O., J. Chevillet, et al. (2004). "Hepsin promotes prostate cancer progression and metastasis." Cancer Cell **6**(2): 185-195.

Klezovitch, O., M. Risk, et al. (2008). "A causal role for ERG in neoplastic transformation of prostate epithelium." Proc Natl Acad Sci U S A **105**(6): 2105-2110.

Koh, C. M., C. J. Bieberich, et al. (2010). "MYC and Prostate Cancer." Genes Cancer **1**(6): 617-628.

Kong, X. T., K. Ida, et al. (1997). "Consistent detection of TLS/FUS-ERG chimeric transcripts in acute myeloid leukemia with t(16;21)(p11;q22) and identification of a novel transcript." Blood **90**(3): 1192-1199.

Konishi, N., M. Nakamura, et al. (2002). "DNA hypermethylation status of multiple genes in prostate adenocarcinomas." Jpn J Cancer Res **93**(7): 767-773.

Kumar-Sinha, C., S. A. Tomlins, et al. (2008). "Recurrent gene fusions in prostate cancer." Nat Rev Cancer **8**(7): 497-511.

Kunderfranco, P., M. Mello-Grand, et al. (2010). "ETS transcription factors control transcription of EZH2 and epigenetic silencing of the tumor suppressor gene Nkx3.1 in prostate cancer." PLoS One **5**(5): e10547.

Kurpios, N. A., L. MacNeil, et al. (2009). "The Pea3 Ets transcription factor regulates differentiation of multipotent progenitor cells during mammary gland development." Dev Biol **325**(1): 106-121.

Kwabi-Addo, B., D. Giri, et al. (2001). "Haploinsufficiency of the Pten tumor suppressor gene promotes prostate cancer progression." Proc Natl Acad Sci U S A **98**(20): 11563-11568.

Lacronique, V., A. Boureux, et al. (1997). "A TEL-JAK2 fusion protein with constitutive kinase activity in human leukemia." Science **278**(5341): 1309-1312.

Lapointe, J., C. Li, et al. (2007). "Genomic profiling reveals alternative genetic pathways of prostate tumorigenesis." Cancer Res **67**(18): 8504-8510.

Lapointe, J., C. Li, et al. (2004). "Gene expression profiling identifies clinically relevant subtypes of prostate cancer." Proc Natl Acad Sci U S A **101**(3): 811-816.

Lawson, D. A. and O. N. Witte (2007). "Stem cells in prostate cancer initiation and progression." J Clin Invest **117**(8): 2044-2050.

Lee, J. M., J. S. Lee, et al. (2012). "EZH2 generates a methyl degron that is recognized by the DCAF1/DDB1/CUL4 E3 ubiquitin ligase complex." Mol Cell **48**(4): 572-586.

Lee, S. T., Z. Li, et al. (2011). "Context-specific regulation of NF-kappaB target gene expression by EZH2 in breast cancers." Mol Cell **43**(5): 798-810.

Lee, T. I., R. G. Jenner, et al. (2006). "Control of developmental regulators by Polycomb in human embryonic stem cells." Cell **125**(2): 301-313.

Leprince, D., A. Gegonne, et al. (1983). "A putative second cell-derived oncogene of the avian leukaemia retrovirus E26." Nature **306**(5941): 395-397.

Liang, C. C., A. Y. Park, et al. (2007). "In vitro scratch assay: a convenient and inexpensive method for analysis of cell migration in vitro." Nat Protoc **2**(2): 329-333.

Liew, C. W., K. D. Rand, et al. (2006). "Molecular analysis of the interaction between the hematopoietic master transcription factors GATA-1 and PU.1." J Biol Chem **281**(38): 28296-28306.

Lilja, H., D. Ulmert, et al. (2008). "Prostate-specific antigen and prostate cancer: prediction, detection and monitoring." Nat Rev Cancer **8**(4): 268-278.

Lin, H. K., Y. C. Hu, et al. (2003). "Suppression versus induction of androgen receptor functions by the phosphatidylinositol 3-kinase/Akt pathway in prostate cancer LNCaP cells with different passage numbers." J Biol Chem **278**(51): 50902-50907.

Lin, J. H., T. Saito, et al. (1998). "Functionally related motor neuron pool and muscle sensory afferent subtypes defined by coordinate ETS gene expression." Cell **95**(3): 393-407.

Lindberg, J., I. G. Mills, et al. (2013). "The mitochondrial and autosomal mutation landscapes of prostate cancer." Eur Urol **63**(4): 702-708.

Liu, W., J. Lindberg, et al. (2012). "Identification of novel CHD1-associated collaborative alterations of genomic structure and functional assessment of CHD1 in prostate cancer." Oncogene **31**(35): 3939-3948.

Longoni, N., M. Sarti, et al. (2013). "ETS transcription factor ESE1/ELF3 orchestrates a positive feedback loop that constitutively activates NF-kappaB and drives prostate cancer progression." Cancer Res **73**(14): 4533-4547.

Macri, E. and M. Loda (1998). "Role of p27 in prostate carcinogenesis." Cancer Metastasis Rev **17**(4): 337-344.

Magee, J. A., S. A. Abdulkadir, et al. (2003). "Haploinsufficiency at the Nkx3.1 locus. A paradigm for stochastic, dosage-sensitive gene regulation during tumor initiation." Cancer Cell **3**(3): 273-283.

Maki, K., H. Arai, et al. (2004). "Leukemia-related transcription factor TEL is negatively regulated through extracellular signal-regulated kinase-induced phosphorylation." Mol Cell Biol **24**(8): 3227-3237.

Manavathi, B., S. K. Rayala, et al. (2007). "Phosphorylation-dependent regulation of stability and transforming potential of ETS transcriptional factor ESE-1 by p21-activated kinase 1." J Biol Chem **282**(27): 19820-19830.

Mani, R. S., S. A. Tomlins, et al. (2009). "Induced chromosomal proximity and gene fusions in prostate cancer." Science **326**(5957): 1230.

Markowski, M. C., C. Bowen, et al. (2008). "Inflammatory cytokines induce phosphorylation and ubiquitination of prostate suppressor protein NKX3.1." Cancer Res **68**(17): 6896-6901.

Maroulakou, I. G. and D. B. Bowe (2000). "Expression and function of Ets transcription factors in mammalian development: a regulatory network." Oncogene **19**(55): 6432-6442.

Marques, R. B., N. F. Dits, et al. (2010). "Bypass mechanisms of the androgen receptor pathway in therapy-resistant prostate cancer cell models." PLoS One **5**(10): e13500.

McCabe, M. T., A. P. Graves, et al. (2012). "Mutation of A677 in histone methyltransferase EZH2 in human B-cell lymphoma promotes hypertrimethylation of histone H3 on lysine 27 (H3K27)." Proc Natl Acad Sci U S A **109**(8): 2989-2994.

McLaughlin, F., V. J. Ludbrook, et al. (2001). "Combined genomic and antisense analysis reveals that the transcription factor Erg is implicated in endothelial cell differentiation." Blood **98**(12): 3332-3339.

Mehra, R., S. A. Tomlins, et al. (2007). "Comprehensive assessment of TMPRSS2 and ETS family gene aberrations in clinically localized prostate cancer." Mod Pathol **20**(5): 538-544.

Migita, T., S. Ruiz, et al. (2009). "Fatty acid synthase: a metabolic enzyme and candidate oncogene in prostate cancer." J Natl Cancer Inst **101**(7): 519-532.

Mosquera, J. M., S. Perner, et al. (2007). "Morphological features of TMPRSS2-ERG gene fusion prostate cancer." J Pathol **212**(1): 91-101.

Muhlbradt, E., E. Asatiani, et al. (2009). "NKX3.1 activates expression of insulin-like growth factor binding protein-3 to mediate insulin-like growth factor-I signaling and cell proliferation." Cancer Res **69**(6): 2615-2622.

Mulholland, D. J., S. Dedhar, et al. (2006). "PTEN and GSK3beta: key regulators of progression to androgen-independent prostate cancer." Oncogene **25**(3): 329-337.

Mulholland, D. J., L. M. Tran, et al. (2011). "Cell autonomous role of PTEN in regulating castration-resistant prostate cancer growth." Cancer Cell **19**(6): 792-804.

Murtaugh, L. C., L. Zeng, et al. (2001). "The chick transcriptional repressor Nkx3.2 acts downstream of Shh to promote BMP-dependent axial chondrogenesis." Dev Cell **1**(3): 411-422.

Nakayama, T., M. Ito, et al. (2001). "Expression of the ets-1 proto-oncogene in human colorectal carcinoma." Mod Pathol **14**(5): 415-422.

Ng, A. P., C. D. Hyland, et al. (2010). "Trisomy of Erg is required for myeloproliferation in a mouse model of Down syndrome." Blood **115**(19): 3966-3969.

Ng, A. P., S. J. Loughran, et al. (2011). "Erg is required for self-renewal of hematopoietic stem cells during stress hematopoiesis in mice." Blood **118**(9): 2454-2461.

Oikawa, T. and T. Yamada (2003). "Molecular biology of the Ets family of transcription factors." Gene **303**: 11-34.

Oikawa, T., T. Yamada, et al. (1999). "The role of Ets family transcription factor PU.1 in hematopoietic cell differentiation, proliferation and apoptosis." Cell Death Differ **6**(7): 599-608.

Okuducu, A. F., U. Zils, et al. (2006). "Increased expression of avian erythroblastosis virus E26 oncogene homolog 1 in World Health Organization grade 1 meningiomas is associated with an elevated risk of recurrence and is correlated with the expression of its target genes matrix metalloproteinase-2 and MMP-9." Cancer **107**(6): 1365-1372.

Osman, I., J. Dai, et al. (2006). "Loss of neutral endopeptidase and activation of protein kinase B (Akt) is associated with prostate cancer progression." Cancer **107**(11): 2628-2636.

Osman, I., H. Yee, et al. (2004). "Neutral endopeptidase protein expression and prognosis in localized prostate cancer." Clin Cancer Res **10**(12 Pt 1): 4096-4100.

Ouyang, X., T. L. DeWeese, et al. (2005). "Loss-of-function of Nkx3.1 promotes increased oxidative damage in prostate carcinogenesis." Cancer Res **65**(15): 6773-6779.

Owczarek, C. M., K. J. Portbury, et al. (2004). "Detailed mapping of the ERG-ETS2 interval of human chromosome 21 and comparison with the region of conserved synteny on mouse chromosome 16." Gene **324**: 65-77.

Papadopoulos, P., S. A. Ridge, et al. (1995). "The novel activation of ABL by fusion to an ets-related gene, TEL." Cancer Res **55**(1): 34-38.

Papas, T. S., D. K. Watson, et al. (1986). "Molecular evolution of ets genes from avians to mammals and their cytogenetic localization to regions involved in leukemia." Gene Amplif Anal **4**: 207-238.

Paramio, J. M., M. Navarro, et al. (1999). "PTEN tumour suppressor is linked to the cell cycle control through the retinoblastoma protein." Oncogene **18**(52): 7462-7468.

Paumelle, R., D. Tulasne, et al. (2002). "Hepatocyte growth factor/scatter factor activates the ETS1 transcription factor by a RAS-RAF-MEK-ERK signaling pathway." Oncogene **21**(15): 2309-2319.

Peeters, P., I. Wlodarska, et al. (1997). "Fusion of ETV6 to MDS1/EVI1 as a result of t(3;12)(q26;p13) in myeloproliferative disorders." Cancer Res **57**(4): 564-569.

Phin, S., M. W. Moore, et al. (2013). "Genomic Rearrangements of PTEN in Prostate Cancer." Front Oncol **3**: 240.

Piunti, A. and D. Pasini (2011). "Epigenetic factors in cancer development: polycomb group proteins." Future Oncol **7**(1): 57-75.

Plath, K., J. Fang, et al. (2003). "Role of histone H3 lysine 27 methylation in X inactivation." Science **300**(5616): 131-135.

Poliseno, L., L. Salmena, et al. (2010). "Identification of the miR-106b~25 microRNA cluster as a proto-oncogenic PTEN-targeting intron that cooperates with its host gene MCM7 in transformation." Sci Signal **3**(117): ra29.

Radu, A., V. Neubauer, et al. (2003). "PTEN induces cell cycle arrest by decreasing the level and nuclear localization of cyclin D1." Mol Cell Biol **23**(17): 6139-6149.

Randi, A. M., A. Sperone, et al. (2009). "Regulation of angiogenesis by ETS transcription factors." Biochem Soc Trans **37**(Pt 6): 1248-1253.

Raouf, A. and A. Seth (2000). "Ets transcription factors and targets in osteogenesis." Oncogene **19**(55): 6455-6463.

Regan, M. C., P. S. Horanyi, et al. (2013). "Structural and dynamic studies of the transcription factor ERG reveal DNA binding is allosterically autoinhibited." Proc Natl Acad Sci U S A **110**(33): 13374-13379.

Riggi, N. and I. Stamenkovic (2007). "The Biology of Ewing sarcoma." Cancer Lett **254**(1): 1-10.

Romana, S. P., M. Mauchauffe, et al. (1995). "The t(12;21) of acute lymphoblastic leukemia results in a tel-AML1 gene fusion." Blood **85**(12): 3662-3670.

Rosen, P., I. A. Sesterhenn, et al. (2012). "Clinical potential of the ERG oncoprotein in prostate cancer." Nat Rev Urol **9**(3): 131-137.

Rostad, K., M. Mannelqvist, et al. (2007). "ERG upregulation and related ETS transcription factors in prostate cancer." Int J Oncol **30**(1): 19-32.

Rouzier, C., J. Haudebourg, et al. (2008). "Detection of the TMPRSS2-ETS fusion gene in prostate carcinomas: retrospective analysis of 55 formalin-fixed and paraffin-embedded samples with clinical data." Cancer Genet Cytogenet **183**(1): 21-27.

Rubin, M. A., C. A. Maher, et al. (2011). "Common gene rearrangements in prostate cancer." J Clin Oncol **29**(27): 3659-3668.

Sahasrabuddhe, A. A., X. Chen, et al. (2015). "Oncogenic Y641 mutations in EZH2 prevent Jak2/beta-TrCP-mediated degradation." Oncogene **34**(4): 445-454.

Sakurai, T., T. Yamada, et al. (2003). "Effects of overexpression of the Ets family transcription factor TEL on cell growth and differentiation of K562 cells." Int J Oncol **22**(6): 1327-1333.

Saramaki, O. R., T. L. Tammela, et al. (2006). "The gene for polycomb group protein enhancer of zeste homolog 2 (EZH2) is amplified in late-stage prostate cancer." Genes Chromosomes Cancer **45**(7): 639-645.

Sartor, A. O., H. Hricak, et al. (2008). "Evaluating localized prostate cancer and identifying candidates for focal therapy." Urology **72**(6 Suppl): S12-24.

Sauvageau, M. and G. Sauvageau (2010). "Polycomb group proteins: multi-faceted regulators of somatic stem cells and cancer." Cell Stem Cell **7**(3): 299-313.

Sawan, C., T. Vaissiere, et al. (2008). "Epigenetic drivers and genetic passengers on the road to cancer." Mutat Res **642**(1-2): 1-13.

Sboner, A., F. Demichelis, et al. (2010). "Molecular sampling of prostate cancer: a dilemma for predicting disease progression." BMC Med Genomics **3**: 8.

Schiewer, M. J., M. A. Augello, et al. (2012). "The AR dependent cell cycle: mechanisms and cancer relevance." Mol Cell Endocrinol **352**(1-2): 34-45.

Schlottmann, S., H. V. Erkizan, et al. (2012). "Acetylation Increases EWS-FLI1 DNA Binding and Transcriptional Activity." Front Oncol **2**: 107.

Schulz, W. A. and M. J. Hoffmann (2009). "Epigenetic mechanisms in the biology of prostate cancer." Semin Cancer Biol **19**(3): 172-180.

Sementchenko, V. I., C. W. Schweinfest, et al. (1998). "ETS2 function is required to maintain the transformed state of human prostate cancer cells." Oncogene **17**(22): 2883-2888.

Setlur, S. R., K. D. Mertz, et al. (2008). "Estrogen-dependent signaling in a molecularly distinct subclass of aggressive prostate cancer." J Natl Cancer Inst **100**(11): 815-825.

Shaikhibrahim, Z., A. Lindstrot, et al. (2011). "Differential expression of ETS family members in prostate cancer tissues and androgen-sensitive and insensitive prostate cancer cell lines." Int J Mol Med **28**(1): 89-93.

Shaikhibrahim, Z. and N. Wernert (2012). "ETS transcription factors and prostate cancer: the role of the family prototype ETS-1 (review)." Int J Oncol **40**(6): 1748-1754.

Sharma, S., T. K. Kelly, et al. (2010). "Epigenetics in cancer." Carcinogenesis **31**(1): 27-36.

Sharrocks, A. D. (2001). "The ETS-domain transcription factor family." Nat Rev Mol Cell Biol **2**(11): 827-837.

Shen, L., J. Cui, et al. (2013). "Update of research on the role of EZH2 in cancer progression." Onco Targets Ther **6**: 321-324.

Shen, M. M. and C. Abate-Shen (2003). "Roles of the Nkx3.1 homeobox gene in prostate organogenesis and carcinogenesis." Dev Dyn **228**(4): 767-778.

Shen, M. M. and C. Abate-Shen (2010). "Molecular genetics of prostate cancer: new prospects for old challenges." Genes Dev **24**(18): 1967-2000.

Shen, X., W. Kim, et al. (2009). "Jumonji modulates polycomb activity and self-renewal versus differentiation of stem cells." Cell **139**(7): 1303-1314.

Shi, B., J. Liang, et al. (2007). "Integration of estrogen and Wnt signaling circuits by the polycomb group protein EZH2 in breast cancer cells." Mol Cell Biol **27**(14): 5105-5119.

Shin, Y. J. and J. H. Kim (2012). "The role of EZH2 in the regulation of the activity of matrix metalloproteinases in prostate cancer cells." PLoS One **7**(1): e30393.

Siegel, R., D. Naishadham, et al. (2013). "Cancer statistics, 2013." CA Cancer J Clin **63**(1): 11-30.

Simon, J. A. and C. A. Lange (2008). "Roles of the EZH2 histone methyltransferase in cancer epigenetics." Mutat Res **647**(1-2): 21-29.

Singh, G. and A. M. Chan (2011). "Post-translational modifications of PTEN and their potential therapeutic implications." Curr Cancer Drug Targets **11**(5): 536-547.

Sneeringer, C. J., M. P. Scott, et al. (2010). "Coordinated activities of wild-type plus mutant EZH2 drive tumor-associated hypertrimethylation of lysine 27 on histone H3 (H3K27) in human B-cell lymphomas." Proc Natl Acad Sci U S A **107**(49): 20980-20985.

Song, H., B. Zhang, et al. (2009). "Loss of Nkx3.1 leads to the activation of discrete downstream target genes during prostate tumorigenesis." Oncogene **28**(37): 3307-3319.

Sparmann, A. and M. van Lohuizen (2006). "Polycomb silencers control cell fate, development and cancer." Nat Rev Cancer **6**(11): 846-856.

Starck, J., M. Weiss-Gayet, et al. (2010). "Inducible Fli-1 gene deletion in adult mice modifies several myeloid lineage commitment decisions and accelerates proliferation arrest and terminal erythrocytic differentiation." Blood **116**(23): 4795-4805.

Stark, G. R., Y. Wang, et al. (2011). "Lysine methylation of promoter-bound transcription factors and relevance to cancer." Cell Res **21**(3): 375-380.

Steadman, D. J., D. Giuffrida, et al. (2000). "DNA-binding sequence of the human prostate-specific homeodomain protein NKX3.1." Nucleic Acids Res **28**(12): 2389-2395.

Strahl, B. D. and C. D. Allis (2000). "The language of covalent histone modifications." Nature **403**(6765): 41-45.

Sun, C., A. Dobi, et al. (2008). "TMPRSS2-ERG fusion, a common genomic alteration in prostate cancer activates C-MYC and abrogates prostate epithelial differentiation." Oncogene **27**(40): 5348-5353.

Tamir, A., J. Howard, et al. (1999). "Fli-1, an Ets-related transcription factor, regulates erythropoietin-induced erythroid proliferation and differentiation: evidence for direct transcriptional repression of the Rb gene during differentiation." Mol Cell Biol **19**(6): 4452-4464.

Tan, J., X. Yang, et al. (2007). "Pharmacologic disruption of Polycomb-repressive complex 2-mediated gene repression selectively induces apoptosis in cancer cells." Genes Dev **21**(9): 1050-1063.

Tay, Y., L. Kats, et al. (2011). "Coding-independent regulation of the tumor suppressor PTEN by competing endogenous mRNAs." Cell **147**(2): 344-357.

Taylor, B. S., N. Schultz, et al. (2010). "Integrative genomic profiling of human prostate cancer." Cancer Cell **18**(1): 11-22.

Taylor, J. M., E. E. Dupont-Versteegden, et al. (1997). "A role for the ETS domain transcription factor PEA3 in myogenic differentiation." Mol Cell Biol **17**(9): 5550-5558.

Teruyama, K., M. Abe, et al. (2001). "Role of transcription factor Ets-1 in the apoptosis of human vascular endothelial cells." J Cell Physiol **188**(2): 243-252.

Thomas, G., K. B. Jacobs, et al. (2008). "Multiple loci identified in a genome-wide association study of prostate cancer." Nat Genet **40**(3): 310-315.

Tie, F., T. Furuyama, et al. (2001). "The Drosophila Polycomb Group proteins ESC and E(Z) are present in a complex containing the histone-binding protein p55 and the histone deacetylase RPD3." Development **128**(2): 275-286.

Tomlins, S. A., B. Laxman, et al. (2007). "Distinct classes of chromosomal rearrangements create oncogenic ETS gene fusions in prostate cancer." Nature **448**(7153): 595-599.

Tomlins, S. A., B. Laxman, et al. (2008). "Role of the TMPRSS2-ERG gene fusion in prostate cancer." Neoplasia **10**(2): 177-188.

Tomlins, S. A., D. R. Rhodes, et al. (2005). "Recurrent fusion of TMPRSS2 and ETS transcription factor genes in prostate cancer." Science **310**(5748): 644-648.

Tootle, T. L. and I. Rebay (2005). "Post-translational modifications influence transcription factor activity: a view from the ETS superfamily." Bioessays **27**(3): 285-298.

Tsuzuki, S., O. Taguchi, et al. (2011). "Promotion and maintenance of leukemia by ERG." Blood **117**(14): 3858-3868.

Van de Sande, T., T. Roskams, et al. (2005). "High-level expression of fatty acid synthase in human prostate cancer tissues is linked to activation and nuclear localization of Akt/PKB." J Pathol **206**(2): 214-219.

van der Vlag, J. and A. P. Otte (1999). "Transcriptional repression mediated by the human polycomb-group protein EED involves histone deacetylation." Nat Genet **23**(4): 474-478.

van Leenders, G. J., D. Dukers, et al. (2007). "Polycomb-group oncogenes EZH2, BMI1, and RING1 are overexpressed in prostate cancer with adverse pathologic and clinical features." Eur Urol **52**(2): 455-463.

Varambally, S., S. M. Dhanasekaran, et al. (2002). "The polycomb group protein EZH2 is involved in progression of prostate cancer." Nature **419**(6907): 624-629.

Vire, E., C. Brenner, et al. (2006). "The Polycomb group protein EZH2 directly controls DNA methylation." Nature **439**(7078): 871-874.

Vlaeminck-Guillem, V., S. Carrere, et al. (2000). "The Ets family member Erg gene is expressed in mesodermal tissues and neural crests at fundamental steps during mouse embryogenesis." Mech Dev **91**(1-2): 331-335.

Wang, C. Y., B. Petryniak, et al. (1992). "Evolutionarily conserved Ets family members display distinct DNA binding specificities." J Exp Med **175**(5): 1391-1399.

Wang, L. C., F. Kuo, et al. (1997). "Yolk sac angiogenic defect and intra-embryonic apoptosis in mice lacking the Ets-related factor TEL." EMBO J **16**(14): 4374-4383.

Wang, S., J. Gao, et al. (2003). "Prostate-specific deletion of the murine Pten tumor suppressor gene leads to metastatic prostate cancer." Cancer Cell **4**(3): 209-221.

Wang, X. and X. Jiang (2008). "Post-translational regulation of PTEN." Oncogene **27**(41): 5454-5463.

Wang, X., M. Kruithof-de Julio, et al. (2009). "A luminal epithelial stem cell that is a cell of origin for prostate cancer." Nature **461**(7263): 495-500.

Wasylyk, B., J. Hagman, et al. (1998). "Ets transcription factors: nuclear effectors of the Ras-MAP-kinase signaling pathway." Trends Biochem Sci **23**(6): 213-216.

Wasylyk, C., A. P. Bradford, et al. (1997). "Conserved mechanisms of Ras regulation of evolutionary related transcription factors, Ets1 and Pointed P2." Oncogene **14**(8): 899-913.

Wei, G., R. Srinivasan, et al. (2009). "Ets1 and Ets2 are required for endothelial cell survival during embryonic angiogenesis." Blood **114**(5): 1123-1130.

Wei, Y., Y. H. Chen, et al. (2011). "CDK1-dependent phosphorylation of EZH2 suppresses methylation of H3K27 and promotes osteogenic differentiation of human mesenchymal stem cells." Nat Cell Biol **13**(1): 87-94.

Weichert, W., A. Roske, et al. (2008). "Histone deacetylases 1, 2 and 3 are highly expressed in prostate cancer and HDAC2 expression is associated with shorter PSA relapse time after radical prostatectomy." Br J Cancer **98**(3): 604-610.

Weischenfeldt, J., R. Simon, et al. (2013). "Integrative genomic analyses reveal an androgen-driven somatic alteration landscape in early-onset prostate cancer." Cancer Cell **23**(2): 159-170.

Welsbie, D. S., J. Xu, et al. (2009). "Histone deacetylases are required for androgen receptor function in hormone-sensitive and castrate-resistant prostate cancer." Cancer Res **69**(3): 958-966.

Whang, Y. E., X. Wu, et al. (1998). "Inactivation of the tumor suppressor PTEN/MMAC1 in advanced human prostate cancer through loss of expression." Proc Natl Acad Sci U S A **95**(9): 5246-5250.

Wood, L. D., B. J. Irvin, et al. (2003). "Small ubiquitin-like modifier conjugation regulates nuclear export of TEL, a putative tumor suppressor." Proc Natl Acad Sci U S A **100**(6): 3257-3262.

Wu, Q. and G. Parry (2007). "Hepsin and prostate cancer." Front Biosci **12**: 5052-5059.

Wu, W., S. Zhang, et al. (2013). "Ets-2 regulates cell apoptosis via the Akt pathway, through the regulation of urothelial cancer associated 1, a long non-coding RNA, in bladder cancer cells." PLoS One **8**(9): e73920.

Wu, Z., M. Conaway, et al. (2006). "Conditional expression of PTEN alters the androgen responsiveness of prostate cancer cells." Prostate **66**(10): 1114-1123.

Xiang, Y., Z. Zhu, et al. (2007). "JMJD3 is a histone H3K27 demethylase." Cell Res **17**(10): 850-857.

Xu, D., J. Dwyer, et al. (2008). "Ets2 maintains hTERT gene expression and breast cancer cell proliferation by interacting with c-Myc." J Biol Chem **283**(35): 23567-23580.

Xu, K., Z. J. Wu, et al. (2012). "EZH2 oncogenic activity in castration-resistant prostate cancer cells is Polycomb-independent." Science **338**(6113): 1465-1469.

Yamane, K., C. Toumazou, et al. (2006). "JHDM2A, a JmjC-containing H3K9 demethylase, facilitates transcription activation by androgen receptor." Cell **125**(3): 483-495.

Yang, B. S., C. A. Hauser, et al. (1996). "Ras-mediated phosphorylation of a conserved threonine residue enhances the transactivation activities of c-Ets1 and c-Ets2." Mol Cell Biol **16**(2): 538-547.

Yang, M., S. A. Kenfield, et al. (2015). "Dietary patterns after prostate cancer diagnosis in relation to disease-specific and total mortality." Cancer Prev Res (Phila) **8**(6): 545-551.

Yang, Y. A. and J. Yu (2013). "EZH2, an epigenetic driver of prostate cancer." Protein Cell **4**(5): 331-341.

Yap, D. B., J. Chu, et al. (2011). "Somatic mutations at EZH2 Y641 act dominantly through a mechanism of selectively altered PRC2 catalytic activity, to increase H3K27 trimethylation." Blood **117**(8): 2451-2459.

Yegnasubramanian, S., J. Kowalski, et al. (2004). "Hypermethylation of CpG islands in primary and metastatic human prostate cancer." Cancer Res **64**(6): 1975-1986.

Yoshimoto, M., J. C. Cutz, et al. (2006). "Interphase FISH analysis of PTEN in histologic sections shows genomic deletions in 68% of primary prostate cancer and 23% of high-grade prostatic intra-epithelial neoplasias." Cancer Genet Cytogenet **169**(2): 128-137.

Yu, J., R. S. Mani, et al. (2010). "An integrated network of androgen receptor, polycomb, and TMPRSS2-ERG gene fusions in prostate cancer progression." Cancer Cell **17**(5): 443-454.

Yuan, Y., Z. R. Qian, et al. (2008). "Reduction of GSTP1 expression by DNA methylation correlates with clinicopathological features in pituitary adenomas." Mod Pathol **21**(7): 856-865.

Zeng, X., S. Chen, et al. (2011). "Phosphorylation of EZH2 by CDK1 and CDK2: a possible regulatory mechanism of transmission of the H3K27me3 epigenetic mark through cell divisions." Cell Cycle **10**(4): 579-583.

Zhang, Y., T. Liu, et al. (2008). "Model-based analysis of ChIP-Seq (MACS)." Genome Biol **9**(9): R137.

Zippo, A., A. De Robertis, et al. (2007). "PIM1-dependent phosphorylation of histone H3 at serine 10 is required for MYC-dependent transcriptional activation and oncogenic transformation." Nat Cell Biol **9**(8): 932-944.

Zong, Y., L. Xin, et al. (2009). "ETS family transcription factors collaborate with alternative signaling pathways to induce carcinoma from adult murine prostate cells." Proc Natl Acad Sci U S A **106**(30): 12465-12470.

Curriculum Vitae

PERSONAL INFORMATION

Name	Laura Curti
Birth Date	28th April 1985
Birth Place	Varese
Nationality	Italian
Contact address	Via Don Maesani 3 21046 Malnate (VA) Italy e-mail: laurti@virgilio.it

EDUCATION

February 2012 to March 2016

Doctoral Programme, Faculty of Pharmaceutical Sciences of the University of Geneva, Switzerland.

December 2007 to March 2010

Master Degree in Applied Biology to Biomedical Research at the Insubria University of Varese, Italy.
Grade: 110/110 *summa cum laude*

September 2004 to December 2007

Bachelor Degree in Medical Biology at the Insubria University of Varese, Italy.
Grade: 110/110 *summa cum laude*

1999-2004

Secondary School: Maturità Scientifica at Liceo Scientifico "G. Terragni" Olgiate Comasco (CO), Italy.
Grade: 100/100

PROFESSIONAL EXPERIENCE

February 2012 to April 2016

Ph.D. student at Institute of Oncology Research (IOR)/Institute of Oncology of Southern Switzerland (IOSI), via Vela 6, Bellinzona, Switzerland. Prostate Cancer Biology group, Giuseppina Carbone, MD (giuseppina.carbone@ior.iosi.ch)

Research topic: study of the mechanisms through which the ETS transcription factor ERG and an important histone modifying enzyme could influence prostate cancer progression.

April 2010 to December 2011

Biologist at Institute of Oncology Research (IOR)/Institute of Oncology of Southern Switzerland (IOSI), via Vela 6, Bellinzona, Switzerland. Prostate Cancer Biology group, Giuseppina Carbone, MD (giuseppina.carbone@ior.iosi.ch)

Research topic: study of ETS transcription factors deregulation in prostate cancer development.

February 2009 to March 2010

Visiting student at Institute of Oncology Research (IOR)/Institute of Oncology of Southern Switzerland (IOSI), via Vela 6, Bellinzona, Switzerland. Prostate Cancer Biology group, Giuseppina Carbone, MD (giuseppina.carbone@ior.iosi.ch)

Reserach topic: training for the preparation of the master degree thesis on the study of UHRF1 and its involvement in prostate cancer progression.

March 2007 to September 2007

Visiting Student at Department of Structural and Functional Biology, University of Varese, via A. Da Giussano, 21052 Busto Arsizio (VA), Italy. Laboratory of General Pathology, Prof Ian Marc Bonapace, PhD (ian.bonapace@uninsubria.it).

Research topic: training for the preparation of the bachelor degree thesis on the study of MeCP2 depletion and its effects on epigenetic modifications of pericentromeric heterochromatin.

POSTERS

Curti L., Zoma M., Mitra A., Rossi S., Shinde D., Albino D., Chiorino G, Thalmann G.N., Catapano C.V. and Carbone G.M.
EZH2-induced methylation and ERG-EZH2 genomic co-occupancy set the basis for extensive transcriptome reprogramming and prostate cancer progression. Poster at AACR Annual Meeting, April 2016.

Curti L., Albino D., Dallavalle C., Genini D., Sarti M., Pinton S., Thalmann G.N, Civenni G., Catapano C.V., Carbone G.M.
The ETS transcription factor ERG alters the epigenetic landscape in prostate epithelial cells. Poster at the meeting "Epigenetics: mechanisms & clinical implication", Nyon November 2013.

Longoni L., Sarti M., Albino D., Civenni G., Pinton S., **Curti L.**, Dallavalle C., Sessa F., Thalmann G.N., Garcia-Escudero R., Chiorino G., Catapano C.V. , Carbone G.M.
The ETS transcription factor ELF3 is involved in a positive feedback loop leading to constitutive NF-kB activation and prostate cancer progression. Poster at Charles Rodolphe Brupbacher Symposium "Breakthroughs in Cancer Research and Therapy", Zurich February 2013.

Albino D., Civenni G., Longoni N., **Curti L**., Dallavalle C., Pinton S., Mello-Grand M., Sarti M., Thalmann G., Chiorino G., Catapano C.V., Carbone G.M.
The ETS factor ESE3/EHF controls differentiation and stemness in human prostate tumors. Poster at Charles Rodolphe Brupbacher Symposium "Breakthroughs in Cancer Research and Therapy", Zurich February 2013.

Kunderfranco P., **Curti L.**, Babbio F., Pistore C., Magistri M., Chiorino G., Bonapace I.M., Catapano C.V., Carbone G.M.
UHRF1 is upregulated in prostate cancer and induces epigenetic silencing of tumor suppressor genes. Poster at AACR 101st Annual Meeting, April 2010.

Babbio F., **Curti L.**, Castiglioni I., Casonato P., Pistore C., Pecoraro D., Bonapace I.M. DBSF, Univ. of Insubria (Busto Arsizio).
MeCP2 (Methyl-CpG-binding protein 2): a new role in nuclear envelope stability? Poster at 10th FISV Congress, Riva del Garda (TN), September 2008.

PUBLICATIONS

Thesis project under submission.

Albino D., Longoni N., **Curti L.,** Mello-Grand M., Pinton S., Civenni G., Thalmann G., D'Ambrosio G., Sarti M., Sessa F., Chiorino G., Catapano CV. and Carbone GM.
ESE3/EHF Controls Epithelial Cell Differentiation and Its Loss Leads to Prostate Tumors with Mesenchymal and Stem-like Features. Cancer Research, 2012. Epub 2012 Apr 13.

Curti L., Babbio F., Pistore C., Kunderfranco P., Brino L., Oudet P., Seiler R., Thalman GN., Roggero E., Sarti M., Pinton S., Mello-Grand M., Chiorino G., Catapano CV., Carbone GM and Bonapace IM.
The SRA protein UHRF1 promotes epigenetic cross-talk and is involved in prostate cancer progression. Oncogene, 2012. Epub 2012 Feb 13.